Development of novel fluorescence-based assays for the investigation of human Organic anion transporting polypeptides, uptake transporters with emerging pharmacological relevance

Ph.D. thesis

Izabel Patik

Supervisor: Csilla Laczka, Ph.D., Institute of Enzymology, RCNS, Budapest, Hungary

Eötvös Loránd University

FACULTY OF SCIENCE

Doctoral School of Biology

Head: Prof. Anna Erdei

Immunology program

Head: Dr. Zsuzsa Bajtay

2020

Budapest

To all my family and friends

Acknowledgements

Above all, I would like to express my endless gratitude to my supervisor **Dr. Csilla Özvegy-Laczka** for all the support, patience, encouragement and mentorship she has given to me through the years. Without her I would have never reached to this point. Thank you for your time and guidance at different stages of my graduate career. You have taught me how to grow as a scientist by creating an open environment and placing trust in me in through my training.

I would like to thank **Éva Bakos** for her very helpful discussions, advices, and for all her help with my projects.

I am also grateful to have the opportunity to work with excellent role models such as Csilla and Éva, as they not only excel in research as women but loving mothers of their children at the same time.

I would like to thank **Dr. Balázs Sarkadi** and **Dr. Gergely Szakács** for their significant contributions in my research training, such as their support, expertise, comments and critical feedback through my student years.

I would like to specifically thank **Nóra Kucsma** and **Györgyi Vermes** for their kindness and for teaching me different experimental techniques that were and will be utilized in my work.

Huge thanks and gratitude go to **Virág Székely** who we worked together for endless hours on multiple projects, hand-in-hand and who she taught me a lot about the value of teamwork. I am grateful for all your help.

I would also like to thank my other two favorite past and present Laczka lab members, **Orsolya Német** and **Réka Rigó** for their contributions to this achievement.

Of course, this work would not have been possible without the assistance of the past and current members of the Institute of Enzymology. Many thanks to **Áron Szepesi**, **György Várady**, **Ágnes Telbisz** and **Melinda Gera**.

I would like to extend a heartfelt thanks to all the faculty and staff at Institute of Enzymology. Furthermore, to the **Szakács, Váradi, Welker**, Sarkadi, Buday and Vértessy lab members for creating a space for life changing conversations, unforgettable memories, growing friendships or just sharing food.

Thanks to our secretary **Krisztina Mohos** for being always helpful and supportive.

A wholehearted thank you goes to **András Váradi** who I am proud to call my mentor. Thanks for all your support, guidance, motivational speaches and friendship through the years that helped me to become a better person. Thank you for everything!

Thanks to **Dey Adwitia** and **Konstantinos Karagiannis** for taking the time to read and comment on this research.

Thanks to the members of the Department of Immunology for all their support, I have learnt a lot through our interactions, meetings and classes.

The work presented would not have been possible without the support of my friends.

Last, but not least, I would like to thank my family for their years of love, guidance and support in making me the person that I am today. Their countless sacrifices and motivation led me to pursue my dreams and become a scientist. Thank you, **Anya**, **Apa** and **Zotya** for everything that you have done for me.

Contents

List of tables

List of figures

Abbreviations

ABC: ATP-binding cassette

ADME: absorption, distribution, metabolism and elimination

AF405: Alexa Fluor 405

BBB: blood-brain barrier

BSA: Bovine serum albumin

CB: Cascade Blue

CT: cancer-type

DDI: drug-drug interaction

DHEAS: dehydroepiandrosterone sulfate

E1S: estrone-3-sulfate

EMA: European Medicines Agency

FBS: Fetal bovine serum

FDA: U.S. Food and Drug Administration

Fl-MTX: fluorescein-methotrexate

GWAS: Genome-wide association studies

hOATP: human organic anion transporting polypeptide

ITS: International Transporter Consortium

LDG: Live/Dead Green

MDD: major depressive disorder

mRNA: messenger ribonucleic acid

MS: mass spectrometry

Na-Fluo: sodium-fluorescein

OATP: Organic anion transporting polypeptides

PDZ: is an initialism combining the first letters of the first three proteins discovered to share the domain; post synaptic density protein (PSD95), Drosophila disc large tumor suppressor (Dlg1), and zonula occludens-1 protein (zo-1)

PK: pharmacokinetics

PSP: progressive supranuclear palsy

PVDF: Polyvinylidene Difluoride

RT-PCR: reverse transcription polymerase chain reaction

SDS-PAGE: sodium dodecyl sulfate polyacrylamide gel electrophoresis

SLC: Solute Carriers

SNPs: single nucleotide polymorphisms

TM: transmembrane

T3: triiodothyronine

T4: thyroxine

Chapter I

1. Introduction

1.1 Transporters and Drugs

The cell membrane contains a plethora of transporter proteins embedded in the lipid bilayer. The interplay between these transporters controls the passage of different compounds from endo- and exogenous origin through the cell. The majority of transporters belong to two superfamilies, the ATP-binding cassette (ABC) transporters and Solute Carriers (SLCs). Multispecific drug transporters with overlapping substrate specificity can be found in both families and they play a crucial role in the absorption, distribution, and elimination of their substrates. These proteins are localized to critical barrier surfaces such as liver, kidney, brain, lung, intestine, testes and placenta. While extensive research has been focused on ABC transporters due to their role in drug resistance and the pathogenesis of several diseases (e.g.: cystic fibrosis, pseudoxanthoma elasticum), recent studies are also focusing on the role of SLCs in drug-drug interactions (DDIs) and pharmacokinetics (PK). One such family, the Organic anion-transporting polypeptides (OATPs) stands out as a major contributor to these findings. The human OATP family has 11 members that are involved in the cellular uptake of various organic compounds, including widely prescribed drugs such as statins, antibiotics, antimycotics, anticancer agents, etc. Modulation of OATP function or expression via pharmacotherapy with OATP substrates/inhibitors or due to polymorphisms affects pharmacokinetics. Moreover, these alterations could manifest themselves into drug toxicities which has been a major concern in drug development. These toxicities can arise from multiple sources, e.g. a combination of drugs and genetically predisposed vulnerabilities (polymorphisms). According to current industry standards, *in vitro* testing for susceptibility to the transport by liver-specific OATP1B1 and OATP1B3 is recommended for drug candidates that are eliminated in part via the liver. Also, OATP1B1 and OATP1B3 are essential in hepatic transport, but they are also known for their role in statin-related DDI risk and have clinically relevant polymorphisms. Although, there is a growing interest in utilizing OATPs for targeted drug delivery, given their broad substrate specificity and their cancer-specific expression, most members of the OATP family are poorly characterized. This is due to multiple factors that complicate the study of this family such as lack of specific substrates and inhibitors, non-standard *in vitro* tools and a limited number of cellular models with well-defined transporter expression.

Hence the objectives of this thesis are to: i) develop a robust assay platform to study the OATPs' function and ii) to describe new OATP-drug interactions. Such knowledge may help us to enhance our understanding of transporter function, interpret observed pharmacological effects and make more accurate predictions of potential adverse and off-target effects.

1.2 The SLCO/OATP family

Organic anion transporting polypeptides (OATPs) are members of the SLC superfamily. This superfamily has 65 families and more than 400 different human transporters accomplishing vital physiological functions from nutrient uptake through neurotransmitter transport to absorption of widely marketed drugs and xenobiotics. The human SLCO gene family (former SLC21) encoding OATPs have 11 members. OATPs are expressed in the membrane of various epithelial and endothelial cells and mediate the sodium and ATP-independent uptake of large organic ions and amphipathic compounds into cells. Although no crystal structure is available yet for any of the OATPs, topology predictions suggest 12 transmembrane helices with intracellular N- and C-termini [1]. OATPs are divided into six subfamilies based on >40% amino acid sequence identity and identified by Arabic numbering (OATP1-OATP6) [2]. Four members of the family have been characterized in detail. These are OATP1A2, OATP1B1, OATP1B3 and OATP2B1 and owing to their role in altering pharmacokinetic parameters of drugs, multispecific substrate profile and cancer-specific expression pattern makes them potential therapeutic targets [3]. Regardless of the growing interest, the biochemical and pharmacological characterization of the family is far from being complete and several members lack the experimental framework required to investigate their transport mechanism and substrate specificity. This chapter aims to give an overview of OATPs in general, their involvement in drug-transporter interactions and *in vitro* methods designed to investigate OATP-drug interactions.

1.2.1 Tissue distribution and localization of OATPs in healthy tissues

OATPs are localized to the plasma membrane of epithelial and endothelial cells and are widely expressed through the human body. The available expression profiles for OATPs are characterized mainly by RT-PCR, which only indicates mRNA levels. However, there are publications that relied on specific antibodies narrowing down their cellular localizations. We have previously published a review where we summarized available data for each OATP in regard of expression patterns and subcellular localization in healthy tissues [4]. **Table 1.1** and **Figure 1.1** contain an updated version of these data (see below).

Gene	Protein	Tissue expression	Localization	Amino Acids	Chromosome location
SLCO1A2	**OATP1A2**	ubiquitous**: blood-brain barrier (BBB)** [5,6], eye (retina)[7,8], intestine [9], **kidney (distal tubule)** [5], **liver (cholangiocytes)**[5], **neurons** [7], **placenta** [10]**, red blood cells** [11]	mainly apical	**670**	**12p12**
SLCO1B1	**OATP1B1**	**liver (hepatocytes)** [12]	basolateral (sinusoidal)	**691**	**12p12**
SLCO1B3	**OATP1B3**	**liver (hepatocytes)** [13], **pancreas (Langerhans islets)** [14], **placenta** [10]	basolateral (sinusoidal)	**702**	**12p12**
SLCO1C1	**OATP1C1**	brain (choroid plexus), **testis** (Leydig cells) [15,16]	basolateral	**712**	**12p12**
SLCO2A1	**OATP2A1**	ubiquitous: **eye (retina, ciliary epithelium)** [17]**, endometrium** [18], **neurons** [19], intestine [20]	n.d.	**643**	**3q21**
SLCO2B1	**OATP2B1**	ubiquitous: **BBB** [6], **liver (hepatocytes)** [21]**, intestine** [1,20], **skeletal muscle** [22], **red blood cells** [11], **retina** [7]	apical (enterocytes) basolateral (hepatocytes)	**709**	**11q13**
SLCO3A1	**OATP3A1**	**brain (choroid plexus, neurons)** [23], **testis** [23], intestine [20]	apical or basolateral (2 diff. isoforms in the brain)	**710**	**15q26**
SLCO4A1	**OATP4A1**	ubiquitous: **eye (ciliary body**) [24], kidney [25], pancreas [25], heart [25], **placenta** [26], intestine[20]	apical	**722**	**20q13.1**
SLCO4C1	**OATP4C1**	**kidney** [27]	basolateral	**724**	**5q21**
SLCO5A1	**OATP5A1**	**breast** [28], heart [29], fetal brain [29], skeletal muscle [29]	n.d.	**848**	**8q13.1**
SLCO6A1	**OATP6A1**	brain [30], testes [31]	n.d.	**719**	**5q21**

Table 1.1 Gene names and their protein products, tissue distribution, amino acid numbers and chromosome localizations of the human OATPs. Tissues and organs highlighted with bold letters represent protein expression data. n.d.: Localization data is not available.

Pharmacologically important members are primarily expressed in tissues important in drug disposition, such as OATP1B1, OATP1B3, OATP2B1 in the liver (OATP2B1 is also highly expressed in the intestine), OATP4C1 in the kidney, and OATP1A2 (and OATP2B1) in the blood-brain barrier

(BBB). Other members are either expressed ubiquitously through the body or have more restricted tissue distribution patterns.

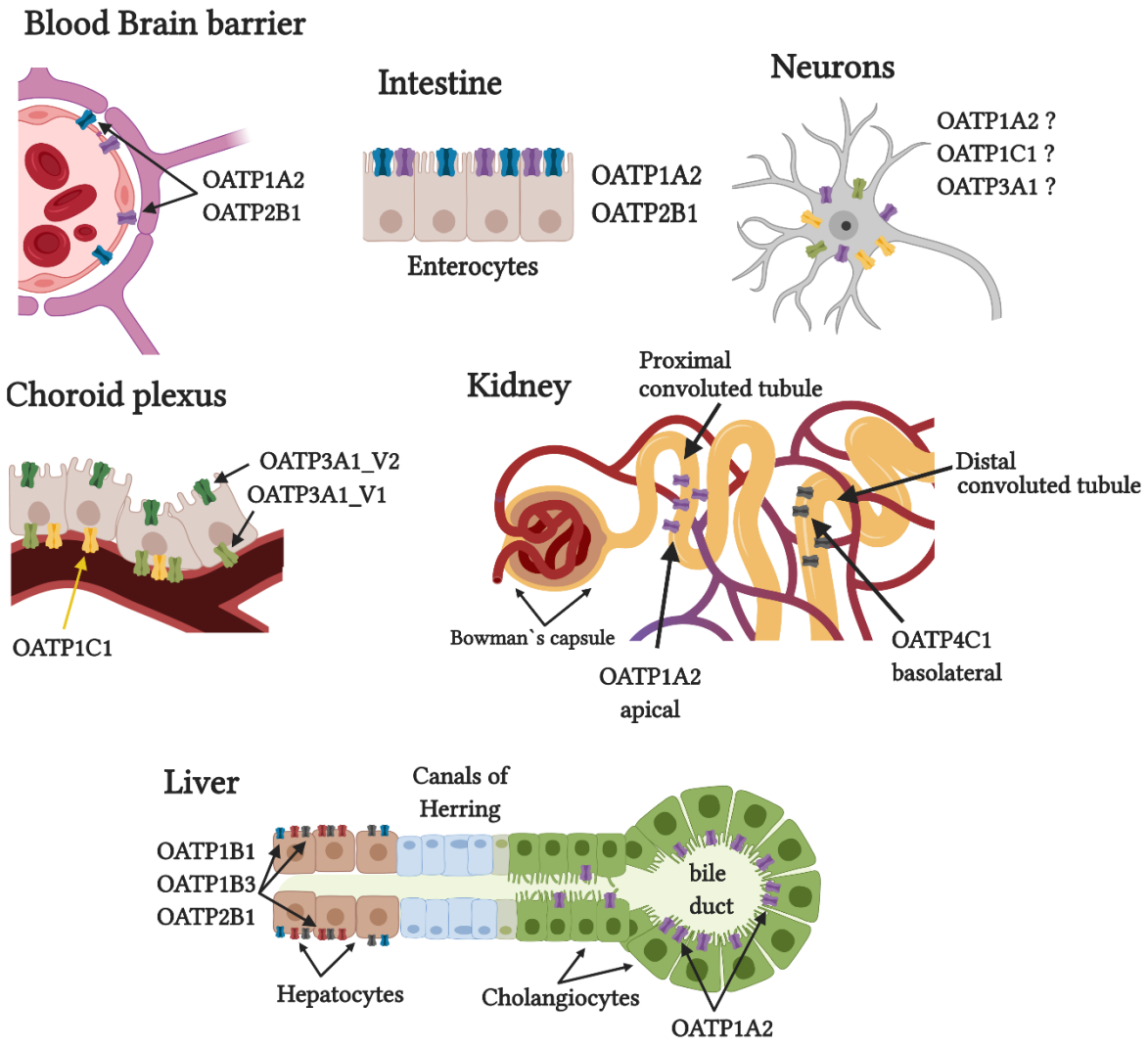

Figure 1.1 Expression of OATPs in selected human epithelial and endothelial cells. Question marks indicate that the expression has been demonstrated but the localization has yet to be shown. OATP3A1 has two isoforms (V1 and V2) with distinct localization. Figure was created with Biorender.com

1.2.2 Structure of human OATPs

Human OATPs share more than 30% amino acid identity and their size range between 634 and 848 amino acids (see **Table 1.1**). Based on hydrophobicity analyses, OATPs are proposed to have a 12 transmembrane segment (TM) topology with both N- and C-termini at the cytoplasmic side of the cell membrane. There are distinct characteristics that help separate OATPs from the rest of the SLC superfamily. For instance, all OATPs share a highly conserved **OATP-signature** sequence: D-X-RW-

(I, V)-GAWW-X-G-(F, L)-L. In OATP1B1 it is located in the boundary of the 3rd extracellular loop and the 6th TM domain [32] (**Figure 1.2.**) and it is important for the surface expression of this protein [33]. The second typical feature is the **large extracellular domain (5th extracellular loop) with conserved cysteines** which is required for the surface expression of OATP2B1 [34,35]. Additionally, in the same loop, previous studies identified a distant homology to the Kazal-type serine protease inhibitors. Although this domain is usually associated with protein kinase inhibitors, there is no existing research showing any relevance for OATPs' function.

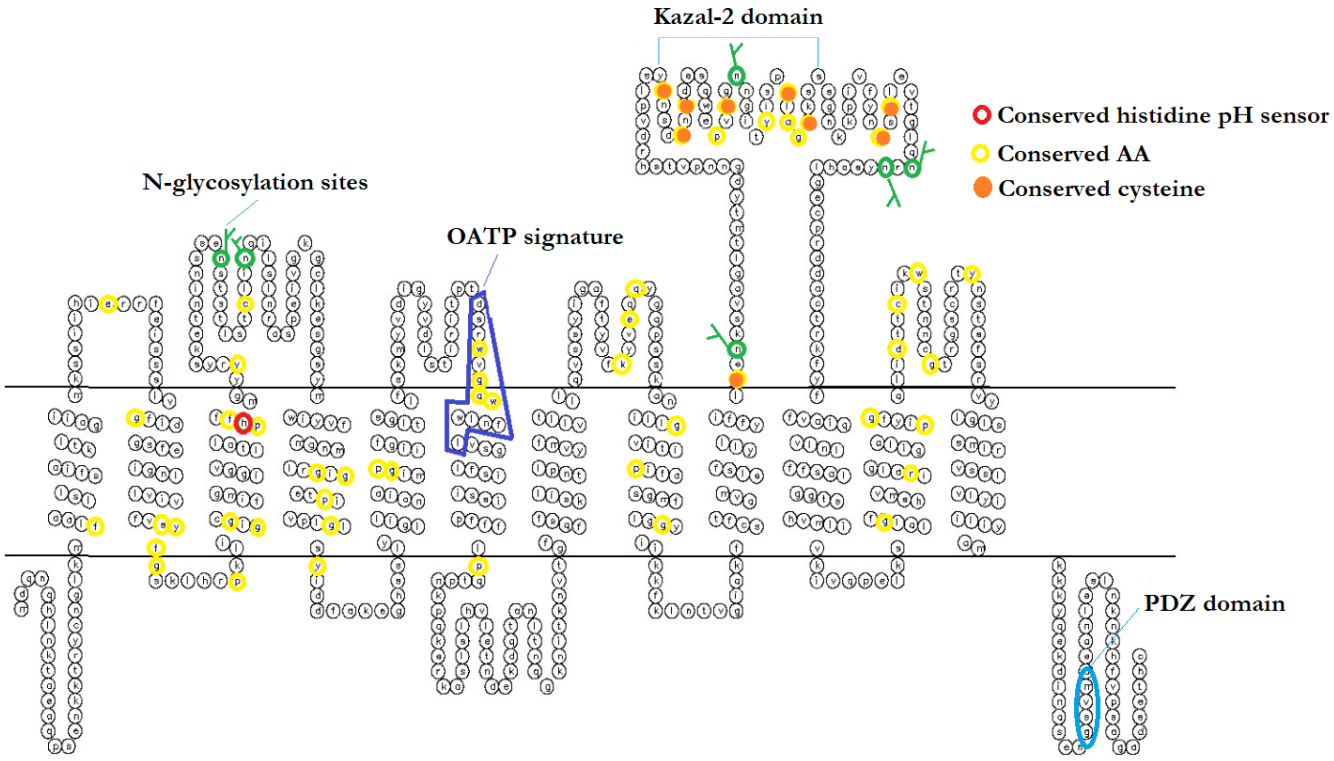

Figure 1.2 Predicted transmembrane structure of OATP1B1. This prediction was created with the help of the HMMTOP server [36].

OATP family members also have a **PDZ consensus sequence** on the C termini. the motif X(S/T)XΦ, where X is any amino acid, and Φ is a hydrophobic amino acid. Wang et al. studied the function of the PDZ domain in *Oatp1a2* (rat) and have found that oligomerization with the PDZK1 protein is essential for proper subcellular localization and function of *Oatp1a2*. In PDZK1 knock-out mice, it was localized to intracellular membranes, resulting in an impaired clearance of bromosulfophtalein [37]. Kato et al. provided further proof, demonstrating that interaction with PDZ proteins are essential for the plasma membrane localization for human OATP1A2, OATP3A1 and

OATP1C1 [38]. OATPs also contain several N-glycosylation sites in their 3rd and 5th extracellular loops. In the case of OATP1B1 N-glycosylation has been shown to dictate proper localization and stability of the protein [39]. Another conserved element in OATPs is the His, found in the 3rd transmembrane segment. This His has been proposed as a pH sensor [40] (read more in 1.2.3). Nevertheless, as there is no OATP crystal structure available, one can only rely on homology models and site-directed mutagenesis studies to predict the structure-function relationships of OATPs [41].

1.2.3 Transport mechanism

The mechanism of OATP-mediated transport is not completely understood. It is generally accepted that the transport is electroneutral, independent of sodium gradient and is not directly coupled to ATP hydrolysis [35]. However, it is unclear whether this involves the coupled movement of another compound or counter ion across the membrane, or if it follows facilitated diffusion through the central pore of the OATP. The proposed transport mechanism for this family is the so-called rocker-switch type mechanism based on the analyses of amino acid conservation patterns, transport activity, substrate specificity and homology modeling [41]. Nevertheless, studies with rat *Oatp* suggest that they act as bicarbonate, glutathione or glutathione conjugate exchangers [23,35]. Also, transport can be enhanced with an acidic extracellular milieu [2,40,42]. There are theories trying to explain why OATPs have a broader substrate specificity and enhanced transporter activity at acidic pH. For example, Varma et al. suggest it might be the result of a change in the degree of protonation of the substrate or the substrate-binding pocket of the transporter. He also used a proton ionophore FCCP (carbonyl cyanide-p-trifluoromethoxyphenylhydrazone) and successfully inhibited OATP2B1-mediated uptake of estrone-3-sulphate and several statins at acidic extracellular pH [43]. Leuthold et al. mutated the highly conserved histidine in the 3rd transmembrane domain, the predicted pH sensor, and argued that the protonation of this conserved His at acidic extracellular pH might responsible for increased affinity toward anionic substrates [40]. There is additional evidence suggesting that the transport might be driven by proton gradient [42]. Additionally, inhibition studies have also shown that different compounds can have different effects on OATP-mediated transport. For example, clotrimazole was shown to stimulate OATP1B3-driven estradiol-17β-glucuronide uptake in stable transfected CHO cells. However, in the same paper they also showed that clotrimazole inhibited OATP1B1-mediated estradiol-17β-glucuronide uptake [44]. It appears that there are significant functional differences within the OATP family, and the function could be influenced in a substrate- and pH-dependent manner.

1.2.4 Substrate specificity

Substrates of OATPs are mainly large amphipathic organic compounds (>300 Da), including steroid hormones, and their conjugates, bile salts, toxins and drugs [30]. Due to their physiological function OATPs are important contributors to bile acid homeostasis (OATPs, 1A2, 1B, 1C1, 2B1, 4A1 and 4C1), bilirubin elimination (OATPs, 1A2, 1B1 and 1B3), inflammatory processes and hormone level adjustments [35,45] (**See Table 1.2** for physiological OATP substrates). On top of that, they are known to recognize wildly prescribed medications such as statins, anticancer agents, and antibiotics [45]. OATPs exhibit a broad and overlapping substrate specificity with other members of the SLC and ABC-transporter families. For instance, OATPs and ABCs work together in the hepatic clearance [46], and toxicity could occur if this essential function is altered by SNPs (single nucleotide polymorphisms), drug-drug or drug-food interactions [47–49]. For instance, co-administration of statins (cholesterol-lowering drugs) with another OATP-inhibitor, cyclosporine A led to toxicity and statin-induced myopathy [22,50]. This helped to recognize the importance of OATPs in drug-transporter interactions. This aspect will be discussed further in the Clinical significance section of this dissertation.

OATP	Physiological substrates
1A2	• atROL [8] • bile salts (taurocholate, cholate, ursodeoxycholic acid) [35,51] •bilirubin [35] • hormones (T4, DHEAS, E1S)[35] • PGE_2 [35] • neuropeptides: SP, VIP [7]
1B1	• bile salts (taurocholate, tauroursodeoxycholate) [35] • bilirubin [35] • eicosanoids (LTC4, LTE4, PGE_2, thromboxane B2) [32] • hormones (E1S, E17βG, T3, T4, DHEAS [35]
1B3	• bile salts (cholate, glycocholate, taurocholate, taurochenodeoxycholate, taurodeoxycholate, tauroursodeoxycholate) [35] • bilirubin [35] • CCK-8 [52] • hormones (T3, T4, E1S, DHEAS, testosterone) [35] • LTC4 [35] • steroid conjugates [30]
1C1	• hormones (E1S, E17βG, thyroid hormones) [30,35]
2A1	• PGs (PGE_1, PGE_2, PGD_2 ,$PGF_{2\alpha}$) [53]
2B1	• DHEAS [54] • E1S [35] • LTC4 [54] • neuropeptides: SP, VIP [7] • PGE_2 [35] • taurocholate [42,54] • thromboxane B2 [53]
3A1	• E1S [15] • PGE_1, PGE_2 [15] • T4 [54] • vasopressin [15]
4A1	• E17βG [35] • E1S [35] • PGE_2 [12] • thyroid hormones (T4, rT3(weak), T3, taurocholate [25])
4C1	• cAMP [27] • E1S [55] • thyroid hormones [27]
5A1	no data

6A1	no data

Table 1.2 Physiological OATP substrates. This table was based on Kovacsics et al., 2016 [4] Abbreviations: **atROL**: all-trans-retinol, **CCK-8**: cholecystokinin, **DHEAS-**dehydroepiandrosterone sulfate, **E1S**: estrone-3-sulphate, **E17βG**: estradiol-17β-glucuronide, **LTC4**: leukotriene C4, **LTE4**: leukotriene E4, **PGE**: prostaglandin E, **PGD**: prostaglandin D, **PGF**: prostaglandin F, **SP:** guinea pig anti-substance P, **T3**: 3,3',5-triiodothyronine, **T4**: thyroxine **VIP:** sheep anti-vasoactive intestinal peptide

1.2.5 Clinical significance

1.2.5.1 OATPs associated with diseases

Several SNPs and mutations in the SLCO genes have been linked to diseases. For example, **OATP1B1** and **OATP1B3** are expressed on the sinusoidal membrane of hepatocytes. They facilitate the uptake of their substrates, such as bilirubin, bile acids, hormones, and drugs. Simultaneous null mutations in SLCO1B1 and SLCO1B3 lead to Rotor-type hyperbilirubinemia, an autosomal recessive disorder characterized by jaundice and elevated serum levels of bilirubin glucuronide [56]. If hepatocytes lack functional OATP1B1 and OATP1B3, there is a failure in the reuptake of conjugated bilirubin from the blood into the liver [56]. Even though OATP1B1 and OATP1B3 have significant roles in drug detoxification, such functional discrepancies are still compatible with relatively normal life and Rotor syndrome is a mild phenotype.

Genome-wide association studies (GWAS) help to identify genetic traits, regions and SNPs that could be associated with certain diseases. Using this approach, a SNP in **SLCO1A2 (rs11568563)** resulting in a Glu172Asp change (causing defective membrane trafficking and decreased function) was found to be involved in progressive supranuclear palsy (PSP). PSP is a Parkinsonian neurodegenerative disorder that presents with predominant specific four repeats (4R) tauopathy in basal ganglia, brainstem and diencephalon with neuronal loss and fibrillary gliosis [57]. Other associations were described between **SLCO6A1** and schizophrenia **(rs6878284, an intron variant)**, bipolar disorder and MDD (major depressive disorder) **(rs7734060, intron variant)** [58,59]. **rs6878284** is significant in the Swedish population; however analysis of Han Chinese population didn't reciprocate the previous finding but found **rs7734060** in strong association with MDD [58]. The primary reason for this discrepancy in schizophrenia could be explained by genetic heterogenicity amongst the Asian and Caucasian populations. In addition, another variant of SLCO6A1 (**rs7705924, intron variant)** was associated with Crohn`s disease in Ashkenazi Jewish cohorts [60].

The first report of deficient OATP1C1 was identified in a 15-year-old patient with severe brain hypometabolism and juvenile neurodegeneration. Exome sequencing revealed the disease causing homozygous missense mutation in the **SLCO1C1** gene resulting in an **Asp252Asn** change. The

mutant protein showed impaired plasma membrane localization and decreased T4 uptake activity [61] Treatment with a T3 analog (Triac) resulted in improved clinical condition and improved quality of life. The group hypothesized that the impaired OATP1C1 function likely reduced T4 uptake in astrocytes and its consequent conversion to T3. Therefore, it has led to reduced bioavailability of T3 in target cells within the central nervous system which might explain the observed developmental delay, abnormal energy metabolism and subsequent neurodegeneration [61]. More on OATP-related diseases check Kovacsics et al., 2016 [4].

1.2.5.2 Ectopic expression of human OATPs

Some OATPs are highly expressed in tumors with low or undetectable expression in corresponding healthy tissues which makes them potential therapeutic targets [62–64]. Increased or ectopic expression of OATPs has been found in breast, liver, colon, lung, pancreatic and ovarian cancers suggesting potential roles for OATPs in tumor development. As most of these OATPs transport chemotherapeutic substrates, their function may sensitize these tissues to cytotoxic agents. Hence targeting these transporters could increase therapy response and might improve overall survival rates. Moreover, given their ability to transport hormones, OATPs might affect cancer development by increasing the proliferation of hormone-sensitive tumors. Therefore, OATPs have been studied to evaluate their potential as diagnostic markers or possible therapeutic targets [65]. Here are a few examples to illustrate how OATPs might affect cancer progression: First, estrone-3-sulfate uptake by OATPs, 1A2 [66], 1B3 [67], 3A1, and 4A1 has been associated to the survival of hormone-dependent breast cancer cells [68]. Second, OATPs also influence disease development in androgen-dependent prostate cancers. The Gly334Thr (rs4149117) allelic variant of OATP1B3 was shown to mediate the increased uptake of testosterone and is associated with decreased patient survival [69]. In another prostate cancer study, they identified a testosterone transport-deficient variant of OATP1B3 (haplotype 334GG/699AA) which was associated with increased survival over 10 years [70]. Similarly, an OATP2B1 variant Arg312Gln (rs12422149), with increased DHEAS (dehydroepiandrosterone sulfate) transport, was correlated with increased patient mortality [69]. At last, as we mentioned above ectopic expression of OATP1B3, identified in cancerous tissues either by immunohistochemistry or based on RT-PCR results, can be found in several types of cancer (colon, breast, prostate, pancreatic, bladder and endometrial) [71]. For several years it has been a generally accepted view that the canonical OATP1B3 (702 amino acid) was identified in cancerous tissues. However, in 2012 and 2013, two cancer-specific isoform (OATP1B3 CT [72] and OATP1B3 V1 [73]) were discovered by two independent groups. The

OATP1B3 CT described by Nagai et al., was found in colon and lung cancer, OATP1B3 V1 was detected in pancreatic and colon cancer tissues. As these proteins are lacking either 47 (OATP1B3 CT) or 28 (OATP1B3 V1) amino acids from the N-terminal end of the canonical OATP1B3 protein, there is an ongoing debate whether these isoforms exhibit plasma membrane localization and transporter function [72–74]. Regardless, they carry a potential to become a diagnostic and prognostic markers for colorectal cancer [75–77]. In **Chapter III** we will take a brief look on their expression, localization and function in different cell lines.

In summary, as a consequence of many contradictory reports, it is hasty to propose whether the presence or absence of a certain OATP in a given cancer is predictive of patient survival or the success of hormonal or antineoplastic therapy. There are comprehensive reviews summarizing OATPs' involvement in cancer: Kovacsics et al., 2016 [4] and Schulte et al., 2019 [64].

1.2.5.3 Drug-transporter interactions

One of the main reasons why OATPs gained recognition was their involvement in drug disposition. It is critical to predict drug-drug, drug-food and drug-transporter interactions and the *in vivo* fate of future/already marketed drugs. Multispecific OATPs, 1A2, 1B1, 1B3 and 2B1 have documented influence on the uptake, disposition and other pharmacokinetic parameters of their substrates. Alterations in their genes may, therefore, account for the interindividual differences in efficacy and toxicity of drugs. Moreover, transporter polymorphisms may not only affect systemic exposure but also local exposure, which is a greater challenge to screen. The family has a plethora of published research on OATP-mediated drug-drug interactions. Excellent reviews summarize the most important ones: Alam et al., 2019 and Shitara et al., 2017 in context of hepatic clearance (OATP1B1 and OATP1B3) [78,79], Ivanyuk et al., 2017 for renal DDIs (OATP1A2 and OATP4C1) [80], and Tamai et al., 2013 for OATP2B1 mediated drug absorption and the potential influence of different fruit juices on OATP2B1 function and expression [81]. Additionally, The U.S. Food and Drug Administration (FDA) published its own list of OATP FDA-approved drug interactions [82]. Consequently, the International Transporter Consortium (ITS) recognizes OATPs, 1A2, 1B1, 1B3, and 2B1 as major determinants of PK and recommends the investigation of these transporters during drug development [83]. The European Medicines Agency (EMA) also agrees with the necessity to describe specific polymorphisms in drug transporters and their possible effect on the efficacy and safety of medicinal products [84]. Collectively, the biggest challenge remains to extrapolate *in vitro* data to relevant *in vivo* predictions. In **Table 1.3** see a summary of the most relevant *in vitro* and *in vivo* OATP-drug interactions.

OATP	Substrates and inhibitors *in vitro*	Drug interactions *in vivo*
1A2	**Antibiotics** •direct **TBPM-PI** (β -lactam antibiotic) uptake [85] **Anesthetics and analgesics** •direct deltorphin II and **DPDPE** transport [86] •direct rocuronium transport inhibited by **APM**, taurocholate, K-strophantoside, **QD**, and **NMQD** [87] **Anticancer drugs** •**ES** uptake inhibited by **MTX** [88] • imatinib transport inhibited by naringin [89] **Antihypertensive drugs** •direct nadolol uptake inhibited by green tea, naringin, verapamil [90] •direct talinolol uptake [91] **Antihistaminic drugs** •direct fexofenadine uptake [92] •direct fexofenadine uptake inhibited by naringin and hesperidin [93] **Antiretroviral drugs** •direct **SQV** uptake [94] **Statins** •direct pravastatin uptake [95] **Toxins** •direct microcystin transport [96] **Others** •direct **ES** uptake inhibited by **atROL**, direct **atROL** transport [8] •direct **TCL** uptake [97] •direct uptake measurements with triptans [98] For further list of interacting molecules see [35,99,100]	•reduced fexofenadine AUC by citrus juices [92,101] •imatinib pharmacokinetics affected by SLCO1A2 SNPs in CML patients [89] •green tea ingestion decreases plasma concentrations of nadolol in humans, presumably in part by inhibition of OATP1A2-mediated intestinal absorption of nadolol [90] •docetaxel transport in humanized mice [102]
1B1	**Antibiotics** •**ES** uptake inhibited by several anti-**TB** drugs [103] •**E17βG** uptake inhibited by novobiocin [104] **Anticancer** •direct docetaxel uptake [105] •direct flavopiridol uptake and increased toxicity [106] •involved in toxicity and disposition of platinum anticancer drugs [107] •**TKI**s as 1B substrates (e.g. direct sorafenib transport) [108] **Antihypertensive drugs** •direct bosentan uptake inhibited by **CsA** and rifampicin [109] •direct valsartan uptake [110] **Anti-inflammatory drugs** •direct mesalazine transport inhibited by budesonide, cyclosporine A, rifampin [111] **Statins** •transport inhibitors: lovastatin acid, pravastatin acid, and simvastatin acid [104] •direct cerivastatin uptake inhibited by **CsA** [112]	•rifampicin as an inhibitor of OATP1B1 and OATP1B3 •Oral or intravenous dose of rifampicin increases exposure of rosuvastatin and pitavastatin [116] •docetaxel transport (humanized mice) [102] •role for OATP1Bs in the elimination of sorafenib (humanized mice) [108]

	•cerivastatin mediated toxicity caused by 1B1 inhibition with gemfibrozil [113] **Toxins** •direct microcystin transport and cytotoxicity [96,114] For further interacting molecules see [35,54,99,100,104,115]	
1B3	**Antibiotics** •**ES** uptake inhibited by several **anti-TB** drugs [103] •direct **E17βG** uptake inhibited by novobiocin [104] **Anticancer drugs** •direct paclitaxel transport [117] •transport inhibitors: mitoxantrone and vincristine 27 [104] •direct docetaxel transport [105] •direct flavopiridol uptake and increased toxicity [106] •1B3 linked toxicity and disposition of cisplatin, carboplatin, and oxaliplatin [107] •**TKI**s as 1B substrates (e.g. direct sorafenib transport)[108] **Anti-inflammatory drugs** •direct mesalazine transport inhibited by budesonide, cyclosporine, rifampin [111] **Antihypertensive drugs** •direct bosentan uptake inhibited by **CsA** and rifampicin [109] •direct valsartan uptake [110] **Toxins** •direct microcystin transport and cytotoxicity [96,114] For an exhaustive list of interacting molecules see: [35,54,99,100,104]	•imatinib pharmacokinetics affected by SNPs in **CML** patients [118] •paclitaxel pharmacokinetics affected by SNPs [117] •docetaxel transport (humanized mice) [102] •role for OATP1Bs in the elimination of sorafenib (humanized mice) [108] •rifampicin as an inhibitor of OATP1B1 and OATP1B3 [116] •rifampicin as an inhibitor of OATP1B1 and OATP1B3 •Oral or intravenous dose of rifampicin increases exposure of rosuvastatin and pitavastatin [116]
1C1	•direct docetaxel transport [105]	
2A1	**Anti-inflammatory drugs** •direct **PGE_2** uptake inhibited by diclofenac and lumiracoxib [119] •direct **PGE_2** uptake induced by indomethacin, ketoprofen, and naproxen [119] **Flavonoids** •direct quercetin transport [120] **Prostaglandin analogs** •direct latanoprost acid uptake [17]	
2B1	**Antibiotics** •direct **ES** uptake inhibited by several **anti-TB** drugs [103] •direct **TBPM-PI** (β -lactam antibiotic) uptake [85] •direct **ES** uptake inhibited by novobiocin [104] **Anticancer drugs** •transport inhibitor: erlotinib [104] •direct flavopiridol uptake and increased toxicity [106] **Anti-inflammatory drugs** •direct mesalazine transport inhibited by budesonide, cyclosporine, rifampin [111] •direct **DCF-AG** transport and toxicity [121] **Antihypertensive drugs** •direct talinolol uptake [91]	

	Prostaglandin analogs •direct latanoprost acid uptake [17] **Statins** •transported by 2B1 [99] •involved in increased cytotoxicity of statins [22] For further interacting molecules see: [35,54,99,100,104]	
3A1	**Antibiotics** •direct benzylpenicillin transport [12] **Antihypertensive drugs** •direct BQ-123 transport [23]	•3A1 as a novel **CD**-associated gene, results higher incidence of bowel perforation in **CD** patients [122]
4A1	**Antibiotics** •direct benzylpenicillin transport [12]	
4C1	**Antidiabetics** •direct sitagliptin transport [123] **Cardiac glycosides** •direct digoxin transport [27,123] •direct digoxin transport increased by bupropion [124] **Statins** •statins increase the expression and function of OATP4C1[125]	•SLCO4C1 overexpression reduced hypertension, cardiomegaly, and inflammation in a rat renal failure model [125]
5A1	**Anticancer drugs** •5A1 expressing cells showed higher resistance to satraplatin [126] **Flavonoids** •direct quercetin uptake [120]	
6A1		

Table 1.3 OATP transporter activity and drug-disposition assessed in vivo (human clinical or rodent data). This table was part of my contribution to the review we published earlier (Kovacsics et al.,2016)[4] **Abbreviations: atROL:** all-trans-retinol; **CsA:** cyclosporin A; **CD:** Crohn's disease; **CML:** chronic myeloid leukemia; **DCF-AG:** diclofenac acyl glucuronide; **DPDPE:** [D-penicillamine2,5]encephalin; **ES:** estrone-3-sulphate; **E17βG:** estradiol-17β-glucuronide; **MTX:** methotrexate; **PGE:** prostaglandin E; **TBPM-PI:** tebipenem pivoxil; **TCL:** trospium chloride; **TKI:** tyrosine kinase inhibitors; **SQV:** saquinavir mesylate

1.3 Methods and models to investigate OATP-drug interactions

1.3.1 Test substrates

Most regulatory agencies require preclinical ADME (absorption, distribution, metabolism and elimination) studies prior to human trials to make better estimates about tissue exposures of potential new drugs and their metabolites. These studies are crucial to select optimal doses and toxicological test systems for future safety evaluation [127]. As yet, the most efficient way to advance our understanding of ADME properties of a drug is to use radioactive isotopes to label and then track a new chemical entity either in *in vivo* or in *in vitro* model systems. So far, radioactively labeled drugs were the best choice to localize and quantify the route of a compound through organs, tissues, and cells. Of course, radiolabeled studies have their limitations, among which is the fact that the measured data reflects both the original compound and its metabolites. Furthermore, it is also costly to tag a compound with [^{14}C] (radiocarbon) or [^{3}H] (tritium), which makes them less favorable for larger-scale substrate-screening experiments [127]. Therefore, efforts have been made to establish newer techniques using mass spectrometry (MS) and compounds with fluorescent tags. Still the use of radioactively labeled compounds in *in vitro* models for screening and estimating drug-transporter interactions has become the standard way to study OATP function. Radiolabeled estrone-3-sulfate, bromsulphthalein, and estradiol 17 β-D- glucuronide have been used for many years to determine the transport activity of several OATPs [42,128–130]. On the other hand, mass spectrometry can also be used to get quantitative ADME or transport data, although it requires more resources, and more efforts to get appropriate standards and to determine individual tissue concentrations. However, mass spectrometry can be applied to follow the metabolism of a drug candidate. Finally, the growing need for imaging-based assays brought attention to fluorescent compounds and they proved to be excellent tools for *in vivo* imaging in drug discovery. The second most popular application of fluorescent compounds is using them in transport inhibition assays. A variety of fluorescent probes (Na-fluorescein [131], fluorescein-methotrexate [132], fluorescein-cAMP [133], various fluorescent bile acids [134,135]) have been used in indirect transport assays to identify OATP1B interacting compounds; however, until recently, no fluorescent assay has been available for other OATPs. Our laboratory was the first to show that sodium-fluorescein (Na-Fluo) is a pan-human OATP substrate and it can also be used to describe poorly characterized OATP family members [136] (See **Chapter I** for details). The value of fluorescein derivatives to develop substrate inhibition assays for OATP1B and OATP2B1 transporters was also

shown in mammalian cells [133]. However, concerns were raised as fluorescein proved to be cell-permeant and its fluorescence intensity is pH-dependent (lowering the pH reduces the fluorescence intensity) [137]. Also, the phenomenon of internal quenching occurs with fluorescein solutions. This means that above a certain concentration in aqueous solutions, the apparent fluorescence of fluorescein will decrease [138]. Therefore, we wanted to identify a pH-independent fluorophore with minimal cell permeability, to perform transport measurements at acidic pH levels desired for the optimal activity of OATPs **(Chapter II)**. Standard and newly developed test substrates of OATPs are listed in **Table 1.4** (also including our findings).

In summary, OATP-drug interaction assays with fluorescent probes are quick, cost-efficient, and suit big compound library screens. However, since the indirect assays do not necessarily distinguish between competitive and non-competitive inhibition, direct transport measurements verified by MS or radioactive labeling should be performed for the compounds identified by such screens.

OATP (human)	Fluorescent or radioactive substrates
1A2	• [^{3}H] atROL [8], • [^{3}H] BSP [90], • [^{35}S] BSP [51], • [tyrosyl-3,5-3H] deltorphin II [86], • [^{3}H] digoxin [139], • [^{3}H] docetaxel [102], • [tyrosyl-2,6-3H(N)] DPDPE [86], • [^{3}H] ES [139], • **Fl-MTX** [136], • [^{3}H] MTX [88], • [^{3}H] nadolol [90], • **LDG**[140], • **LDV**[140], • **LorD488**[140], • **Na-Fluo** [136], • [^{3}H] PGE2 [139], • [^{3}H] quercetin [120], • [^{3}H] quinidine [87], • Rhodamine 123 [141], • [^{3}H] N- methyl-quinine [139], • **SRB**[140], • **SRG**[140], • **SR101**[140], • [^{14}C] SQV [94], • [^{3}H] TCL [97], • **ZV** [140]
1B1	• **AF405**[142], [142]• [^{3}H] BSP [143], • [^{3}H] BPS [144], • **CB**[142], • DCF and DBF [133], • [^{3}H] docetaxel [105], • [^{3}H] E17βG [145], • [^{3}H] ES [143], • Fl-MTX [132], • Fluo-3 [44], • Flutax-2 (Oregon Green 488-Paclitaxel) [35], • **LDG**[142], • **LDV**[142], • Na-Fluo [131], • Oregon green [133], • [^{3}H] TC [145], **ZV**[142]
1B3	• **AF405**[142], • [^{3}H] BSP [13], • [^{3}H] BPS [144], • **CB**[142], • [^{3}H] CCK-8 [52], • DBF [133], • [^{3}H] docetaxel [105], • [^{3}H] E17βG [13], • [^{3}H] ES [139], • Fl-MTX [132], • Fluo-3 [133], • Na-Fluo [131], • **LDG**[142], • **LDV**[142], • Oregon green [133], • [^{3}H] TC [145], • [^{125}I]-T3 [139], • [^{125}I]-T4 [139], • **ZV**[142]
1C1	• [^{3}H] BSP [16], • [^{3}H] docetaxel [105], • [^{3}H] E17βG [16], • [^{3}H] ES [16], • **LDG** [140], • **LDV** [140], • **LorD488** [140], • **Na-Fluo** [136], • SR101 [140,146], • **SRB** [140], • **SRG**[140]
2A1	• **Na-Fluo** [136], • [^{3}H] PGE2 [53], • [^{3}H] PGE1 [53], • [^{3}H] quercetin [120]
2B1	• **AF405** [142], • [^{3}H] BSP [139], • **CB** [142], • DCF and DBF [133], • [^{3}H]-ES [12], • Fl-MTX [136], • LDG [142], • LDV [142], • **Na-Fluo** [136], • Oregon green [133], • [^{3}H] quercetin [120], • [^{3}H] PGE2 [12], • **SR101**[140], • [^{3}H]TC [42], • **ZV**[142]
3A1	• [prolyl-3,4(N)-^{3}H]-BQ-123 [23], • [^{3}H]-ES [12], • **Na-Fluo** [136], • [^{3}H] PGE2 [23], • [^{3}H] PGE1 [23], • [tyrosyl-3,5(N)-^{3}H]-vasopressin [23]
4A1	•[^{3}H] ES [12], •[^{3}H] PGE2 [12], • **Na-Fluo** [136], •[^{3}H] TC [25], •[^{125}I] T4 [25]

4C1	• [^{3}H] digoxin [27], • [^{3}H] ES [40,55], • **Na-Fluo** [136], • [^{14}C] and [^{3}H] sitagliptin [123]
5A1	• **Na-Fluo** [136], • [^{3}H] quercetin [120]
6A1	• **Na-Fluo** [136]

Table 1.4 Fluorescent and radiolabeled substrates used to study OATP function. An updated version of a table previously published by our group (Kovacsics et al.,2016)[4] **Abbreviations:** **AF405:** Alexa Fluor 405 NHS Ester; **BPS**: Beraprost Sodium; **BSP**: Bromsulphthalein/ sulfobromophthalein; **CB:** Cascade Blue hydrazide; **CCK-8**: cholecystokinin; **DBF**: 4',5'-dibromofluorescein; **DCF**: 2',7'- dichlorofluorescein; **DHEAS-**dehydroepiandrosterone sulfate; **DPDPE**: [D-penicillamine^{2,5}]encephalin; **ES**: estrone-3-sulphate; **E17βG**: estradiol-17β-glucuronide; **Fl-MTX**: fluorescein-methotrexate; **LDG:** Live/Dead Green; **LDV:** Live/Dead Violet; **LorD488:** Live-or-Dye 488; **Na-Fluo**: sodium-fluorescein; **PGE**: prostaglandin E; **SR101**: sulforhodamine 101; **SRB:** sulforhodamine B; **SRG:** sulforhodamine G; **SQV**: saquinavir mesylate; **TC**: taurocholate; **TCL**: trospium chloride; **T3**: 3,3',5-triiodothyronine; **T4**: thyroxine. Highlighted with bold letters represent the substrates that were described by our laboratory.

1.3.2 *In vitro* models

Nowadays a plethora of cellular models are available for the investigation of OATPs. The first established and still popular cell-based model to study OATP transport activity is based on cRNA-injected ***Xenopus laevis* oocytes**. Although this model could offer only transient OATP-expression, it has been used for many years to characterize OATPs' function and substrate-specificity [117,147–150]. Sf9 (*Spodoptera frugiperda*) **insect cells** have also been used for the investigation of OATPs [23,135,136,151].

Although several **mammalian cell lines** (Caco-2 [152,153], CHO [154], HeLa [155], HEK-293 [108,154,156,157], HepG2 [74,158], Huh7 [158] etc.) were created to stably overexpress OATPs, there is evidence that generation of these cell lines is challenging [159]. We also experienced difficulties generating stable OATP expressing cell lines (see more in **Chapter II**). One possible explanation to this phenomenon is the uptake of toxic compounds from cell culture media by overexpressed OATPs causing metabolic distress. There is another concern with loss or gain of function studies, as other endogenous transporters with overlapping substrate specificities can compensate for the metabolic changes which could baffle the results obtained with these studies [159].

During the *in vivo* route of a drug through the human body the compound interacts with various transporters and may be modified by metabolic enzymes. To recapitulate the *in vivo* tissue environment and better understand this network, more complex methods are required. Keeping the pharmacological goal in mind, there were multiple options from which to choose. The simplest are cell lines expressing or co-expressing influx and efflux transporters and biotransformation enzymes [160]. More complex stem-cell-derived organoid cultures [161,162], precision-cut intestinal slices [163,164], 3D cell cultures [163] and bioreactors [165] are used to try to recapitulate the tissue heterogeneity.

Also, we should be mindful of the interpretation of the data we acquire with the cell-based *in vitro* systems. There are known prediction methods and guidelines that help to predict whether a new drug has the potential to inhibit OATP1B1 function. Vaidyanathan et al., 2016 compared the reliability of these prediction methods based on *in vitro* data. They concluded that they can reasonably predict a potential risk of OATP1B1-mediated clinical DDI, although we should better understand the variability in inhibition potency, and standardization of these prediction methods is the key [166].

1.3.3 *In vivo* models

As mentioned above, it is important to predict potential DDIs during the preclinical phase of drug development. It is a difficult task to extrapolate *in vitro* data to more complex *in vivo* processes. Therefore, animal models that may offer a better picture of drug disposition in the human is always of interest. Hepatic OATPs have been studied in mice, rats and primates at the systemic level. There are Oatp1a/1b knockout [167] and a *Oatp1b2* (homolog of OATP1B1/1B3) knockout mice strains that have been used to study the liver and plasma distribution of toxins (phalloidin, microcystin- LR), cholesterol-lowering drugs (cerivastatin, lovastatin acid, pravastatin, and simvastatin acid), and antibiotics (rifampicin and rifamycin SV) [128,168]. Alas, for some OATP members, no orthologs have been found in preclinical animal models such as rodents, and dogs [49]. Hence better model is "humanized mice". These are knockouts for the rodent *Oatp*, but have organ-specific expression of OATP1B1, OATP1B3 [108,169]. Such, OATP1A and OATP1B knockout and transgenic mice demonstrated the importance of OATPs in the plasma and hepatic clearance of anticancer drugs such as taxanes, irinotecan/SN-38, methotrexate, doxorubicin, and platinum compounds [170]. However, it is important to point out that OATP1A2 is also expressed in the hepatocytes of the "humanized" mouse model, while OATP1A2 expression is limited to cholangiocytes in humans [168]. Currently, there is no rodent model for OATP2B1. To help to better understand the role of OATPs in the liver, positron emission tomography (PET) imaging has been used to visualize OATP-mediated hepatobiliary transport in humans [171], rats [172] and mice [173]. Cynomolgus monkeys share more than 90% of gene and amino acid sequence identity for human OATP1B transporters [15,49,174]. Therefore, cynomolgus monkeys have been assessed as a more human-like model to study OATP1B-mediated DDIs. They have been used to study the inhibitory potential of cyclosporin A and DDIs reported for rosuvastatin [175], pitavastatin and atorvastatin [174]. These studies concluded that there is a need using several probe substrates and a pre-incubation step when performing *in vitro* inhibition studies [174]. This also emphasizes how difficult the task is when we want to extrapolate *in vitro* data to more relevant *in vivo*

processes. Not only due to species differences in tissue localization and substrate recognition but also due to interindividual differences in dosing, tissue exposure and mechanisms involved in drug clearance.

There are exceptional reviews on the *in vitro-in vivo* extrapolation of OATP-mediated DDIs: Chu et al., 2012 [49] and Ufuk et al., 2018 wrote excellent summaries on interspecies differences and DDIs and Shen et al., 2016 assessed Coproporphyrins I and III as probes for OATP1B1 [176].

Chapter II

Expression of Human Organic anion transporting polypeptides in insect cells reveals that sodium fluorescein is a general OATP substrate

(The work presented in this chapter has been published in Biochemical Pharmacology (2015) [136])

2.1 Abstract

Organic anion transporting polypeptides (OATPs) are plasma membrane proteins encoded by the SLCO gene family. OATPs are sodium-and ATP- independent transporters mediating the uptake of a wide variety of amphipathic or negatively charged compounds [45]. There are 11 human members, and two of them -OATP1B1 and OATP1B3- have been extensively studied in the past decade [56,78,177,178]. Besides their physiological importance in the hepatic reuptake of bile acids and bilirubin, they are also influencing drug disposition/pharmacokinetics and are sites of DDIs [47,78]. In addition, extensive research shows altered expression patterns in multiple cancer types for several other OATPs (see overview in Chapter I). Due to the reasons mentioned above, regulatory agencies, as the US Food and Drug Administration (FDA) and the European Medicines Agency (EMA) and the International Transporter Consortium recommend determining the relative contribution of certain OATPs (e.g.: OATP1B1 and OATP1B3) to *in vivo* pharmacokinetics of drugs [179,180]. Even though there is a growing interest, most members of the family remain poorly characterized, owing to the limited availability of test substrates and functional assays and lack of suitable expression systems with well-defined protein expression.

The existing preclinical models designed to typify the OATPs' substrate profile rely on mass spectrometry (MS) or radioactive test substrates such as tritiated estrone-3-sulfate, bromosulfophtalein and estradiol-17β-glucuronide [127,181]. Although these methods proved to be excellent tools for initial small-scale transporter-drug interaction tests, they are not suitable for larger-compound screenings given their cost and time requirements, and limited substrate availability. Substantial efforts have been made to develop fluorescent probes to substitute radioactive labeling since they are sensitive, affordable and carry a potential for scaled-up automated compound discovery. For instance, sodium-fluorescein (Na-fluo), fluorescein-methotrexate (Fl-MTX), indocyanine green and fluorescent bile acids were identified previously as fluorescent substrates for OATP1B1 and/or OATP1B3 [131,132,134,149,182], but none were available for other members of this family. Moreover, there is no known

substrate for OATP6A1. Thus, there is a significant gap in the ability to predict OATP-mediated drug disposition.

Therefore, in this chapter, I describe a new fluorescence-based functional assay that can be used to study the function of human OATPs. We expressed all 11 human OATPs in a baculovirus-infection based insect cell system and measured the accumulation of Na-Fluo or Fl-MTX. We measured time- and concentration-dependent, and inhibitor sensitive uptake of these compounds. Moreover, we demonstrated that an acidic extracellular microenvironment led to a stimulation of substrate transport. We found that Na-Fluo is a pan-OATP substrate, while Fl-MTX can only be transported by OATPs, 1A2, 1B1, 1B3 and 2B1. We also identified new molecular interactions between OATP2B1 and Imatinib, OATPs, 3A1, 5A1 and 6A1 and estradiol-17β-glucuronide, and OATPs, 1C1 and 4C1 and prostaglandin E_2.

Na-fluorescein is the first fluorescent substrate that can be used to characterize the entire human OATP family and the insect-cell based assay is a useful tool to identify OATP substrates. This system might help to elucidate structure-function relationships, predict interactions of pre- and clinical drugs which could lead to better dosage guidelines and less drug-related toxicity.

2.2 Materials and methods

2.2.1 Materials

Cholic acid (CA), glycocholic acid (GC), propidium iodide, prostaglandin E2 (PGE2), rifampicin (Rif), sodium fluorescein salt (Na-Fluo), taurocholic acid (TC) and ursolic acid (UA) were purchased from Sigma–Aldrich (Budapest, Hungary). Fluorescein-methotrexate (Fl-MTX) was obtained from Biotium, Inc. (Hayward, CA, US). Restriction endonucleases were from New England Biolabs, Ltd. (Ipswitch, MA, US)

2.2.2 Plasmid constructs

To generate the plasmids carrying the gene of human OATPs, we first tailored unique restriction sites that enabled us to insert the gene of each human OATP into the baculoviral transfer vector pAcUW21 (BD Biosciences, San Jose, CA, US). The modified plasmid, termed pAcUW-L2, was constructed by inserting oligonucleotide linkers between the BamHI and NotI sites of pAcUW21-L/ABCG2, a vector generated previously in our lab [183].

5`-GGCCGTGAATTCGGTACCTCGAGCTCGCGGCCGCT-3`

5`-GATCAGCGGCCGCGAGCTCGAGGTACCGAATTCAC-3`

Full-length cDNA sequences encoding human OATPs were then introduced into pAcUW-L2 using the appropriate restriction sites. cDNAs of OATPs, 1A2, 1B3, 1C1, 2A1, 2B1, 4A1, 5A1 and 6A1 were obtained from the Harvard PlasmID Repository (Harvard Medical School, Boston, MA, US), and the cloning of OATP1B1 (Gene ID: AB026257), OATP3A1 variant 1 (AB031050) and OATP4C1 (353189) was performed using the previously constructed vector, pSPORT1 [23,139]. OATP1B1 and OATP3A1 transfer vectors were constructed by isolating the corresponding full-length OATP cDNA from pSPORT1, and then subcloning into the pAcUW21-L2 plasmid between the KpnI and NotI restriction endonuclease sites. Sequence analysis revealed that the OATP1B1 cDNA encodes a polymorphism (N130D, rs2306283), therefore, we reverted the sequence to wild-type (Q9Y6L6.2) using site-directed mutagenesis. The primers used in the mutagenesis reaction were: 1B1-N130N for 5`-ACTAATATCAATTCATCAGAAAATTCAACA-3`, 1B1- N130N rev 5`-TGTTGAATTTTCTGATGAATTGATATTAGT-3`. To generate the OATP6A1 construct, the corresponding cDNA was removed from a pBluescriptR vector (BC034976, HsCD00333181) using NotI and BamHI restriction enzymes, and subcloned into pAcUW21-L/ ABCG2. Sequencing revealed that the vector HsCD00333181 contains a shorter isoform of 6A1, which is missing amino

acids 206–267, compared to the canonical sequence (Q86UG4-1). The cDNA corresponding to the missing region was synthesized by ShineGene Molecular Bio-Technologies, Inc. (Shanghai, China), and subcloned into the pAcUW-21-L/OATP6A1 isoform 2 vector between the NdeI and SpeI sites. The open reading frames of OATP1A2 (BC042452, HsCD00333163), OATP1B3 (BC141525, HsCD00348132), OATP1C1 (BC022461, HsCD00332885), OATP2A1 (BC041140, HsCD00338568), OATP2B1 (BC041095.1, HsCD00378878), OATP4A1 (BC015727, HsCD00334491), OATP4C1 and OATP5A1 (BC137424, HsCD00342690) were amplified by HF PCR (Phusion® High-Fidelity PCR Kit, NEB, Ipswitch, MA, US) following the manufacturer's instructions and using the following primers:

1A2 for 5`-GGAAGATCTGCGGCCGCGCCACCATGGGAGAAACTGAGAA-3`
rev 5`-ATTGAGCTCCTGCAGTTACAATTTAGTTTTCAAT-3`
1B3 for 5`-GTAAATGCGGCCGCAACTCGAGGCCACCATGGACCAACATCAACAT-3`
rev 5`-GTACATGCGGCCGCACTGCAGTTAGTTGGCAGCAGCATT-3`
1C1 for 5`-TGTTTAAACTCTAGAGCCACCATGGACACTTCATCCAAAGAA-3`
rev 5`-TAACCTGCAGGCGGCCGCGTTTCTAAAGTTGAGTTTCCTTG-3
2A1 for 5`-GTAAATGCGGCCGCAAGAATTCGCCACCATGGGGCTCCTGCCCA-3`
rev 5`-GTACATGCGGCCGCTAAGCTTTCAGATGAGGCCTGCCGC-3`
2B1 for 5`-GTAAATGCGGCCGCAAGAATTCGCCACCATGGGACCCAGGATAGG-3`
rev 5`-GTACATGCGGCCGCTAAGCTTTCACACTCGGGAATCCTC-3`
4A1 for 5`-GGAAGATCTGATATCGCCACCATGCCCCTGCATCAGCTG-3`
rev 5`-ATTGAGCTCAAGCTTTCAGACGCTGCTCTGGAG-3`
4C1 for 5`-GGAAGATCTGCGGCCGCGCCACATGAAGAGCGCCAAAGGT-3`
rev 5`-ATTGAGCTCAAGCTTTCACCCTTCTTTTACTAT-3`
5A1 for 5`-TGTTTAAACTCTAGAGCCACCATGGACGAAGGCACTGGACTGC-3`
rev 5`-TAACCTGCAGGAGCGGCCGCCTTCTTCCATTTTCAAGCTTCAGGAGG-3`

The amplified fragments were digested using the following restriction enzymes (OATPs, 1A2, 4A1 and 4C1: BglII and SacI, OATP1B3: XhoI and NotI, OATP2A1 and OATP2B1: EcoRI and NotI, and OATP1C1 and OATP5A1: PmeI and NotI) and subcloned into the pAcUW21-L2 plasmid. Because sequencing of the OATP4A1 construct revealed that the purchased cDNA contains a known SNP of OATP4A1 (232G > A (V78I), rs1047099), the canonical sequence (Q96BD0-1) was generated via Quick Change mutagenesis using the following primers: 5`-AGGTGCGGTACGTCTCGG-3`

(4A1 for and 5`-CCGAGACGTACCGCACCT 30 (4A1 reverse). The DNA sequences for all constructs were verified by sequencing.

2.2.3 Growth and maintenance of Sf9 insect cell line and generation of recombinant baculoviruses

Spodoptera frugiperda (Sf9) cells were grown in suspension culture using TNM-FH insect medium (Sigma–Aldrich, Budapest, Hungary) supplemented with 10% fetal bovine serum (FBS), 100 units/ml penicillin and 100 mg/ml streptomycin, at 27°C. Recombinant baculoviruses, carrying the different human OATP cDNA sequences, were generated using the BaculoGold Transfection Kit (BD Biosciences, San Jose, CA, US) following the manufacturer's instructions. After amplification, the virus stocks were stored at 4°C. For the uptake experiments, we choose virus stocks giving the highest protein expression (after Western blot-based quantitation).

2.2.4 Immunoblot analysis of OATPs

Whole cell lysates of Sf9 cells (5–10 μg) were separated on 7.5% Laemmli SDS-PAGE. Protein transfer to PVDF membrane was performed using the Bio-Rad mini Protean 3 system. Protein concentrations were determined using the Lowry method using BSA as standard. Membranes were incubated overnight with polyclonal antibodies. The antibodies used for the detection of OATPs, 1A2, 1B1, 1B3, 1C1, 2B1, 3A1_v1 and 4A1 were provided by Bruno Stieger [23,44,139]. Antibodies against OATP2A1 (HPA013742), OATP4C1 (HPA036516), OATP5A1 (HPA025062) and OATP6A1 (HPA054126) were purchased from Atlas Antibodies (Stockholm, Sweden). Antibody dilutions: 1:250 for OATP5A1, 1:500 for OATPs, 1A2, 1B1, 2A1, 4C1 and 6A1, and 1:1000 for OATPs, 1B3, 1C1, 2B1, 3A1_v1 and 4A1. After O/N incubation, PVDF membranes were incubated with 10,000–20,000x diluted, HRP-conjugated anti-rabbit secondary antibodies (Jackson ImmunoResearch, Suffolk, UK) for 1h. Luminescence was detected using the Luminor Enhancer Solution kit by Thermo Scientific (Waltham, MA, US).

2.2.5 Cell-based dye uptake assay and measuring OATP transport activity

OATP-transduced Sf9 cells were harvested 40 h post infection into one of the following buffers: **Buffer pH 7.4–8.4**: 125 mM NaCl, 4.8 mM KCl, 1.2 mM CaCl2, 1.2 mM KH_2PO_4, 12 mM $MgSO_4$, 25 mM HEPES, and 5.6 mM glucose, with the pH adjusted to 8.4 or 7.4 using 10 N NaOH or 10 N HCl, respectively. **Buffer pH 4.5–7.4**: 125 mM NaCl, 4.8 mM KCl, 1.2 mM $CaCl_2$, 1.2 mM KH_2PO_4,

12 mM $MgSO_4$, 25 mM MES, and 5.6 mM glucose, with the pH adjusted to 7.4, 6.5, 5.5 or 4.5 using 10 N NaOH or 1 M HEPES.

Cells (2–5 $x10^5$/reaction) were pre-incubated in the presence or absence of inhibitors for 5 min at 37°C. The reaction begun with the addition of two times concentrated Fl-MTX or Na-Fluo to a final concentration of 1 μM except for the measurement of concentration dependence. Uptake was stopped after 10 min (unless stated otherwise) of incubation at 37°C by adding 1 ml of ice-cold phosphate-buffered saline. The cells were kept on ice until flow cytometry analysis. The cellular fluorescence of 10,000 live cells was measured by an Attune® Acoustic Focusing Cytometer (Applied Biosystems, Life Technologies, Carlsbad, CA, US) at an excitation wavelength of 488 nm and an emission wavelength of 530 nm. Dead cells were excluded by propidium iodide (1 μg/ml) staining. As a control, we used Sf9 cells expressing a Drosophila melanogaster telomerase subunit (the plasmid encoding this nuclear protein was a generous gift from Dr. Imre Boros at the Biological Research Center in Szeged, Hungary). Transporter activities were calculated by subtracting the background fluorescence (measured in control cells) from fluorescence measured in Sf9 cells expressing human OATPs. Each data point represents the mean of at least 3 independent experiments.

2.2.6 Data analysis

Kinetic parameters of dye uptake were calculated using non-linear curve fitting (Hill fit) and Graph Pad Prism 8 software. A Student's t- test was used to calculate any statistical significance. The p-value for statistical significance was set at 0.05 (*), 0.01 (**) or 0.001 (***).

2.3 Results

2.3.1 Baculovirus-infection based insect cells are suitable to express functional human OATP1B1 and OATP1B3

Sf9 insect cells were derived from the pupal ovarian tissue of the fall army worm (*Spodoptera frugiperda*). This cell line provides the host for the baculovirus-based expression system. Sf9 cells have been used to express various human proteins for more than 20 years [184]. Some of the main advantages of this system, compared to mammalian cell lines are time- and cost efficiency and higher protein expression levels. Moreover, if compared to prokaryotic expression systems, some human proteins require post-translational modifications to be functionally active (like phosphorylation, disulfide bond formation, N-and O-linked glycosylation and signal peptide cleavage which has an impact on the protein folding). This system provides an excellent platform to express and study the function of membrane transporter proteins (e.g. ABC-transporters) [185–188]. Interestingly, except for OATP2B1, this system to study human OATPs has not yet been described [151]. The baculovirus-insect cell system has a transient nature, hence viral infection results in cell lysis after time giving its minor flaw. However, carefully measuring the viability and the protein levels following infection, it has been previously demonstrated that, 25-30 % of the cells 36-40h post-infection still have intact plasma membranes and they expressed the protein of interest near to the maximum levels [183].

To test the applicability of this system to study human OATPs, first we expressed the two best characterized members of the family, OATP1B1 and OATP1B3 in Sf9 cells. **Fig.2.1** shows the successful expression of these proteins in Sf9 cells.

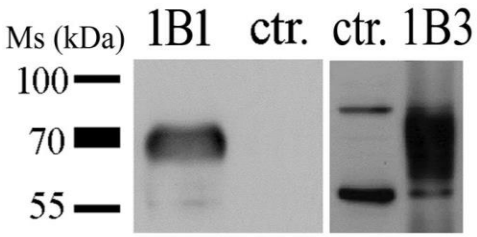

Figure 2.1 Immunodetection of OATP1B1 and OATP1B3 expressed in Sf9 cells. 5 μg whole-cell lysates were separated on 7.5%SDS gels and then transferred to PVDF membranes. The membranes were incubated in milk with anti-OATP1B1 (1:500) and anti-OATP1B3 (1:1000) polyclonal antibodies. HRP-conjugated, polyclonal anti-rabbit secondary antibody was used in a 1:10000 dilution. Control (**ctr.**) shows Sf9 cells overexpressing an unrelated protein.

Next, we tested the functionality of OATP1B1 and OATP 1B3. 40 hours after infection, we measured the cellular accumulation of two previously described substrates, Na-Fluo and Fl-MTX. We could

selectively measure the uptake of Na-Fluo and Fl-MTX in intact cells expressing OATP1B1 or OATP1B3 by flow cytometry (see **Figure 2.2**). This technique enabled us to exclude potential false positives, such as dead cells with compromised membranes by propidium iodide co-staining.

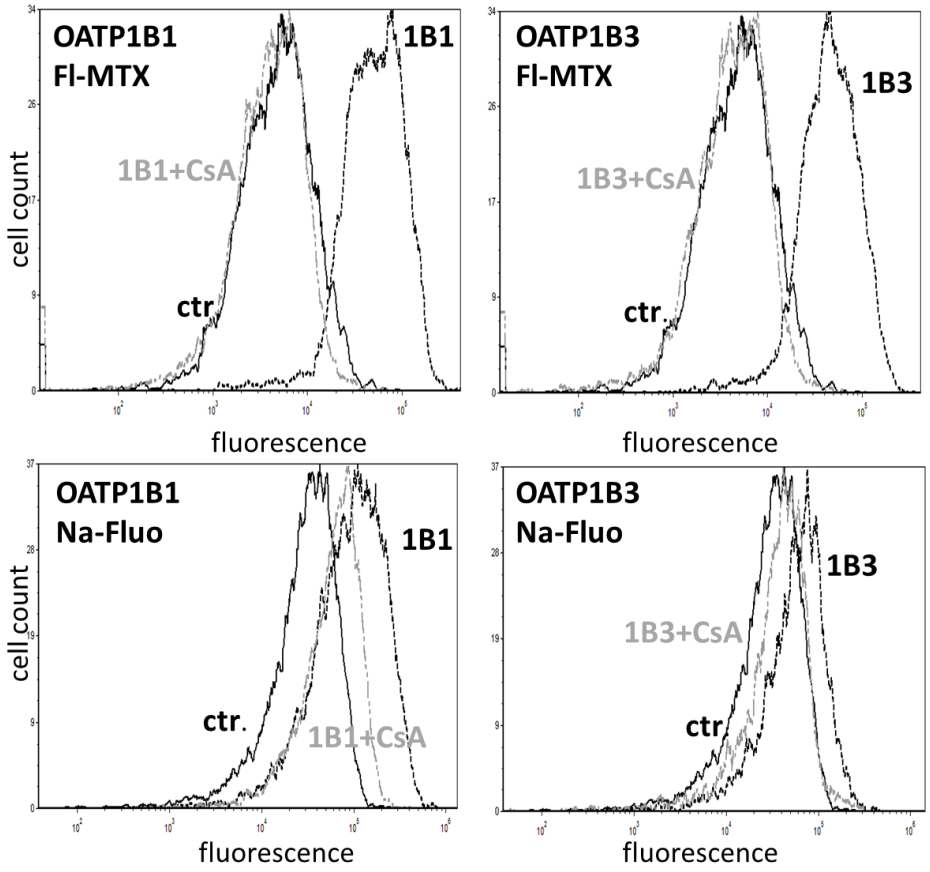

Figure 2.2 1 µM fluorescein methotrexate (Fl-MTX) and 1.5 µM sodium fluorescein (Na-Fluo) uptake in Sf9 cells overexpressing OATP1B1 or OATP1B3 in the presence or absence of 20 µM cyclosporin A (CsA). The transport was measured for 10 min at 37°C and pH 7.4. Dead cells were excluded based on propidium-iodide positivity. Figure was published in [136].

The transport of the fluorescent compounds was rapid, showed saturation kinetics and could be inhibited with a known inhibitor, cyclosporin A (**CsA**) [112] as shown on **Figure 2.3** for Fl-MTX. The transport showed similar kinetics for sodium-fluorescein (**see Figure 2.4**).

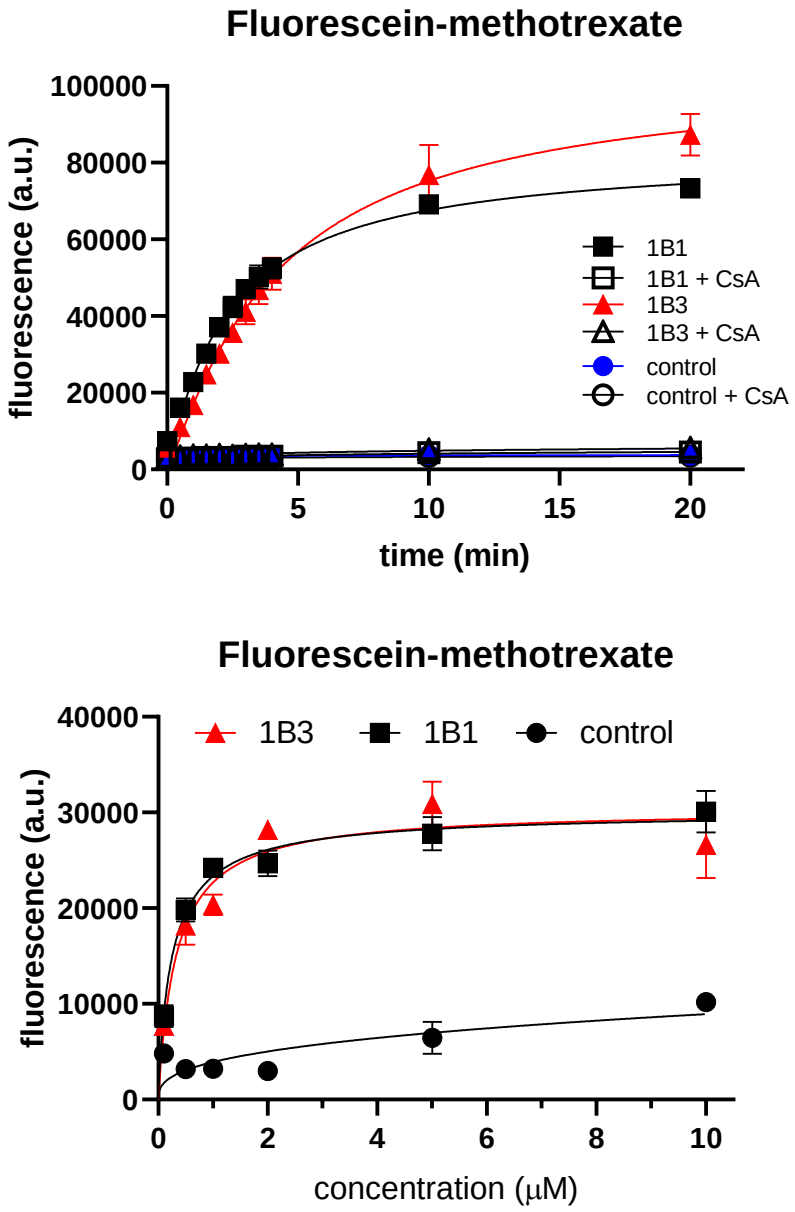

Figure 2.3 Time- and concentration-dependent accumulation of Fl-MTX in Sf9 cells expressing human OATP1B1 or OATP1B3 measured by flow cytometry. Upper panel: 1 μM Fl-MTX was added and cellular fluorescence was measured for 0.5-20 min at 37°C, pH 7.4 in the presence or absence of 20 μM Cyclosporin A (CsA). **Lower panel:** concentration-dependent accumulation of Fl-MTX after 2 min incubation with the substrate. Figures show geomean fluorescence measured by flow cytometry. Data points represent the average of at least three independent measurements ±SD values.

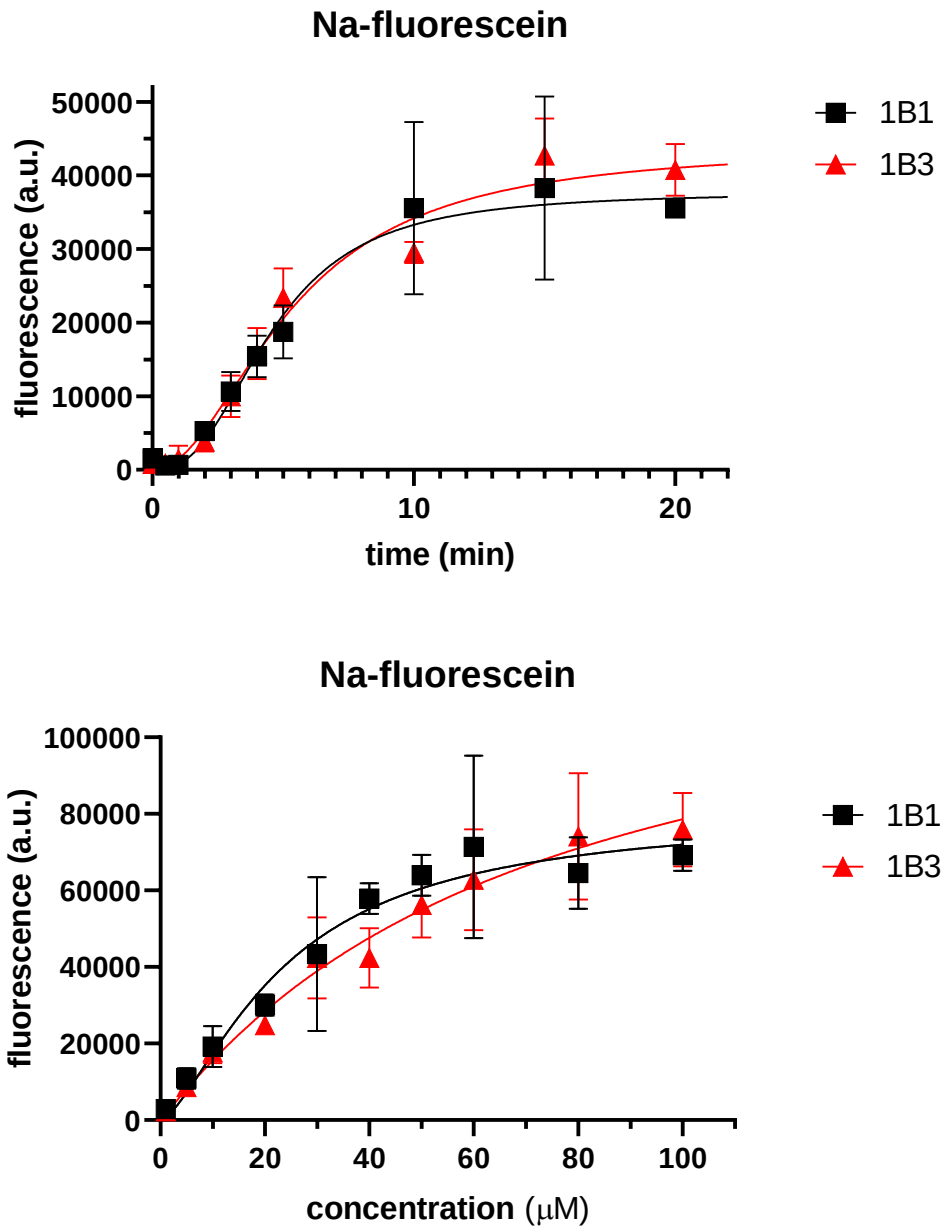

Figure 2.4 Time- and concentration dependent accumulation of sodium-fluorescein in Sf9 cells expressing human OATP1B1 or OATP1B3. Upper panel: 1 μM Na-Fluo was measured between 0.5-20 min at 37°C, pH 7.4. **Lower panel**: concentration-dependent accumulation of Na-Fluo after 4 min incubation with the substrate at 37°C, at pH 7.4. Figures show geomean fluorescence measured by FACS (background fluorescence was subtracted based on fluorescence measured in cells expressing an unrelated protein). Data points represent the average of at least three independent measurements ± SD values.

Kinetic parameters of the transports are summarized below for both substrates. The OATP-mediated uptake was absent at 4°C (data not shown). Comparing these data with the *in vitro* results obtained from other studies, our results correspond well to those measured in mammalian cells [131,132].

	Na-Fluo		Fl-MTX	
Protein	**OATP1B1**	**OATP1B3**	**OATP1B1**	**OATP1B3**
$t_{1/2}$ (min)	6.71±2.33	5.58±0.11	2.64±0.53	4.16±0.28
K_m (μM)	25.73±4.68	38.55±15.00	0.23±0.04	0.53±0.4

Table 2.1 Kinetic parameters of Na-Fluo and Fl-MTX transport measured in Sf9 cells expressing OATP1B1 or OATP1B3.

In order to further validate and characterize OATP1B1/1B3-mediated transport in Sf9 cells, we tested the inhibitory effect of several previously described OATP-interacting compounds on the uptake of Na-Fluo and Fl-MTX (**Figure 2.5)**. Most of the tested inhibitors attenuated OATP1B1/1B3 mediated transport, confirming that the overexpressed proteins are indeed fully functional and that these dyes can be applied to detect OATP1B1/1B3 drug interactions. OATPs are thought to have multiple binding sites which might explain the observed differences in the inhibition of the two fluorescent compounds [45].

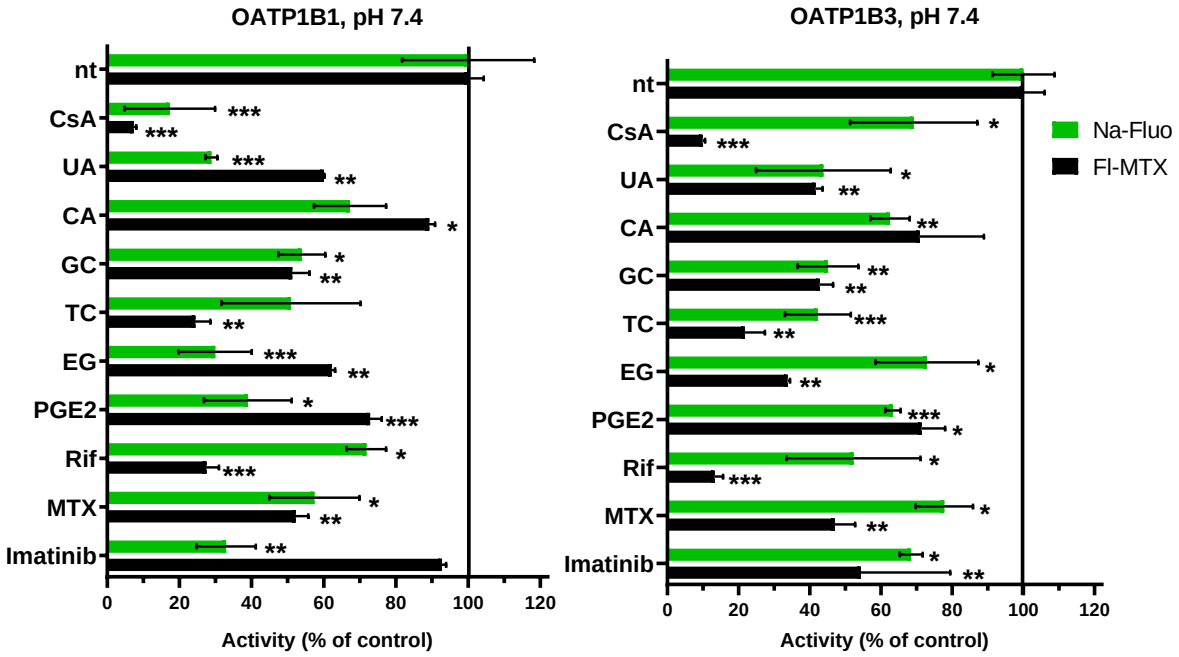

Figure 2.5 OATP1B1 and OATP1B3-mediated Fl-MTX and Na-Fluo transport in Sf9 cells. A panel of OATP-interacting compounds was assessed for 1 μM Fl-MTX and 1 μM Na-Fluo transport activity for 10 min at 37°C and pH 7.4. Transporter activity shown as percentage of control: which was baseline uptake measured with Na-fluo or Fl-MTX alone (100%) after corrected for the uptake by control cells. Bars represent averages of at least 3 independent measurements (±SD). **nt**: non-treated control**, CsA**: 20 μM cyclosporin A, **UA**: 20 μM ursolic acid, **CA**: 150 μM cholic acid, **GC**: 150 μM glycocholate, **TC**: 150 μM taurocholate, **EG**: 50 μM estradiol-17β-glucuronide, **PGE2**: 5 μM prostaglandin E2, **Rif**: 10 μM rifampicin, and **MTX**: 10 μM methotrexate. Significance: *$p < 0.05$, **$p < 0.01$, ***$p < 0.001$

2.3.2 Expression of the human OATP family in insect cells reveals sodium fluorescein as a pan-OATP substrate

After successfully showing that the insect cell-based system is, indeed, useful for the functional expression of OATP1B1 and OATP1B3, our next aim was to express all human OATPs in Sf9 cells. The protein levels of OATPs; 1A2, 1C1, 2A1, 2B1, 3A1, 4A1, 4C1, 5A1 and 6A1 were determined by Western blot (see **Figure 2.6**). Based on the predicted size of the proteins we assumed that the bands in our blots correspond to the core-glycosylated form of our overexpressed proteins [165]. Glycosylation in insect cells is not complete compared to mammalian cell lines. Although N-glycosylation in Sf9 cells results in simple oligo-mannose sugar chains, the glycoprotein will lack complex sugar groups with terminal sialic acids [189]. However, it has been previously demonstrated for many membrane transporters, that this system produces proteins with relevant biological functions [151,187,190–192]. Therefore, it is a suitable system for functional transporter studies.

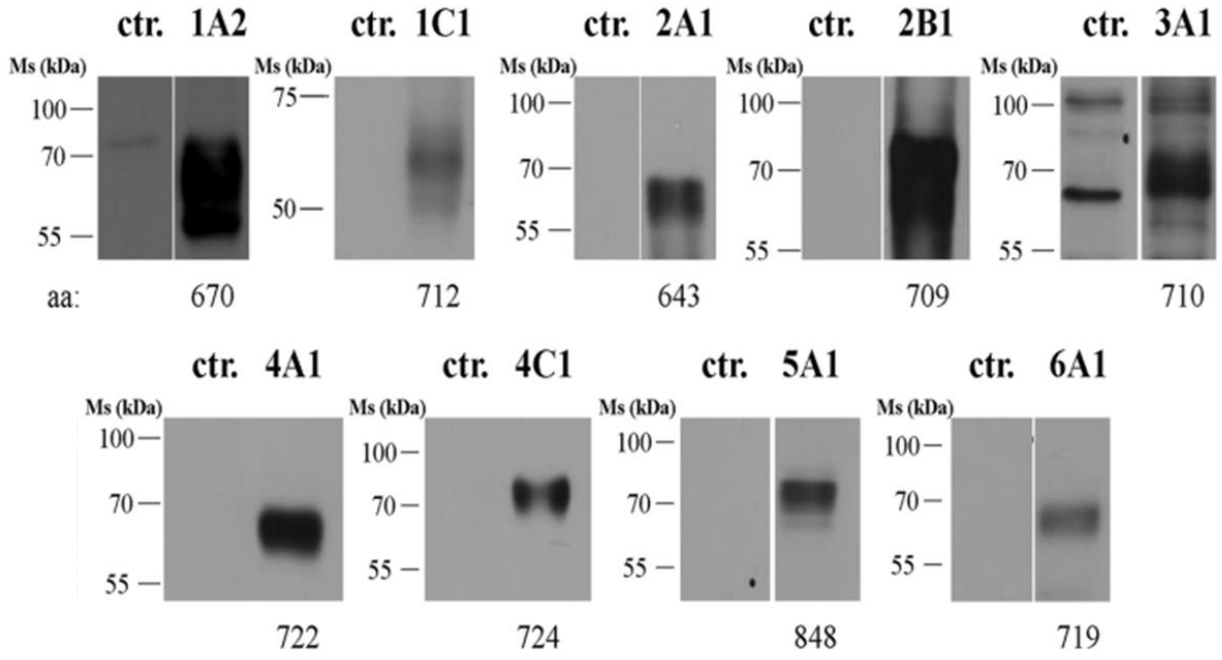

Figure 2.6 Human OATPs overexpressed in Sf9 cells. Whole cell lysates were loaded onto 7.5% Laemmli gels. 5 μg protein was loaded for OATPs, 1C1, 2B1, 4A1, 4C1 and 10 μg for OATPs, 1A2, 2A1, 3A1, 5A1 and 6A1. Control (ctr.) represents Sf9 cells expressing an unrelated protein.

To see if there is an interaction between other human OATP family members and the fluorescent OATP1B1/1B3 substrates, we measured Fl-MTX and Na-Fluo transport under the same conditions as we have optimized for OATPs, 1B1 and 1B3 (10 min incubation at 37°C, pH 7.4, using 1 μM fluorescent substrate). In these experiments, Fl-MTX was transported only by OATP1B1 and

OATP1B3, but surprisingly, all members of the hOATP family were able to show uptake of Na-Fluo (see **Figure 2.7**)

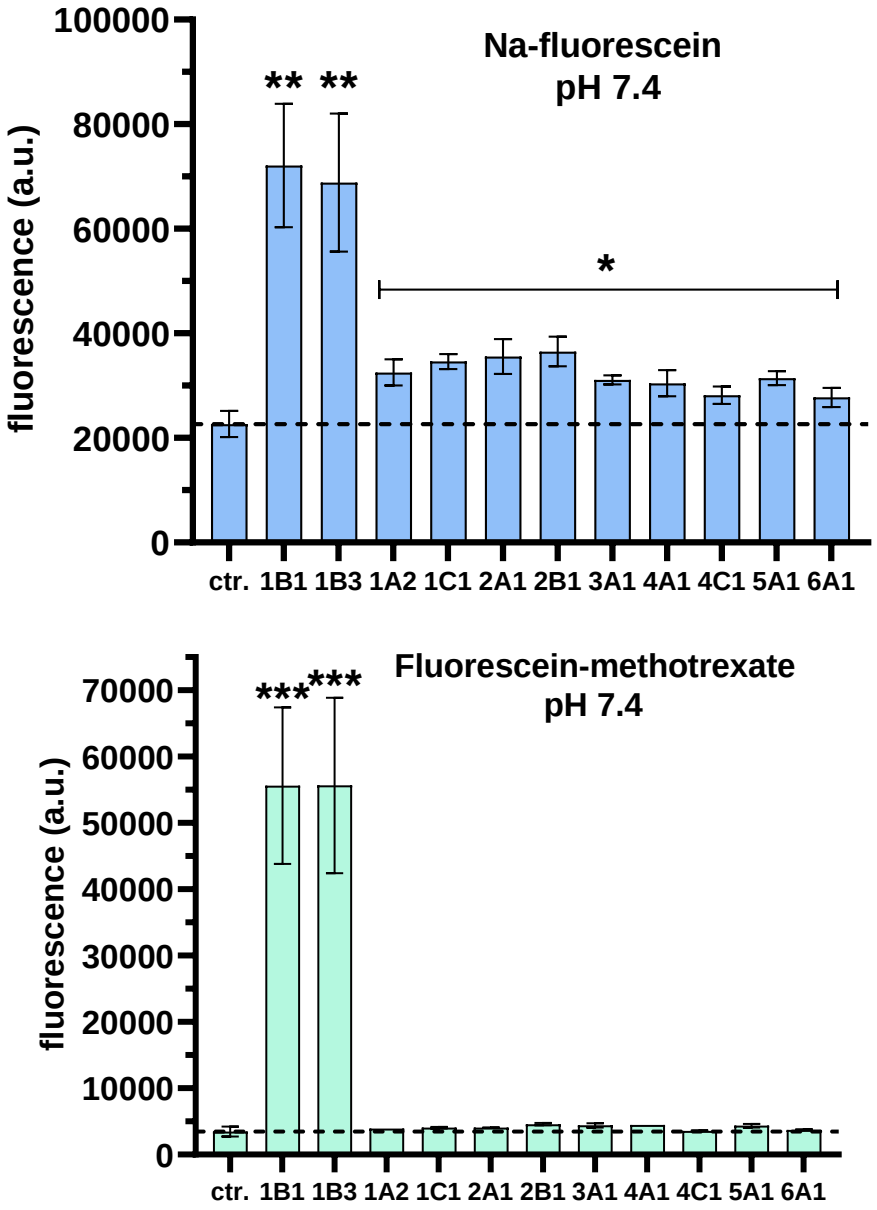

Figure 2.7 Sf9 cells overexpressing human OATPs (see axis x) or an unrelated protein (ctr.). Cells were incubated with 1 μM Na-Fluo (upper panel) or 1 μM Fl-MTX (lower panel) at 37°C for 10 min at pH 7.4. Intracellular fluorescence was measured by flow cytometry. Graphs show geomean fluorescence, bars represent the average of at least three independent experiments ±SD values. Significance: *$p < 0.05$, **$p < 0.01$, ***$p < 0.001$.

2.3.3 Effect of the pH on Na-fluorescein and Fl-MTX transport

The transport mechanism of OATPs is not completely understood, but they`ve been shown to be organic anion exchangers. This is based on existing data showing that substrate transport is accompanied by the extrusion of bicarbonate or glutathione [155]. Also, several papers were published on the pH dependency of OATPs, demonstrating that a low extracellular pH may lead to an increase of substrate transport by all human OATPs, and Rat *Oatp1a1* and *Oatp1b2* [1,40,140,193]. Therefore, we were interested to see, how the pH influences Fl-MTX and Na-Fluo transport in insect cells. Sf9 cells are grown at pH 6.2 which might intercept the optimal H^+ gradient formation to facilitate the pH-sensitive OATP-driven transport. Thus, we tested various buffers adjusted to different pH values, ranging from pH 4.5 to 8.5 in Sf9 cells expressing either OATP1B1 or OATP1B3. Uptake of Fl-MTX and Na-Fluo by OATPs, 1B1 and 1B3 showed distinct pH dependence. As shown on **Figure 2.8** Na-Fluo transport was significantly higher under acidic assay conditions, supporting the concept of a proton gradient-driven uptake mechanism. It is important to note here, that the fluorescence intensity peak of Na-Fluo reduces as the pH is lowered [137,138], therefore the observed increase in transport was due to the increased OATP1B1 or OATP1B3-mediated uptake not due to increased fluorescence of the dye. As I summarized in Chapter I, different theories are trying to explain how the pH might have a stimulatory effect on OATP function. One possible explanation is a change in the protonation levels either in the substrate itself or in amino acids (more precisely the conserved His) of the binding pocket of the transporter, which will change the affinity toward the substrate and result in increased uptake [43]. Fluorescein has a carboxyl and a phenol group which can be ionized. As the pH changes, it could become a cation (pH 1), a neutral quinonoid or lactonoic (pH 2-4), a monoanion (pH 5) or a dianion (≥pH 6.4) molecule. Hence, in the case of fluorescein we expect a neutral molecule at pH 4.5, a monoanion at pH 5.5 and a dianion above 6.4. While the conserved His (pk=6) would be protonated below pH 6. Hence the observed phenomenon can be attributed to the changes in the charge of the substrate; however, it does not fit in any of the existing mechanisms of OATP transport, e.g. the observed highest transport of the neutral fluorescein molecule at pH 4.5.

Interestingly, Fl-MTX uptake showed less pronounced pH dependence, and in contrast to Na-Fluo maximal dye uptake could be observed at or close to neutral pH. In the case of fluorescein-methotrexate, based on the calculated pKa values we expect a monoanion in the pH range between 4.5 and 8, therefore we conclude that the conserved His may not be involved in the recognition of Fl-MTX.

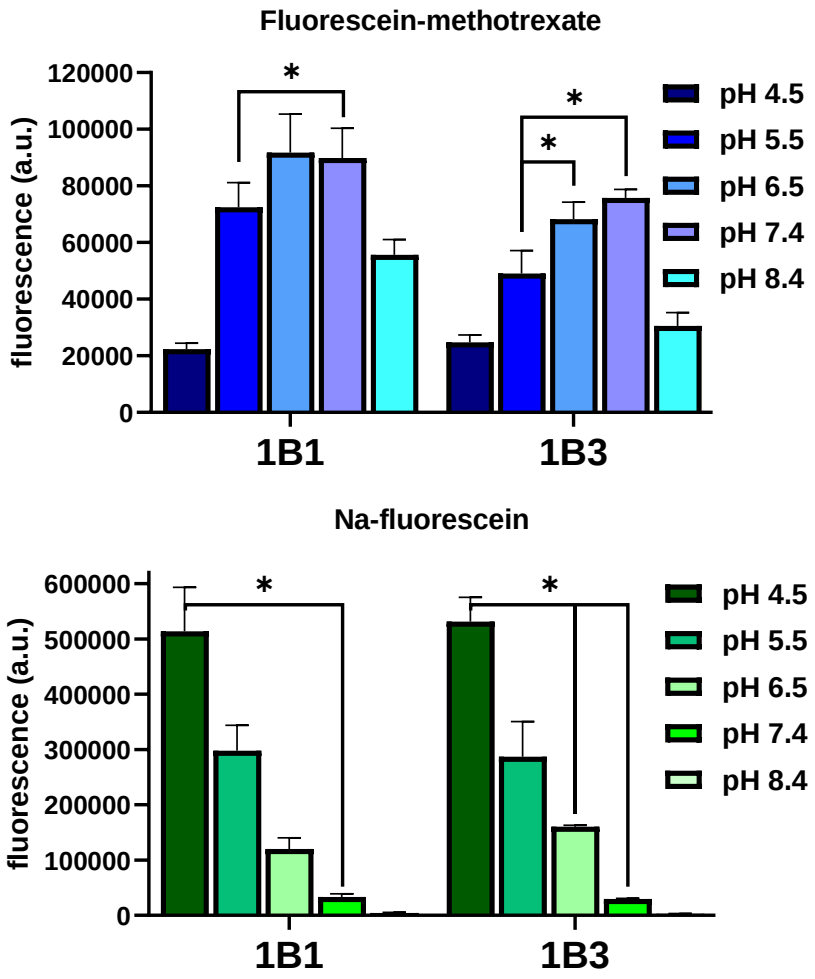

Figure 2.8 pH-dependent uptake of 1 µM Fl-MTX (upper panel) or 1 µM Na-Fluo (lower panel) in Sf9 cells overexpressing OATP1B1 or OATP1B3. Transport was measured for 10 min at 37°C in uptake buffer where the pH ranged from 4.5 to 8.4. Data shows geomean values from three independent experiments ±SD values minus the background fluorescence detected in control cells. Significance: *$p < 0.05$

Because we observed a significant enhancement in transporter activity under acidic assay conditions for Na-fluo, we also wanted to test the entire human OATP panel at acidic pH. The optimized assay conditions for Fl-MTX were between pH 6.5-7.4 and between pH 4.5-5.5 for Na-Fluo. To achieve maximum transport activity closer to physiologically relevant conditions (although local H^+ gradients may be different), we choose to measure transport at pH 6.5 for Fl-MTX and pH 5.5 for Na-Fluo. Consistent with our previous results for OATP1B1 and OATP1B3, lowering the extracellular pH resulted in increased Na-Fluo transport by all human OATPs, despite the increased background fluorescence (**Figure 2.9**). However, when we measured Fl-MTX transport, only OATP1A2 and OATP2B1 showed transporter activity, the other OATPs stayed inactive (**Figure 2.9**).

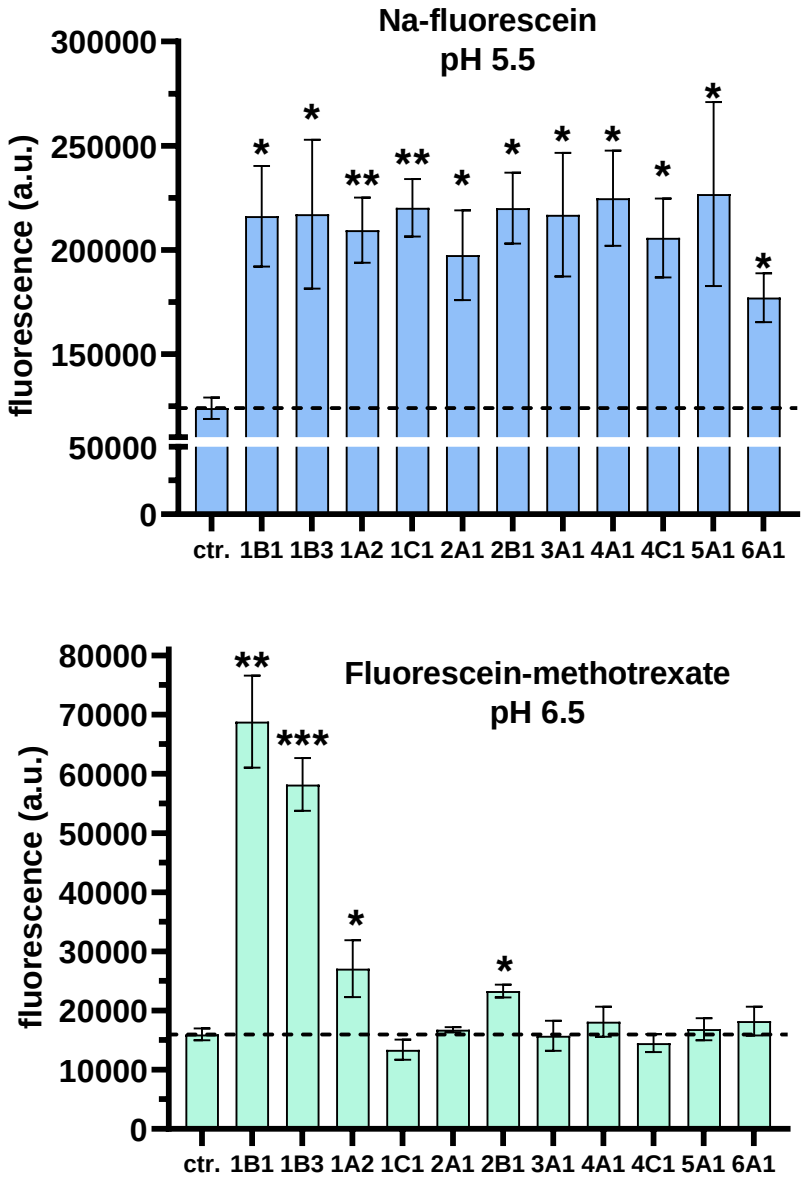

Figure 2.9 Na-fluorescein and Fl-methotrexate uptake in Sf9 cells expressing hOATPs. Cells overexpressing OATPs were incubated with 1 μM Na-Fluo at pH 5.5 (upper panel) or 1 μM Fl-MTX at pH 6.5 (lower panel) for 10 min at 37°C. Data represents geomean values of the average of three independent measurements (±SD values). Significance: *$p < 0.05$, **$p < 0.01$, ***$p < 0.001$

2.3.4 Effect of inhibitors on Na-Fluo and Fl-MTX transport

Following our initial success in confirming that the insect-cell based system is suitable for expressing fully functional human OATPs, and then proving that Fl-MTX and Na-fluo are high affinity substrates for some of these transporters, we also wanted to use this platform to detect OATP interactions. Therefore, we choose a set of previously described OATP-interacting compounds and measured Na-

Fluo transport in all 11 human OATPs in the presence of these drugs. As shown on **Figure 2.10**, the transport activity of each OATP could be altered by at least one compound. Cyclosporin A inhibited OATP-mediated Na-Fluo transport in cells expressing OATP1B3, OATP1A2, OATP2A1 and OATP2B1. Prostaglandin E_2 decreased the Na-Fluo uptake in cells expressing OATP1A2, OATP1C1, OATP2A1, OATP2B1 and OATP4C1. Strikingly, estradiol-17β-glucuronide and ursolic acid enhanced the OATP-mediated transport for several members of the OATP family.

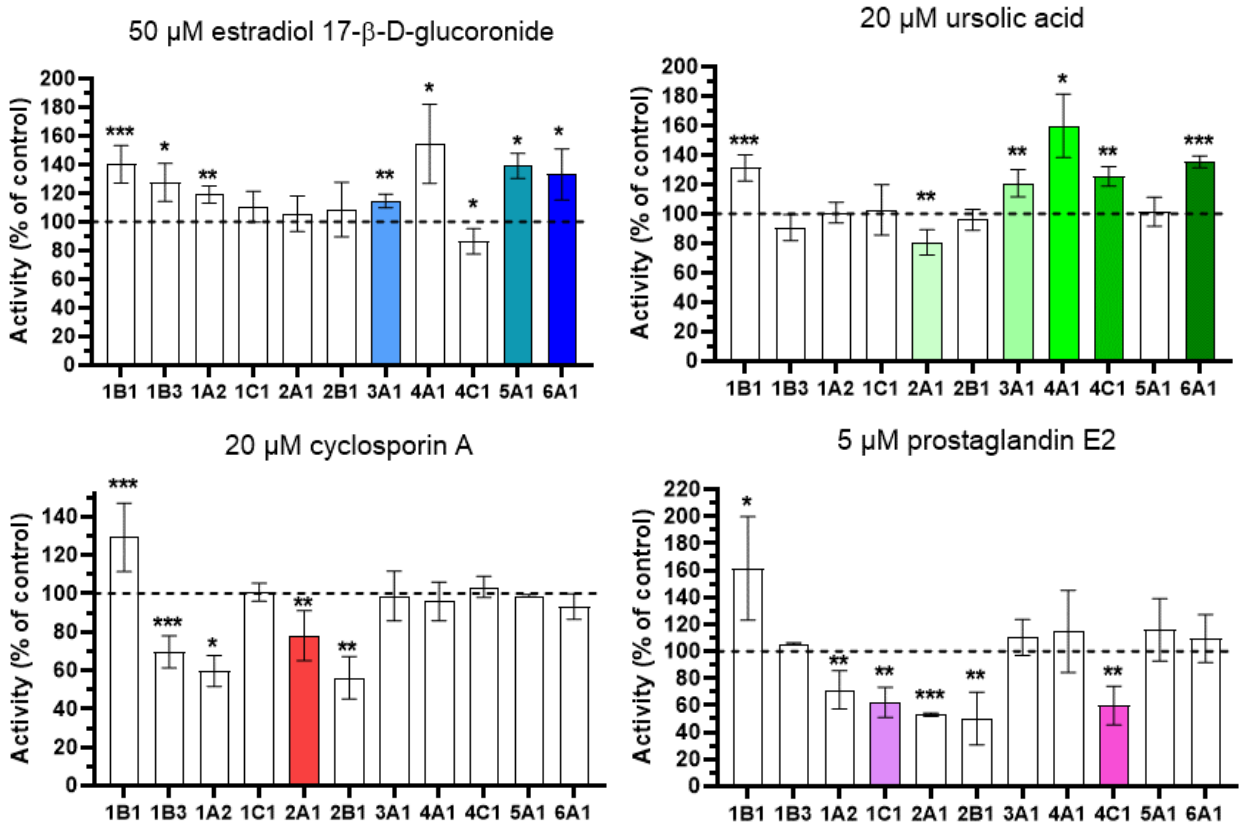

Figure 2.10 Sodium-fluorescein uptake is changed by a variety of compounds. Sf9 cells were incubated with 1 µM Na-Fluo at pH 5.5 for 10 min in the presence of estradiol-17β-glucuronide, ursolic acid, cyclosporin A or prostaglandin E_2. Baseline Na-Fluo uptake represented as 100% (dashed line), columns are showing transporter activity altered by the OATP-interacting compound as a percentage of baseline fluorescence. Colored bars indicate newly defined interactions. Significance: *$p < 0.05$, **$p < 0.01$, ***$p < 0.001$

The stimulatory effect of the compounds can be explained by allosteric activation or by co-transport. Allosteric activation was described earlier for OATP2B1 (where progesterone enhanced the OATP2B1-dependent pregnenolone sulfate transport) [194] and for OATP1B1 and OATP1B3 where pravastatin uptake was further stimulated by non-steroid anti-inflammatory drugs (NSAIDs) [195]. Allosteric activation could be an important contribution to the transporter-mediated DDIs and

demonstrates that a drug doesn`t necessarily have to act as an inhibitor or substrate to modulate the transport activity.

Additionally, as OATP1A2, OATP1B1 and OATP2B1 were able to transport Fl-MTX, we measured Fl-MTX accumulation in the presence of these previously described OATP-interacting compounds. As **Figure 2.11** shows; cyclosporin A, ursolic acid, bile acids, prostaglandin E_2, methotrexate and Imatinib inhibited the OATP-mediated Fl-MTX uptake.

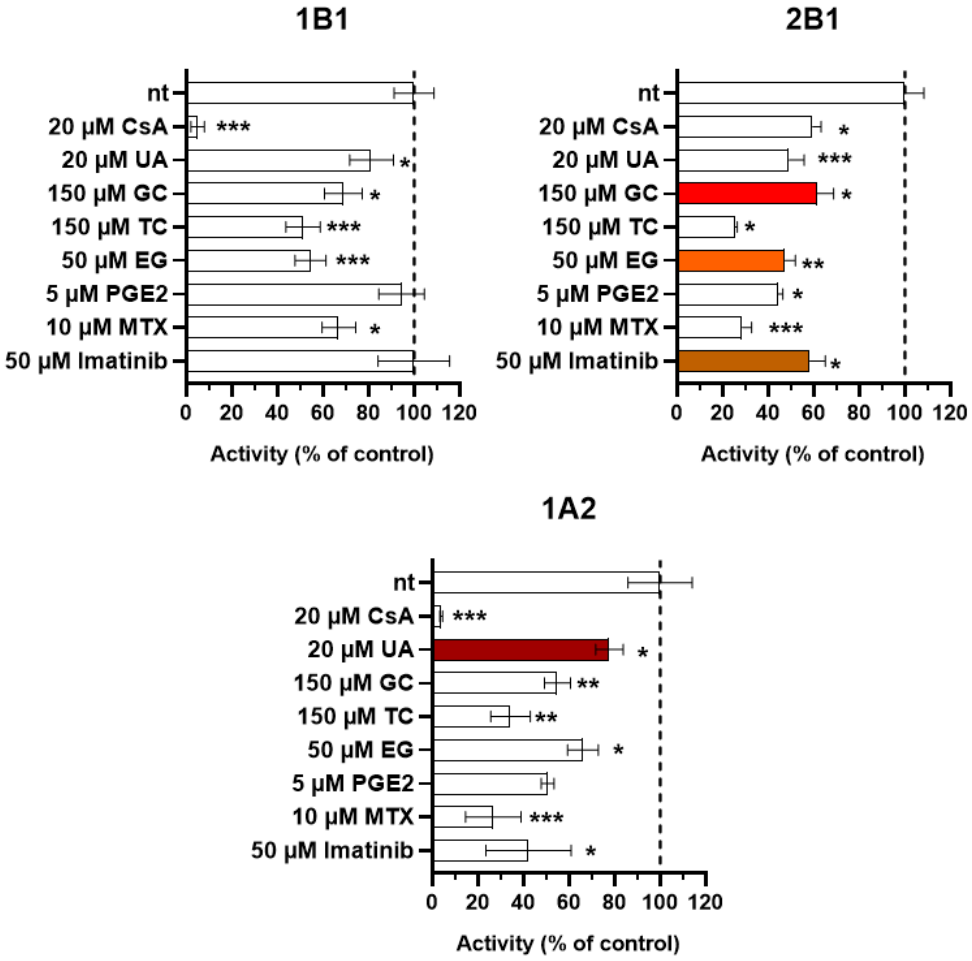

Figure 2.11 Fluorescein-methotrexate uptake inhibited by a variety of compounds. Sf9 cells were incubated with 1 µM Fl-MTX at pH 6.5 for 10 min in the presence of cyclosporin A (**CsA**), ursolic acid (**UA**), glycocholate (**GC**), taurocholate (**TC**), estradiol-17β-glucuronide (**EG**), prostaglandin E_2 (**PGE2**), methotrexate (**MTX**) and **Imatinib**. Baseline Fl-MTX uptake values measured without the compounds represented as 100% (dashed line and **nt**). Columns show activity as a percentage of baseline uptake. Measurements were repeated at least 4 times, data shows average ±SD values. Colored bars indicate novel OATP-interactions.

In summary, optimizing the assay conditions helped us to describe new interactions between OATPs and drugs or naturally occurring compounds (colored bars on **Figure 2.10** and **Figure 2.11**). These findings are nice additions to the hitherto described OATP-interacting compounds. Furthermore, we

were able to show interactions for poorly characterized members of the OATP-family, such as OATP5A1 and OATP6A1. So far OATP5A1 was only demonstrated to transport quercetin [120], but with our functional assay, we detected interaction with estradiol 17-β-D-glucuronide. OATP6A1, whose function and substrate profile remains unknown, showed altered Na-fluorescein uptake in the presence of estradiol-17β-glucuronide and ursolic acid (pentacyclic triterpenoid found in fruit rind).

2.4 Discussion

There is growing evidence that OATPs are important contributing factors in drug disposition and their function is also altered by widely marketed drugs. Given the absence of suitable functional assays, most members of the human OATP family remain poorly characterized. So far, the main hurdles have been the limited availability of radioactively- and fluorescently labeled substrates and the lack of cell-based models to investigate OATP-function. In this current study, we established an insect cell-based fluorescent transport assay which is suitable for the functional expression of all human OATPs and for OATP-drug interaction screens. The main benefit of using insect cells compared to mammalian expression systems is the relatively high level of protein expression levels, therefore lower background transporter activity. Although OATP2B1 expressed in insect cells was shown to transport [^{3}H] estrone-3-sulphate before (Tschantz et al., 2008) [151], our assay provides the first comprehensive system to express all human OATPs. It is important to emphasize before we highlight the main advantages of this system; with this approach, our target proteins are transiently expressed and the baculovirus infection eventually leads to the death of our cells. However, choosing the right time point where the cells are still viable and our protein is expressed in high levels, we can measure the OATP-mediated intracellular accumulation of fluorescent test substrates. One could also argue that the proteins expressed in the Sf9 insect cell system are only core glycosylated [165], therefore they might not be fully functional. To assess this concern, we used known OATP substrates to test the transport activity of OATP1B1 and OATP1B3, the two best-characterized members of the family. They both showed saturable, inhibitor sensitive uptake of Na-fluorescein and fluorescein-methotrexate (**Figure 2.3, 2.4 and 2.5**) comparable to the data measured in mammalian cells [131,132] further validating the applicability of this method.

Using the same expression system has its unique advantage; it allows a systemic comparative study of OATPs without having to consider the varying assay conditions and the different cellular models used by other laboratories.

The pH-sensitive transport activity of human OATPs was proven by several other groups in the past. Being able to respond to changes in the microenvironment might be a way to regulate transporter function. We also investigated the pH-dependent transport activity of OATP1B1 and OATP1B3 and we found that the optimal condition for Fl-MTX transport is at pH 7.4, while Na-Fluo transport is increased with an acidic extracellular milieu (**Figure 2.7, 2.8 and 2.9**). Other OATPs exhibited lower Na-Fluo transport at neutral pH. However, they all showed a significant increase in Na-Fluo uptake at pH 5.5, further demonstrating that Na-Fluo is a pan-OATP substrate. Fl-MTX transport is less affected by changing the pH. There are attempts to explain why a low extracellular pH could influence transporter activity. OATPs (except OATP1C1) have a conserved pH-sensitive histidine (His) in the 3rd transmembrane domain which could serve as a pH sensor. Leuthold et al. demonstrated that the transport activity of OATP1C1 lacking this His is not activated by acidic pH [40]. In contrast to this, in my work OATP1C1-mediated Na-Fluo transport was activated by a lower proton gradient. In addition, the most recent publication of our laboratory also showed an increased transport of the fluorescent viability dye Live or Dye 488 by OATP1C1 at pH 5.5 compared to pH 6.5 or 7.4 [140]. Therefore, pH may have various influence on the transport depending on the substrate used.

The primary goal for less-characterized OATP-family members would be the identification of physiological substrates and exogenous compounds that might interfere with their function. Our functional assay may serve as a new tool to achieve this goal. Here we have shown this system is suitable for the identification of new substrates and molecular interactions. We validated our assay by reconfirming previously published interactions between OATP1A2, OATP1B1, OATP1B3 and OATP2B1 with bile acids, cyclosporin A, prostaglandin E_2 and methotrexate (**Figure 2.5, 2.10 and 2.11**). Moreover, we also identified new molecular interactions between ursolic acid and OATP1A2, OATP2A1, OATP3A1, OATP4A1 and OATP6A1, cyclosporin A and OATP2A, estradiol-17β-glucuronide and OATP3A1, OATP5A1 and OATP6A1, prostaglandin E_2 and OATP1C1 and OATP4C1 (**Figure 2.10 and 2.11**). These findings might suggest new roles in hormone transport for OATPs, 3A1, 5A1 and 6A1. As OATPs show ectopic expression in several tumors they might affect the survival of hormone-dependent tumors [64].

This assay also revealed surprising interactions. Contrary to De Bruyn et al., we saw significant OATP2B1-mediated Na-Fluo transport at pH 7.4 [131] (**Figure 2.7**). Interestingly, Na-Fluo transport at pH 5.5 in OATP1B1 was stimulated rather than inhibited by cyclosporin A, estradiol-17β-glucuronide, prostaglandin E_2 and ursolic acid (**Figure 2.10**). This effect appears to be pH-specific, as these compounds inhibited Na-Fluo uptake at pH 7.4 (**Figure 2.5**). In other experiments, we observed a

similar, pH-dependent stimulation in Fl-MTX transport by several known interacting compounds (data not shown). Correspondingly, we saw a similar activating effect by estradiol-17β-glucuronide on OATP3A1, 5A1, 6A1-mediated Na-Fluo transport activity, and ursolic acid on OATP3A1, OATP4A1, OATP4C1 and OATP6A1 transport (**Figure 2.10**). This data suggests that transport activity is allosterically controlled, as previously documented for OATP1B3 and OATP2B1 [194,195].

However, it is important to point out that our system cannot reveal the true mechanism of this substrate-dependent interaction even though several compounds can seemingly inhibit or stimulate the uptake of our test substrates with different degrees of interaction. This might be explained by the level of interaction between the compounds and OATPs' two binding sites [132]. Consequently, the transport of the potential substrates should be tested by direct transport measurements e.g. by using mass spectrometry or radioactively labeled substrates.

In summary, we developed a new cell-based assay which can be used to express human OATPs and may be applicable for inhibitor and substrate screening and to assess risk for possible drug-drug interactions. It might also be a new tool to compare pharmacologically relevant OATP variants and elucidate structure-function relationships.

Chapter III

Identification of novel cell-impermeant fluorescent substrates for testing the function and drug interaction of Organic anion transporting polypeptides, OATP1B1/1B3 and 2B1

(The majority of work presented in this chapter has been published in Patik et al., Scientific Reports (2018)[142])

3.1 Abstract

OATP1A2, OATP1B1, OATP1B3 and OATP2B1 have been shown to have multispecific transport capabilities as they transport not only endogenous substrates (bile acids, bilirubin and hormones) but a wide range of pharmacologically relevant compounds (e.g. statins, antibiotics, antivirals and chemotherapeutics). OATP1B1 and OATP1B3 are known to mediate drug-drug and drug-food interactions, leading to altered pharmacokinetics and unexpected toxicity; while the pharmacological role of the ubiquitously expressed OATP2B1 is less well characterized.

Testing the interaction between a new molecular entity and OATP1Bs is recommended at the initial stages of drug development. In broad terms, the strategy to study OATPs has been based on radiolabeled substrates. However, radioactive isotopes are continuously challenged by a new generation of fluorescent labels. Fluorescent substrates eliminate the hazards associated with the use of radioactive compounds, the resulting laboratory waste doesn't require special disposal, therefore it is safer to use. Fluorescent substrates are better suited for OATP-drug screens; even more in high-throughput setups, given their relatively low cost, similar or even higher sensitivity and greater flexibility in multicolor labeling.

There were attempts to set up fluorescent substrate-based transport assays to measure OATP1B1 and OATP1B3 transport function and drug interactions [55,131,196]; however, these do not necessarily meet high-throughput drug screening criteria, and a fluorescence-based screening assay for OATP2B1 is entirely missing.

The following research provides an alternative framework to study OATP-drug interactions. We describe novel, pH-independent, fluorescent substrates for OATP1B and OATP2B1 with minimal passive cellular uptake and high signal to noise ratio. We show the OATP-mediated uptake of commercially available fluorescent dyes including Zombie Violet, Live/Dead Violet, Live/Dead Green, Cascade Blue and Alexa Fluor 405. The uptake measured in cells expressing hepatic OATPs

are time and concentration-dependent and sensitive to inhibitors. Furthermore, our results strongly suggest that Live/Dead Green can be utilized for OATP function-based sorting. This method could be a new tool for the selective enrichment of OATP proteins in different cell lines.

The fluorescence-based transport assay measuring the uptake of the best-performing substrates opens the way to the development of sensitive high-throughput assays for the detection of OATP drug interactions. Development of experimental strategies such as this may assist in explaining different aspects of OATP function and help gaining a deeper and more comprehensive understanding of the pharmacokinetics of drugs.

3.2 Materials and methods

3.2.1 Materials

Fluorescent dyes: Zombie dyes (Violet and Green) were bought from Bio Legend® (San Diego, CA, US). LIVE/DEAD® Fixable Cell Stain Dye panel, Cascade Blue hydrazide, Alexa Fluor 405 succinimidyl ester were bought from Thermo Fischer Scientific (Waltham, MA, US), and fluorescein-methotrexate triammonium salt from Biotium (Hayward, CA, US). Restriction endonucleases were from New England Biolabs Ltd. (Ipswitch, MA, US). All other materials, if not indicated otherwise, were purchased from Sigma Aldrich, Merck (Budapest, HU).

3.2.2 Generation of plasmid constructs

Generation of baculovirus expression vectors (pAcUW21-L/OATP and pAcUW21-control) was described in **Chapter II**. OATP2B1 expressing cells were generated with transposase mediated genomic insertion of the OATP2B1 cDNA (BC041095.1, HsCD00378878). OATP2B1 cDNA was amplified (Phusion1 High-Fidelity PCR Kit, NEB, Ipswitch, MA, US) from the vector ordered from Harvard PlasmID Repository (Harvard Medical School, Boston, MA, US) by using the following primers: forward 5': GTAAAT GCGGCCGC AA GAATTC GCCACCATGGG ACCCAGGATAGG and reverse 5' GTACAT GCGGCCGC T AAGCTT TCACACTCGGGAATCCTC. The PCR fragment was cloned between the NotI-HindIII sites of the pSB-CMV vector [197].The cDNAs of OATP1B3-V1 and OATP1B3-ct were amplified by HF PCR from the pAcUW21-L/OATP1B3wt vector using the following forward primers:
5' ACTAGTTTAAACGCCACCATGTTCTTGGCAGCCCTG (OATP1B3-V1), ACTAGTTTAAACGCCACCATGAAAATTTCCATCACT (1B3-ct) and reverse primer 5' GTACATGCGGCCGCACTGCAGTTAGTTGGCAGCAGCATTGTC. After digestion with PmeI and PstI restriction enzymes the PCR fragments were cloned to the corresponding sites of the pRRL-CMV-MCS-IRES-ΔCD4 vector (). The base order of the cDNAs in all constructs was verified by sequencing.

OATP1B1 and OATP1B3, OATP1B3 V1 overexpressing mammalian cells were created by lentivirus transduction. The lentiviral vector (pRRL-CMV-MCS-IRES-ΔCD4) was generated by replacing the GFP sequence with a multicloning site of the pRRLSIN.cPPT.PGK-GFP.WPRE (Addgene #12252) plasmid (Didier Trono, Lausanne, Switzerland). An IRES (Internal ribosome entry site) was cloned between the PmlI and XbaI sites of the MCS (forward: 5'-ACACGTGTCCGGACTAGTCCACCTTGCC TTACACATGAAGAG, reverse: 5'-

ATCTAGAATGATCAGCCATATTATCATCGTGTTTTTCAAAG). The plasmid also contains a truncated CD4 receptor sequence enabling to monitor the virus transfection. Truncated CD4 cDNA was PCR amplified by the following primers (based on Liu et al. [198]: 5'-GATTCTAGAGCCACCATGAACCGGGGAGTCCCTTTTAGGC and 5'-GTAGTCGACTTAGCGCCTTCGGTGCCGGCAC from the pCMV-SPORT6-CD4 (Harvard Plasmid Repository). After digestion with XbaI-SalI enzymes, the PCR fragment was cloned to the corresponding sites of the pRRL-CMV-MCS-IRES vector. The open reading frames of OATP1B1 (Gene ID: AB026257) and OATP1B3 (BC141525, HsCD00348132) were amplified by HF PCR (Phusion1 High-Fidelity PCR Kit, NEB, Ipswitch, MA, US) from the pAcUW-21-L/ OATP1B1-wt vector and from the plasmid obtained from Harvard PlasmID, respectively, using the following primers: OATP1B1: forward 5' TATTATTCGAAGCCACCATGGACCAAAATCAACAT, reverse 5' CATGTAACTAGTTTAACAATGTGTTTCACTATCT. OATP1B3: forward 5' ACTAGTTTAAACGCCACCATGGACCAACATCAACAT and reverse 5' GTACATGCGGCCGCACTGCAGTTAGTTGGCAGCAGCATTGTC. After cleaving with BstBI and SpeI (OATP1B1) or PmeI-PstI (OATP1B3) the PCR fragments were cloned to the corresponding sites of the pRRL-CMV-MCS-IRES-ΔCD4 vector. The sequence of the cDNAs in the final vector was verified by sequencing. Empty vectors (pSB-CMV and pRRLdCD4) were used as negative controls (indicated as mock on the figures).

3.2.3 Expression in insect cells

Transient expression of human OATP1B1, OATP1B3 and OATP2B1 in Sf9 (*Spodoptera frugiperda*) cells was accomplished as described in **Chapter II**. Baculovirus infected Sf9 cell were collected 36–40 hours post-infection and were used for transport measurements.

3.2.4 Generation of mammalian cell lines.

A431, MDCKII, HEK293T cells (ATCC) were transfected with 1 μg plasmid DNA (OATP2B1) + 100 ng plasmid containing the transposase [197,199] using Fugene HD reagent (Promega, Madison, WI, US) following the supplier's protocol. 48 h following transfection, we added puromycin (1 μg/ml) to the media. After 14 days of selection with puromycin, cells were kept in DMEM (Gibco, Thermo Fischer Scientific, Waltham, MA, US) supplemented with 10% fetal calf serum, 2 mM L-glutamine, 100 U/ml penicillin, and 100 μg/ml streptomycin at 37°C with 5% CO_2 and 95% humidity, without puromycin. OATP1B1 and OATP1B3 overexpression in A431,HCT 8, HCT 116 cells were achieved by recombinant lentiviruses as described in Tatrai et al. [200]. Briefly, HEK-293 T human embryonic

kidney cells (1.8×10^6 cells were plated onto 60mm X15mm Petri dishes) were transfected with (6 μg) pRRL-CMV-MCS-IRES-ΔCD4/OATP1B1 or OATP1B3, 2.2 μg pMDG and 4 μg psPax2 vectors[200] using $CaPO_4$ precipitation. The supernatant, containing lentiviral particles was collected 72 h following transfection. Using the supernatant, A431, HCT 8 and HCT 116 cells were transfected with the virus. Cells were kept in DMEM (A431) or RPMI (HCT 8, HCT 116) (Gibco, Thermo Fischer Scientific (Waltham, MA, US)) supplemented with 10% fetal calf serum, 2 mM L-glutamine, 100 U/ml penicillin, and 100 μg/ml streptomycin at 37°C with 5% CO_2 and 95% humidity. The multiplicity of infection was approximately 1.

3.2.5 Determination of dye uptake with flow cytometry

Uptake measurement were carried out as described in Chapter II, using the uptake buffer (125 mM NaCl, 4.8 mM KCl, 1.2 mM CaCl2, 1.2 mM KH2PO4, 12 mM MgSO4, 25 mM MES, and 5.6 mM glucose, with the pH adjusted to 8.5, 7.4, 6.5, 5.5 or 4.5 using 10 N NaOH or 1 M HEPES) in a final volume of 100 μl. The exact concentrations and incubation times are indicated in the Figure legends. Viability dyes were reconstituted with DMSO following the manufacturers' protocols. The reaction was stopped by adding 1 ml ice-cold phosphate-buffered saline (PBS). The cells were kept on ice until flow cytometry analysis. The fluorescence of min. 20,000 live cells were measured using an Attune Acoustic Focusing Cytometer (Applied Biosystems, Life Technologies, Carlsbad, CA, US). Dead cells were excluded by propidium iodide (PI, 1 μg/ml) positivity. Functional data represents the mean of at least 3 independent experiments done on different days. In the case of A431 cells, cells were collected after trypsinization (0.1% trypsin) and the uptake experiments were performed in the same way as described for insect cells (**Chapter II**). Histogram figures were generated by the FCS Express software.

3.2.6 96-well microplate-based assay.

OATP-expressing A431 cells were plated (6×10^4 cells in 200 μl final volume/well) onto 96-well plates and grown for 16–24 h at 37°C, 5% CO_2. The supernatant was removed the following day and the cells were washed 3-times with 200 μl of PBS. When we used inhibitors, the cells were pre-incubated with the inhibitors (dissolved in DMSO) for 5 min at 37°C (usually in 50 μl volume). The amount of DMSO was kept below 0.5% throughout the study. Side note: this amount of the solvent did not influence the fluorescence of the dyes. The reaction was started with the addition of 50 μl fluorescent dye (1–40 μM final concentration or 0.05 μl–1.2 μl in a final volume of 100 μl) and the plate was

incubated at 37°C for 2–30 minutes. The reaction was stopped by adding 200 µl ice-cold PBS. The supernatant was immediately removed, and then, the cells were washed 3-times with 200 µl ice-cold PBS. Lastly, 200 µl PBS was added to the cells and fluorescence was measured at room temperature using an Enspire fluorescent plate reader (Perkin Elmer) at wavelengths indicated in **Table 3.1**.

3.2.7 Cell sorting

Cells were sorted based on Live/Dead Green (LDG) positivity (this dye labels dead cells and cells when it gets taken up by OATP-mediated transport). Briefly, cells expressing OATP1B1, OATP1B3 or OATP2B1 (2–4 × 10^6 cells/sample) were incubated with 0.8–1.2 µl LDG in 100 µl uptake buffer (sterile filtered), pH 5.5 at 37°C for 30 minutes. Cells were washed with 1 ml DMEM and centrifuged at 300 g for 4 minutes. After removing the supernatant, cells were resuspended in 500 µl DMEM. Cellular fluorescence was measured using a BD FACSAria III Cell sorter (BD Biosciences, San Jose, CA, US). Cells with the highest fluorescence (see the applied gate ("LDG+") on **Figure 3.1**) were sorted for further analysis. Cells kept in culture for maximum 20 passages were used for the experiments.

3.2.8 Western blot

Whole-cell lysates of Sf9 or A431 cells (10–50 µg) were separated on 7.5% Laemmli SDS-PAGE gels. Protein transfer to PVDF was performed using the Bio-Rad miniProtean 3 system. Protein concentrations were determined using the Lowry method using BSA as standard. PNGase F (New England BioLabs) digestions were carried out following the manufacturer's protocol. Membranes were incubated overnight with polyclonal antibodies. The antibodies used for the detection of OATP1B1 and OATP2B1 were kind gifts from Dr. Bruno Stieger (Department of Clinical Pharmacology and Toxicology, University Hospital, 8091 Zurich, Switzerland) [139]. Other antibodies were anti-β-actin (A1978, Sigma) and anti-OATP1B3 (AMAb9123, Atlas Antibodies, Stockholm, Sweeden). After O/N incubation, PVDF membranes were incubated with 10,000–20,000x diluted HRP-conjugated anti-rabbit or anti-mouse secondary antibodies (Jackson ImmunoResearch, Suffolk, UK) for 1h. Luminescence was detected using the Luminor Enhancer Solution kit by Thermo Scientific (Waltham, MA, US).

3.2.9 Immunofluorescent staining and confocal images

Cells (2 x 10^5) were seeded onto 8 well µ-Slide (Ibidi, 80826) and cultured for 16-24 h at 37°C, 5% CO_2. Cells were washed twice with 300 µl PBS and fixed with 100 µl 4%PFA-PBS for 15 min and washed three times with 300 µl PBS. Cells were blocked in PBS supplemented with 0.5% BSA, 0.5 % fish gelatin, 0.1% Triton-X and 5 % goat serum for 1 h at RT. Then, the primary antibody was added, and cells were incubated at 4°C O/N. The slides were washed with PBS 3 times the following morning and incubated with the secondary antibody for 1h at RT. On the end, the slides were washed 4 times with PBS and kept in PBS+ 0.1% sodium-azide solution until microscopy. Fluorescence was imaged by Zeiss LSM 710 confocal microscope with 40x oil immersed objective. Images were captured and analyzed by Zen 2 (Blue edition) Software.

3.2.10 Toxicity testing

5×10^3 A431 cells were seeded onto 96-well plates in a final volume of 100 µl DMEM. The following day, the cells were washed with PBS and 0.4 or 1.6 µl Live/Dead Green or Zombie Violet was added/5×10^5 cells in a 100 µl final volume of uptake buffer. After 30 min of incubation, the cells were washed twice with PBS, and 200 µl DMEM was added to the cells. 144 hours later, the viability of the cells was determined with PrestoBlue (Thermo Fischer Scientific) assay. Briefly, the medium was removed, and cells were incubated for 60 mins at 37°C in 100 µl 5% PrestoBlue in PBS. Absorbance was detected at 583 nm with an Enspire fluorimeter (Perkin Elmer). Cells incubated with the uptake buffer alone served as control. Background signal was calculated by absorbance measured in empty wells filled with 5% PrestoBlue.

3.2.11 Data analysis and statistics

Z-factor was calculated as follows: $1-((3\times SD_{\text{negative control}}\ 3\times SD_{\text{positive control}})/(Mean_{\text{positive}}-Mean_{\text{negative}}))$ based on Zhang et al. [201]. Kinetic parameters of dye uptake or inhibition were analyzed by Hill fit curve fitting using the GraphPad Prism 8 software. Statistical significance was calculated by Student's t-test. The p value for statistical significance was set at 0.05 (*), 0.01 (**) or 0.001 (***).

3.3 Results part I-Assay development

3.3.1 Zombie Violet is a novel substrate for human OATP1B1, OATP1B3 and OATP2B1

As our aim was to find better fluorescent substrates for the hepatic OATPs, we reviewed the literature in search for dyes with low membrane permeability and pH independent fluorescence. Viability dyes seemed to fit these characteristics, as they show low membrane permeability. Furthermore, repurposing commercially available viability dyes for studying transporter function was shown before; as Calcein, an acetoxymethyl ester (AM) derivative has been used extensively to study P-glycoprotein (ABCB1) and MRP (ABCC) function [192]. As described in **Chapter II**, we have developed an insect cell-based assay to measure OATP-transporter activity. Therefore, we used this system to screen potential substrate candidates. Measuring the cellular uptake of an amine-reactive fluorescent viability dye, Zombie Violet (**ZV**) in OATP1B1 expressing cells turned out to be our first promising hit. To distinguish staining between dead cells and transporter-mediated dye uptake, we counterstained the cells with propidium-iodide (**PI**). Comparing control cells to OATP1B1 expressing cells, we observed marked differences in the stained cell populations. While control cells stained with ZV were always accompanied by PI positivity, OATP1B1 expressing cells showed two separate subpopulations: one ZV positive and PI negative and one double-positive indicating that ZV can penetrate the cells via OATP-mediated uptake (**see Figure 3.1**). Further measurements confirmed that ZV uptake is mediated by OATP1B1 function, and the transport showed saturable and inhibitor-sensitive uptake (**Figure 3.2**). It needs to be noted here, that the chemical structure of the viability dyes, including ZV could not be obtained from the supplier, hence Km values for the viability dyes cannot be determined.

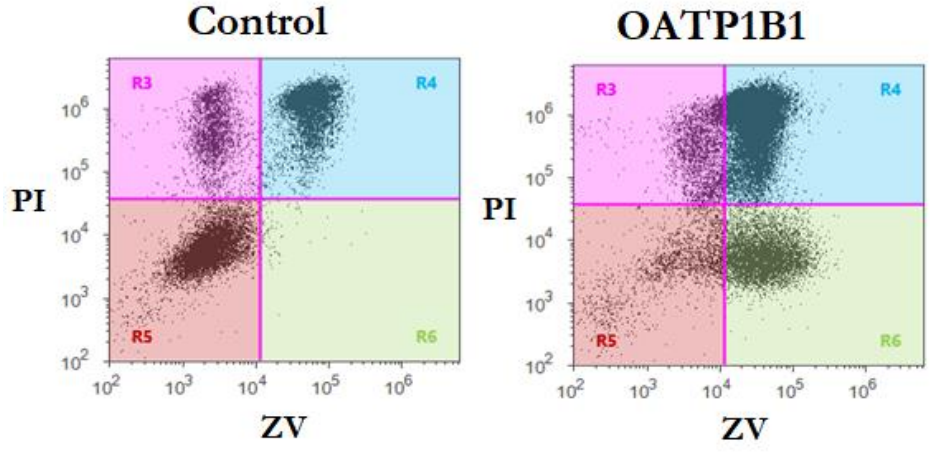

Figure 3.1 ZV uptake in Sf9 cells. 0.2 µl dye in 100 µl uptake buffer was measured at 37°C in pH 5.5 uptake buffer for 15 min. Dead cells were identified by PI positivity. One representative experiment is shown.

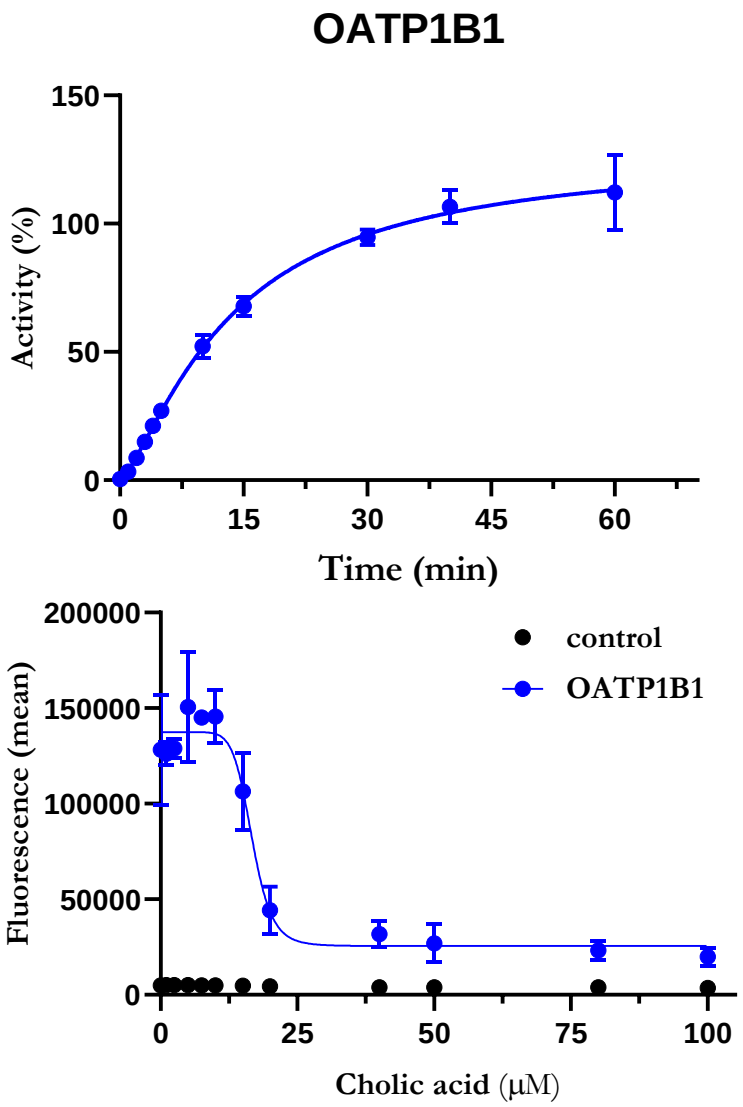

Figure 3.2 <u>**Upper panel:**</u> **Time-dependent ZV uptake in Sf9 cells expressing OATP1B1.** Uptake rates were normalized to the fluorescence values measured for OATP1B1 (minus the fluorescence in control cells) incubated with 2 μl ZV for 30 min. <u>**Lower panel**</u>*:* **OATP1B1-mediated transport inhibited by cholic acid** (a known inhibitor of OATP1B1 function). Intracellular accumulation of 0.1 μl ZV/ $5x10^5$ cells in 100 μl was measured with increasing concentrations of cholic acid (0.1–100 μM) for 20 min. Data show the means ± SD of 3 independent experiments. Sf9 cells overexpressing an unrelated protein were used as control (see **Chapter II-Methods**).

In the next set of experiments, we tested whether any other human OATP would show transporter-mediated ZV uptake. We found that OATP1B3 and OATP2B1 expressing Sf9 cells were also able to mediate ZV uptake, although to a lesser degree (**Figure 3.3**). Since the expression levels of the different human OATPs cannot be compared in the lack of a pan anti-OATP antibody, it cannot be defined whether these differences in the transport rate are due to different expression levels or due to differences in the affinity toward ZV.

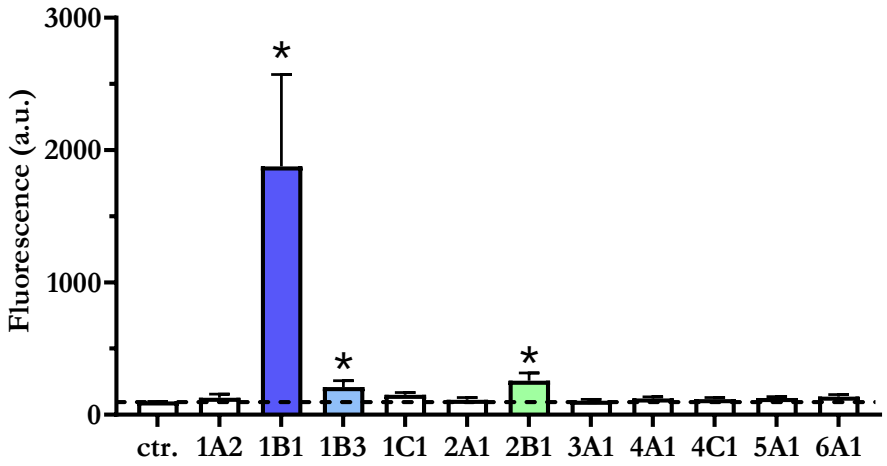

Figure 3.3 Zombie Violet (ZV) uptake measured in Sf9 cells expressing human OATPs. Cells were incubated with 0.2 µl/100 µl uptake buffer adjusted to pH 5.5 for 30 min at 37°C. Control cells (**ctr.**) were expressing an unrelated protein [136]. Average of at least three independent measurements with duplicates ±SD values are shown. Student t-test were used to determine significance, *p< 0.05

As OATP1B1, OATP1B3 and OATP2B1 were able to transport Zombie Violet in our preliminary screens we further characterized the uptake. The transport in these cells was sensitive to the pH-**Figure 3.4**). The highest OATP-mediated transport rate was observed at pH 5.5 for all three transporters which we were able to inhibit with previously described OATP-interacting compounds (**Figure 3.5**). Furthermore, OATP1B1 and OATP1B3 demonstrated transport at pH 7.4, while OATP2B1 stayed inactive at neutral pH. No transport could be observed at pH 8.5. These experiments demonstrated that Zombie Violet is a bona fide OATP1B1, OATP1B3 and OATP2B1 substrate.

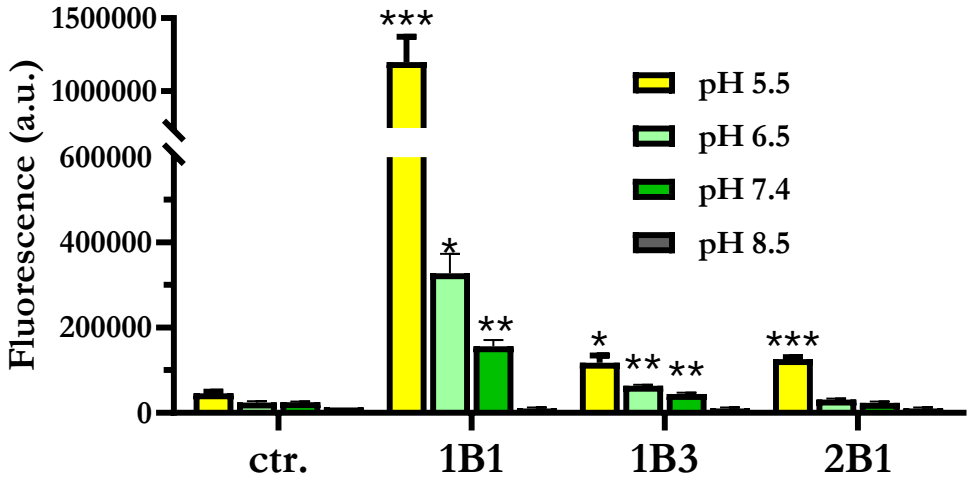

Figure 3.4 pH dependent ZV uptake in Sf9 cells. Cells were incubated with 0.2 µl ZV/5x10^5 cells uptake buffer adjusted to pH 5.5 for 10 min at 37°C. Control cells (**ctr.**) were expressing an unrelated protein [136]. Bars

represent the average of three independent experiments ±SD values. Significance: $p < 0.05$ (*), $p < 0.01$ (**) or $p < 0.001$ (***).

Besides, we also tested two other fixable amine-reactive viability dyes, Zombie Green (**ZG,** Bio Legend) and Live/Dead Green (**LDG**, Life Technologies). Although ZG was not transported by OATPs, we found that LDG was a substrate of OATP1B1, OATP1B3 and OATP2B1 (**Figure 3.6)**.

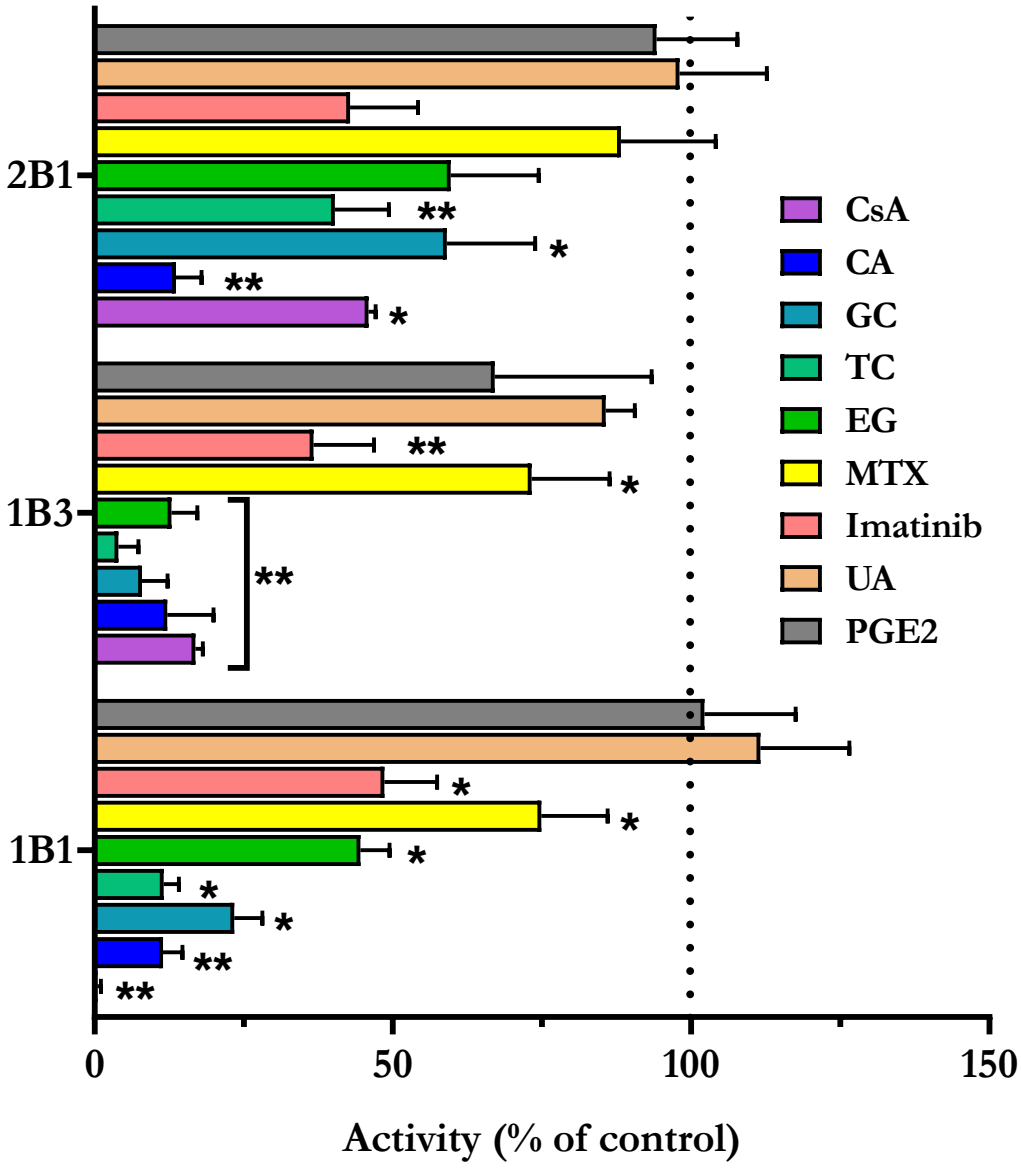

Figure 3.5 Inhibition of ZV uptake in Sf9 cells expressing OATP1B1, OATP1B3 or OATP2B1. Uptake of 0.2 µl ZV/5x10^5 cell was measured in the absence or presence of the following compounds after 30 min incubation in uptake buffer pH 5.5 at 37°C: 20 µM cyclosporin A (**CsA**), 150 µM cholic acid (**CA**), 150 µM glycocholic acid (**GC**), 150 µM taurocholate (**TC**), 50 µM estradiol 17-β-D-glucuronide (**EG**), 10 µM methotrexate (**MTX**), 50 µM **imatinib**, 20 µM ursolic acid (**UA**), 5 µM prostaglandin E_2 (**PGE2**). Fluorescence measured in control cells (**ctr.**) expressing an unrelated protein [136] were subtracted. Transport measured in cells

with ZV alone was set 100% and the effect of the compounds was compared to this value. Bars represent the average of three independent experiments ±SD values. Significantly different from the control: *p < 0.05, **p < 0.01.

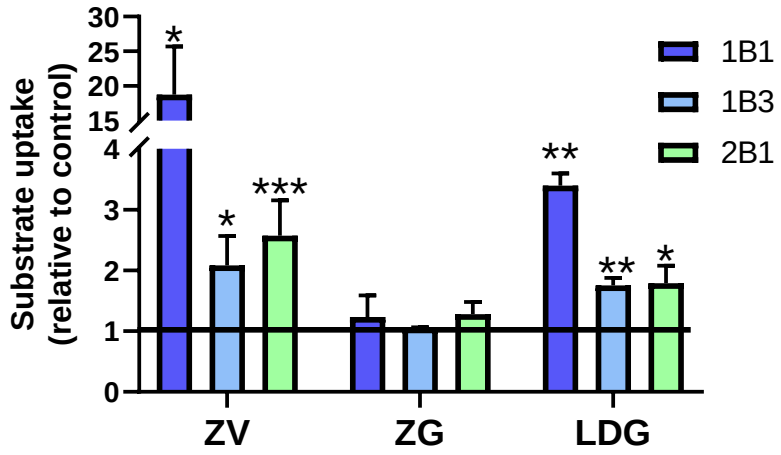

Figure 3.6 ZV and LDG uptake in Sf9 cells expressing OATP1B1, OATP1B3 or OATP2B1. Dye uptake was measured after 30 mins of incubation at pH 5.5, 37°C (0.2 µl dye/ $5x10^5$ cells). Data points represent the average of at least three independent measurements ±SD values. Cells expressing an unrelated protein were used as control. Significance: $p < 0.05$ (*), $p < 0.01$ (**) or $p<0.001$ (***).

3.3.2 Establishment of a novel viability dye-based cell sorting method to create cell lines with high OATP1B1, OATP1B3 and OATP2B1 expression

Although the baculovirus insect cell system proved to be an excellent tool for initial substrate screens, the transient nature of its protein expression is not compatible with high-throughput screening methods (HTS). As our primary goal with this project was to build a robust screening platform to study OATP drug interactions, human-derived cell lines with stable expression of OATP1B1, OATP1B3 or OATP2B1 were required to adapt our transport measurements for a 96-well plate-based setup. We choose A431 cells (human epidermoid carcinoma) because of its strong adherence. Our first attempt to overexpress hepatic OATPs in this cell line resulted in a well-detectable OATP2B1 overexpression. However, regardless of repeated lentiviral transduction, we could only detect low OATP1B1 and OATP1B3 protein levels. If we compared the protein levels between Sf9 cells and A431 cells, we saw apparent differences in the overall OATP expression levels (as shown on **Figure 3.7).**

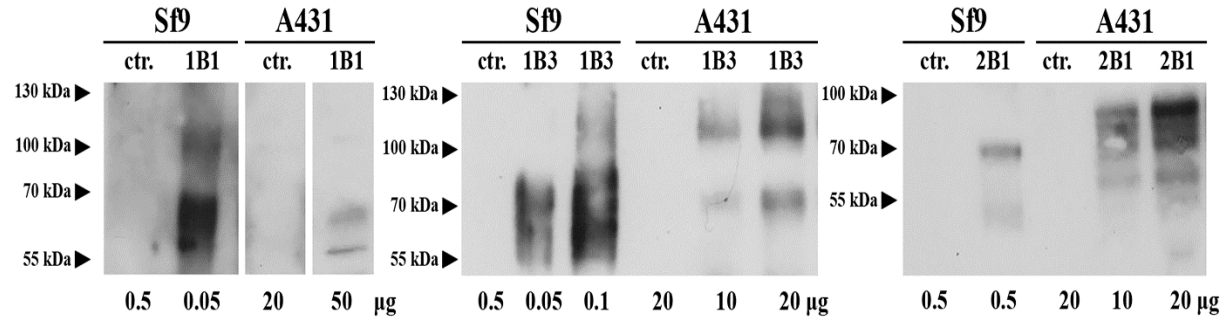

Figure 3.7 Low level of OATP1B expression in A431 cells demonstrated by Western blot. Controls (**ctr**.) represent either Sf9 cells expressing an unrelated protein or mock-transfected A431 cells. Whole-cell lysates were separated on 7.5% Laemmli SDS-PAGE. Different migratory bands most probably represent different glycosylated forms of OATPs.

Subsequently, Fl-MTX (a common hepatic OATP substrate, see more in **Chapter II**) uptake in these cells was low. Additionally, we could only measure convincing Fl-MTX, ZV and LDG uptake in OATP2B1 overexpressing A431 cells (**Figure 3.8a**). Transduction with viral vectors usually results in a high degree of target protein expressing cells, however the transduction efficiency is never 100%. Additionally, the substrate uptake should be proportional to protein expression and function. Thus, we were interested to see if we could identify the subpopulations of cells with elevated OATP expression based on increased substrate accumulation. As LDG didn't seem to be toxic (data not shown here but present in the publication[142]), we sorted cells with the highest LDG signal transduced with OATP1B1, OATP1B3 or OATP2B1. This also included dead cells as they had high LDG signal, but as these cells were dead, they have washed away after the first passage. Sorted cells were then further maintained and grown. These cell populations showed significantly higher OATP expression and improved function compared to the unsorted cells (**Figure 3.8b** and **Figure 3.9**). The expression levels were stable for at least 2 months, about 20 passages. Our results strongly suggest that OATP function-based sorting is possible with LDG. This method could be a new tool for the selective enrichment of OATP proteins in different cell lines.

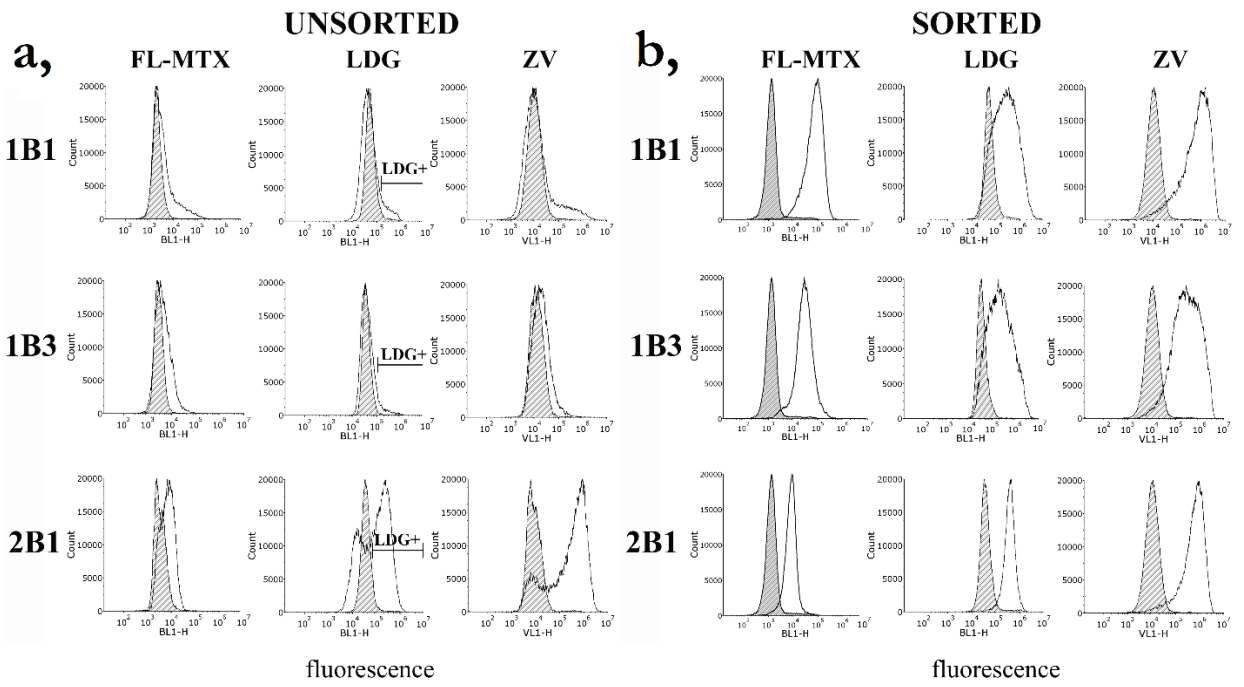

Figure 3.8 Fluorescent substrate uptake in A431 cells. Uptake of 1 μM fluorescein-methotrexate (**Fl-MTX**), 0.4 μl Live/Dead Green (**LDG**) or Zombie Violet (**ZV**)/ 5x10^5 cells were measured before (**a**) and after (**b**) sorting of LDG positive cells. Mock transfected cells were used as controls (indicated by filled histograms). Cells were incubated for 15 min (Fl-MTX) or 30 min (LDG and ZV) at 37°C in pH 5.5 uptake buffer. Dead cells were excluded based on PI staining. This experiment was repeated several times, histograms show the results of one representative experiment.

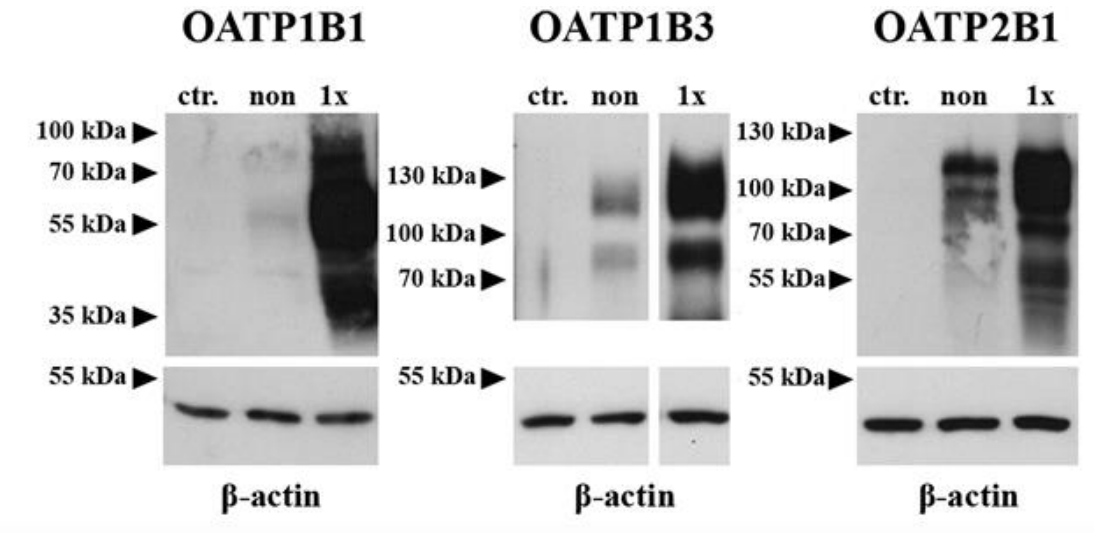

Figure 3.9 Sorting with LDG results in increased OATP protein expression. Controls (**ctr**.) represents mock transfected A431 cells and β-actin serves as an internal control. Whole cell lysates (20 μg each) were separated on 7.5% Laemmli SDS-PAGE. One representative blot is shown. Multiple bands probably represent diverse glycosylation levels of these proteins.

To further demonstrate that our novel method is suitable for OATP function-based sorting, we sorted freshly transduced HEK-293T and MDCKII cell lines. After recovery, the cells were cultured and tested for transporter-mediated substrate accumulation. Ultimately, we obtained cell lines expressing OATP1B1, OATP1B3 or OATP2B1 with measurable transporter activity (**Figure 3.10**). See more examples of the successful application of this sorting strategy later in this chapter.

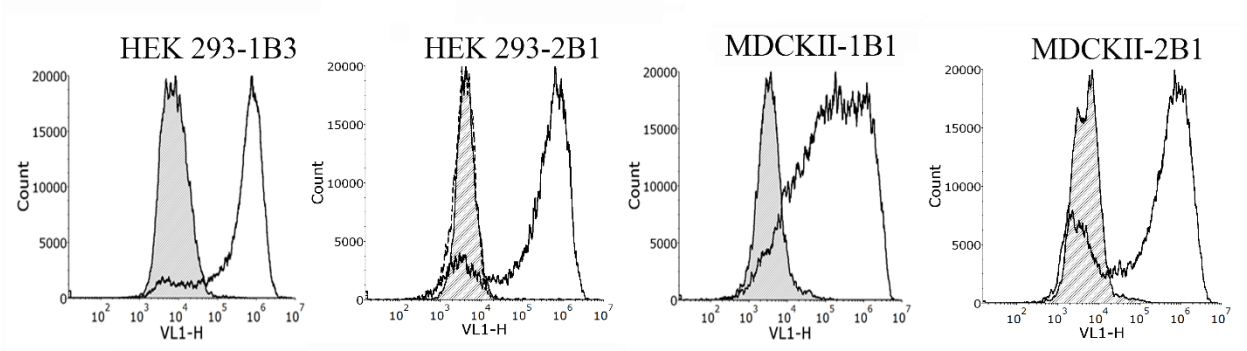

Figure 3.10 Zombie Violet (ZV) uptake in HEK-293 and MDCKII cells expressing OATPs, 1B1, 1B3 or 2B1. Intracellular accumulation of 0.1 µl ZV / $5x10^5$ cells in 100 µl was measured at pH 5.5 for 30 min. Dead cells were excluded based on PI staining (1 µg/ml). Experiments were repeated at least two times. One representative experiment is shown. Filled histograms show fluorescence measured in cells transfected with the empty vector.

3.3.3 A semi-high throughput assay for OATP-drug interaction screens

3.3.3.1 Other commercially available fluorescent substrates for the hepatic OATPs

Our initial hits were from a family of amine-reactive dyes used for live/dead cell discrimination. There are quite a few more commercially available dyes designed for the same purpose. Additionally, we also found other cell impermeant dyes, such as Cascade Blue hydrazide (**CB**) and Alexa Fluor 405 succinimidyl ester (**AF405**). Both of these compounds are used in cell permeability assays and for protein labeling [202]. Thus, we put together a panel of possible substrates and tested whether they show OATP-mediated cellular accumulation (See **Table 3.1** for the tested compounds). We plated the cells on a 96-well plate and tested our candidates under the same conditions used in our flow cytometric experiments.

Distributor	Dye	Abbreviations	Ex/Em optimum (nm)
Bio Legend	Zombie Green	ZG	488/515

	Zombie Violet	**ZV**	**405/423**
Thermo Fisher (Life Technologies)	**Live/Dead Blue**	**LDB**	**350/450**
	Live/Dead Aqua	**LDA**	**267/526**
	Live/Dead Violet	**LDV**	**416/451**
	Live/Dead Yellow	**LDY**	**400/475**
	Live/Dead Green	**LDG**	**495/520**
	Live/Dead Red	**LDR**	**595/615**
	Live/Dead Far-red	**LDFR**	**650/665**
	Live/Dead near-IR	**LDNIR**	**750/775**
	Alexa Fluor 405 NHS ester	**AF405**	**401/421**
	Cascade Blue hydrazide	**CB**	**400/419**

Table 3.1 Fluorescent dyes used in the current study to screen for novel fluorescent OATP substrates. All dyes were tested in A431 cells expressing OATP1B1, OATP1B3 and OATP2B1.

Our results showed transporter-mediated uptake of some of these dyes. Moreover, ZV, LDG, CB and AF405 surpassed Fl-MTX signal intensity (see later on **Figure 3.12** and **Table 3.2**), indicating that these dyes are a better fit for fluorescence-based OATP-studies. (Alas, the other compounds listed in **Table 3.1** were not transported by the investigated OATPs.)

3.3.3.2 A microplate-based functional assay

With the aim of optimizing the protocol and to find the ultimate dye for semi high-throughput uptake measurements we characterized the uptake of the new OATP1B and OATP2B1 substrates. We measured the transport of our newly identified substrates in A431 cell expressing OATP1B1, OATP1B3 and OATP2B1 seeded in 96-multiwell plates (**Figure 3.11**).

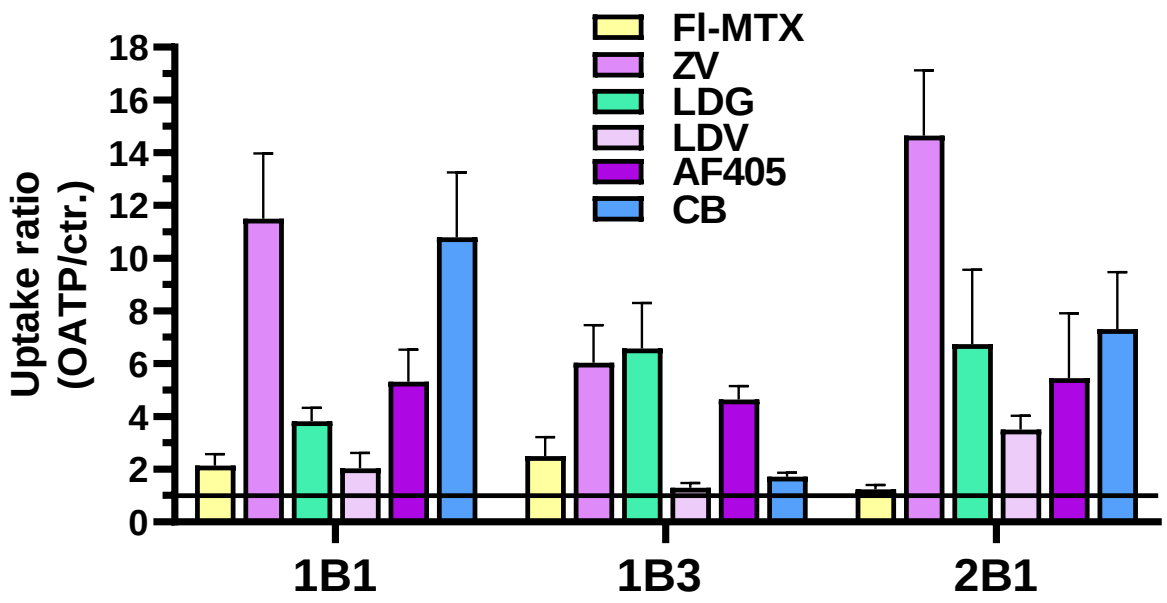

Figure 3.11 Additional hepatic OATP substrates. Transport was measured in A431 cells overexpressing OATP1B1, OATP1B3 and OATP2B1. Cells were seeded onto 96-well plates. 1 µl ZV, LDV, LDG, 1 µM (or 4 µM for OATP2B1) Fl-MTX or 20 µM CB and AF405 for 30 minutes at 37 °C in buffer with pH 5.5, in final reaction volume of 100 µl. Fluorescence was determined using a fluorescent plate reader. The activity was calculated by dividing fluorescence measured in A431-OATP cells with that measured in A431 mock-transfected cells. Average of at least three independent measurements with triplicates ± SD values are shown.

As we optimized the assay conditions, the highest transport ratios for OATP1B1 and OATP2B1 were observed at pH 5.5. **Figure 3.12** shows the pH-dependent ZV, CB and AF405 uptake in A431 cells (LDG is not shown here).

Our results show a rapid uptake of these compounds with a strong and stable signal. Opposed to Na-fluo and Fl-MTX, amine-reactive dyes stably bind to proteins upon entry into the cytoplasm. The cells retained a robust signal for more than 60 minutes without significant loss of the fluorescence intensity. Sadly, patent protects the commercially available viability dyes, thus the chemical structures and dye concentrations are not available. However, **Alexa Fluor 405 NHS ester**: (Tris(N,N-diethylethanaminium)8-[2-(4-{[(2,5-dioxopyrrolidin-1-yl)oxy]carbonyl}piperidin-1-yl)-2-oxoethoxy]pyrene-1,3,6-trisulfonate) and **Cascade Blue hydrazide**: ([(3,6,8-trisulfo-1-pyrenyl)oxy]-,1-hydrazide) are well documented dyes. Consequently, we choose to continue characterizing these two compounds. The saturation kinetics of their uptake; K_m and V_{max} is shown in **Figure 3.13**.

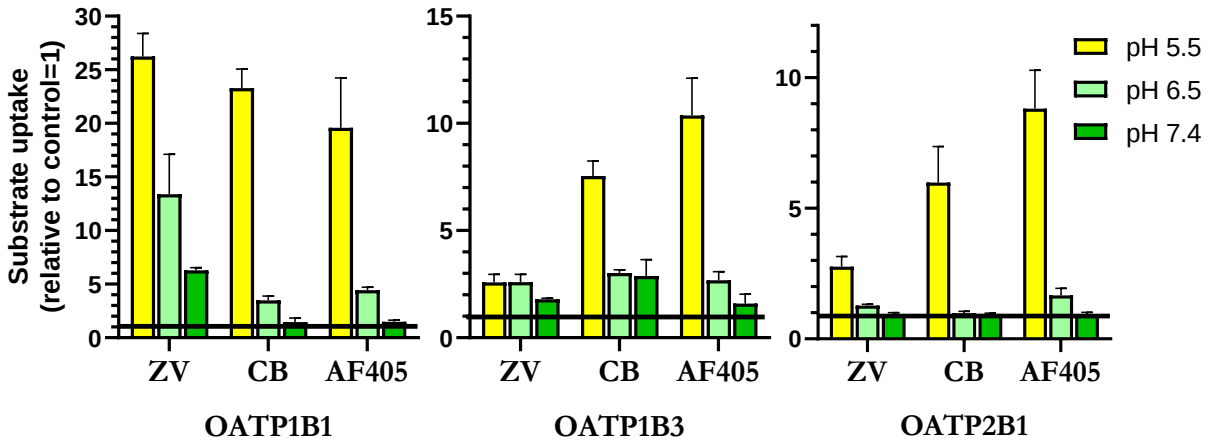

Figure 3.12 pH-dependent dye uptake in A431 cells. Transport was measured in 96-multiwell plates containing 1.2 x 10^5 cells/well. Cells were incubated with the dyes for 30 minutes in uptake buffer pH 5.5, 6.5 or 7.4. Dyes were added as follows: A431-OATP1B1 0.2µl/100 µl ZV, 2 µM CB and 1 µM AF405; A431-OATP1B3 0.2 µl/100 µl ZV, 20 µM CB and 5 µM AF405; A431-OATP2B1 0.2 µl/100 µl ZV, 5 µM CB and 2.5 µM AF405. Experiments were performed in triplicates with three parallels in each biological replicate. Average ± SD values are shown.

As seen on **Figure 3.13**, **Fl-MTX** uptake was similar for OATP1B1 and OATP1B3, while OATP2B1 has a lower affinity for this compound. Even though Fl-MTX was shown to be higher affinity substrate opposed to CB and AF405, the V_{max} of Cascade Blue transport for OATP1B1 and OATP2B1 was 2-3-fold higher, as their transport significantly exceeded that of Fl-MTX. Although OATP1B3 is also able to transport CB, the best substrate for OATP1B3 seems to be Alexa Fluor 405 as the V_{max} is 3-fold-higher compared to Fl-MTX. The important note here that the expression levels of the three OATPs cannot be directly compared, as there isn't any antibody that recognizes all three proteins. Therefore, the maximum uptake rates cannot be directly compared.

After optimizing the assay conditions, we measured OATP-mediated uptake for each dye. In summary, ZV showed the highest fluorescent signal (OATP vs. mock transfected control) for all three OATPs. CB proved to be an equally good substrate for OATP1B1 and OATP2B1 as ZV. The preferred substrates for OATP1B3 are ZV, LDG and AF405 (activity ratios are reviewed in **Table 3.2**).

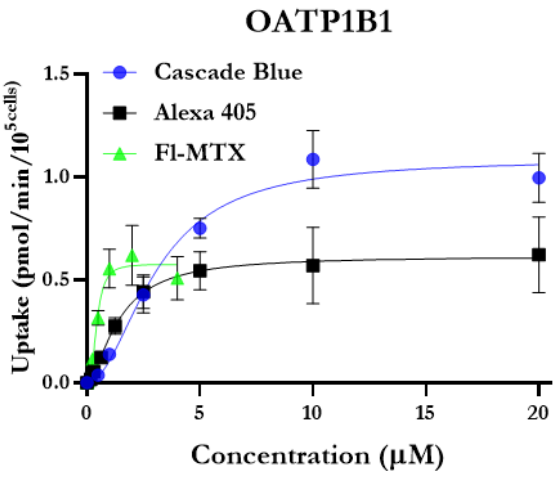

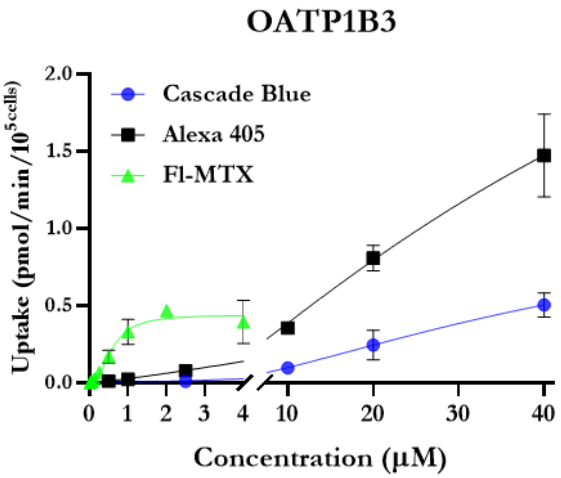

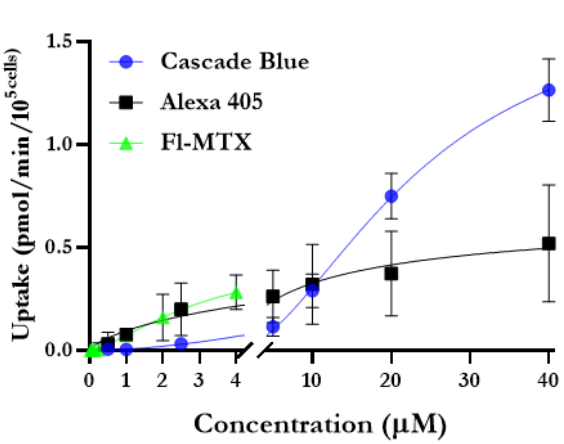

	K_m (µM)			V_{max} (pmol/min/1.2 x 10^5 cells)		
	1B1	1B3	2B1	1B1	1B3	2B1
Alexa Fluor 405	1.29 ± 0.04	16.98 ± 4.95	4.10 ± 0.72	0.57 ± 0.01	1.37 ± 0.57	0.37 ± 0.04
Cascade Blue	2.63 ± 0.13	20.98± 2.65	20.55 ± 1.29	1.07 ± 0.07	0.62 ± 0.08	1.58 ± 0.09
Fl-MTX	0.48 ± 0.03	0.58 ± 0.04	1.94 ± 0.13	0.60 ± 0.05	0.49 ± 0.03	0.34 ± 0.02

Figure 3.13 Concentration-dependent uptake kinetics of fluorescein-methotrexate (Fl-MTX), Cascade Blue and Alexa Fluor 405 (Alexa 405) measured in A431 cells expressing OATP1B1, OATP1B3 or OATP2B1. Transport was assessed in 96-well plates in the linear phase of uptake (2.5 minutes for Fl-MTX, 10 minutes (1B1, 2B1) or 15 minutes (1B3) for Cascade Blue, and 15 minutes for Alexa 405). Transport capacity was calculated based on calibration with known amounts of the dyes. Data points represent the average transport rates after background subtraction (measured in mock-transfected cells) from three independent measurements ±SD values.

	Transport ratio compared to control			z-factor		
	1B1	**1B3**	**2B1**	**1B1**	**1B3**	**2B1**
Fl-MTX	2.14 ± 0.44	2.49 ± 0.72	1.24 ± 0.16	**0.59**	**0.77**	-1.8
Zombie Violet	**11.05 ± 2.47**	**6.03 ± 1.43**	**14.65 ± 2.47**	**0.61**	**0.61**	**0.71**
Live/ Dead Violet	2.03 ± 0.59	1.33 ± 0.21	3.50 ± 0.53	**0.55**	-0.42	**0.79**
Live/ Dead Green	3.82 ± 0.51	**6.58 ± 1.73**	**6.74 ± 2.82**	**0.84**	**0.76**	**0.62**
Cascade Blue	**10.79 ± 2.46**	1.71 ± 0.16	**7.31 ± 2.17**	**0.73**	0.26	**0.66**
Alexa Fluor 405	**5.32 ± 1.22**	**4.65 ± 0.51**	**5.46 ± 2.46**	**0.59**	**0.64**	**0.57**

Table 3.2 A431 cells (seeded in 96-well plates) were incubated with the dyes at pH 5.5 for 30 minutes in order to reach the maximum fluorescent signal. Data were calculated from at least 3 independent measurements. Dyes were applied in the following concentrations/amounts: Fl-MTX 1 μM (OATP1B1 and 1B3) and 4 μM (OATP2B1); ZV, LDV and LDG 1-1 μl; CB and AF405 10 μM (OATP1B1 and 2B1) and 20 μM (OATP1B3). A z-factor above 0.5 is considered to be an excellent assay [201]. Numbers in bold indicate dyes meeting these criteria. Dyes defined as best candidates for HTS are indicated in bold.

3.3.3.3 Inhibition assay for OATP-drug interaction screening using Cascade Blue and Alexa Fluor 405

After finding the ideal dyes and optimal assay conditions (incubation time, pH and dye dilutions), we tested the applicability of the assay for the detection of OATP-drug interactions using known OATP1B and OATP2B1 interacting compounds. Our results showed that the transport of Cascade Blue and Alexa Fluor 405 was inhibitor sensitive (**Figure 3.14**).

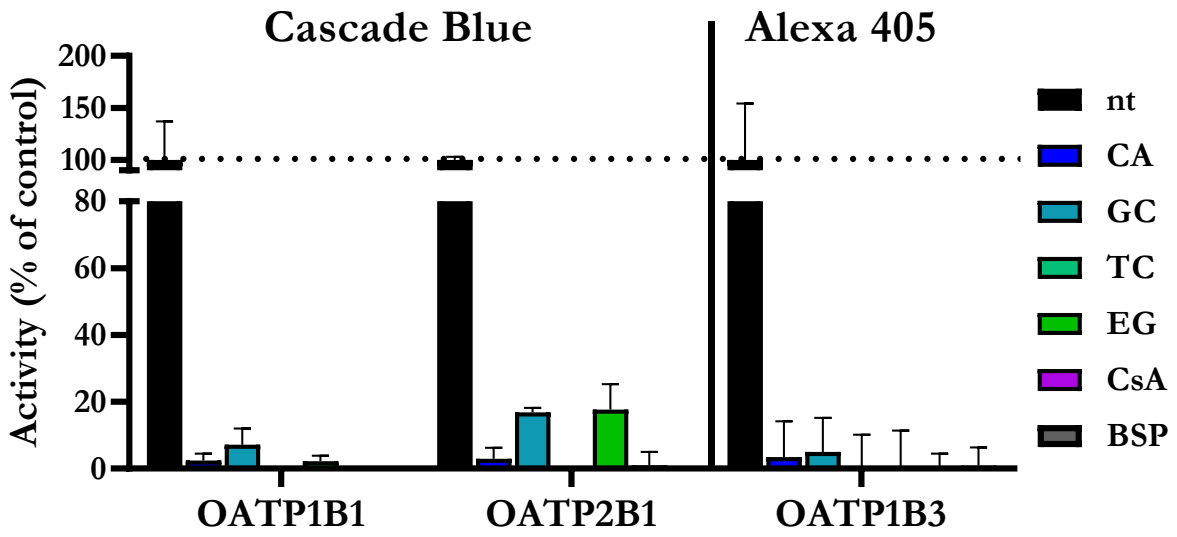

Figure 3.14 Inhibition of 10 µM Cascade Blue or 5 µM Alexa Fluor 405 uptake in A431 cells expressing OATP1B1, OATP1B3 and OATP2B1. Fluorescence was measured after 30 min incubation at 37°C, pH 5.5. Uptake was inhibited with the following compounds: 150 µM cholic acid (**CA**), 150 µM glycocholic acid (**GC**), 150 µM taurocholate (**TC**), 50 µM estradiol 17-β-D-glucuronide (**EG**), 20 µM cyclosporin A(**CsA**), 100 µM bromsulphthalein (**BSP**). Transport measured in cells with the dye alone was set 100% and the effect of the compounds was compared to this value. Bars represent the average of at least three independent experiments ±SD values.

Furthermore, we measured the concentration-dependent inhibition kinetics for cyclosporin A (CsA) and estrone-3-sulfate (ES) (**Figure 3.15**). CsA is a well-known inhibitor [112,203] and estrone-3-sulfate is a substrate for hepatic OATPs [43,193]. The measured IC_{50} values obtained in the novel fluorescence assay were comparable to the ones using radiolabeled substrates (**Table 3.3**). Z-factor is used to determine the robustness of a HTS assay [201]. Here we found that almost all the assays show a z-factor above 0.5 (summarized in **Table 3.2**), indicating that they are suitable for HTS OATP-drug interaction screens.

	OATP1B1		**OATP1B3**		**OATP2B1**	
	our data	**literature**	**our data**	**literature**	**our data**	**literature**
CsA	0.07± 0.04	0.1 [133,143], 0.2 [204], 1.3 [205]	0.18±0.05	0.2 [204], 1.2 [205]	1.45±0.11	36 [205]
E1S	0.22±0.004	0.05[133,204]	9.5±0.13	20 [204]	0.56±0.05	no data

Table 3.3 Comparing IC_{50} values between our and literature data. IC_{50} (µM) values were obtained using 2 or 10 µM CB (OATP1B1 or OATP2B1) or 5 µM AF405 (OATP1B3). Literature data shows IC_{50} values obtained in assays using estradiol-17-β-D-glucuronide, estrone-3-sulfate, 8-fluorescein-cAMP or dichlorofluorescein as probe substrates.

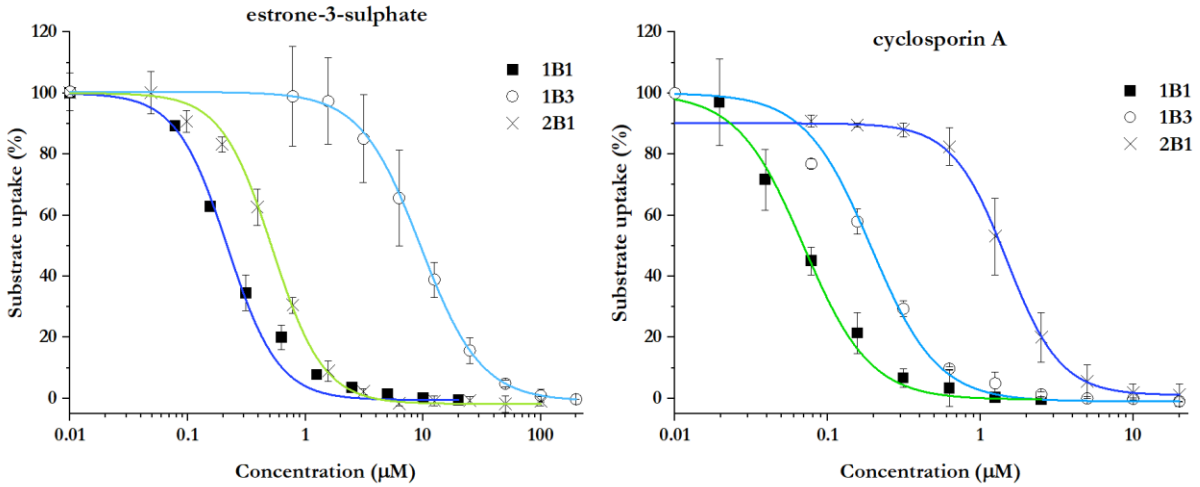

Figure 3.15 Inhibition of OATP-mediated Cascade Blue (CB) and Alexa Fluor 405 (AF405) uptake in A431 cells. 2 µM CB for OATP1B1, 10 µM CB for OATP2B1 and 5 µM AF405 for OATP1B3. Transport was measured after 30 min incubation in uptake buffer, pH 5.5 at 37°C. Data represents transport activity corrected with background fluorescence measured in mock transfected cells. Figures show the average of three independent measurements performed with three parallels ±SD values.

3.4 Results part II-Assay applications

3.4.1 The use of Cascade Blue to confirm new OATP2B1 interactions

(These results were published in Windt et al, Archives of Toxicology, 2019 [206])

The A431-OATP2B1 cell line established in my work has already been utilized for OATP2B1 related functional studies. In this particular study, we screened drugs that might contribute in OATP2B1-mediated toxicity. Although several chemotherapeutics have already been identified as OATP2B1 substrates, the OATP2B1-mediated sensitization of the cells toward cytostatics has not yet been demonstrated. By screening the toxicity of 101 FDA approved drugs our group investigated the influence of key drug-transporters, including OATP2B1 on the toxicity of approved anticancer drugs. In these experiments performed by my colleagues, several chemotherapeutic compounds were identified causing increased toxicity in OATP2B1 expressing cells. This toxicity can be explained by increased anticancer drug uptake by OATP2B1. In order to verify these new interactions, we used our Cascade Blue based assay and measured CB uptake in the presence of these compounds. If a drug alters CB uptake (both inhibition and activation can be expected) it proves the interaction with OATP2B1. As shown in **Figure 3.16** and **Table 3.4** the putative OATP2B1 substrates identified by the cytotoxicity screen inhibited CB uptake.

NSC number	Compound	IC_{50} values
NSC-125066	Bleomycin	64.15±6.1
NSC-712807	Capecitabine	124.01±6.42
NSC-628503	Docetaxel	11.32±0.38
NSC-616348	Irinotecan	17.03±1.46
NSC-180973	Tamoxifen	10.99±0.7
NSC-740	Methotrexate	265.50±31.38
NSC-122819	Teniposide	4.59±0.4
NSC-141540	Etoposide	1.88±0.32
NSC-6396	Thioplex	574.28±282.7

Table 3.4 Inhibition of OATP2B1-mediated Cascade Blue (CB) uptake by the putative OATP2B1 substrates identified in the cytotoxicity screen. Transport was measured as indicated under **Figure 3.15.** Experiments were performed in triplicates with three parallels in each biological replicate. Average ± SD values of IC_{50} values are shown

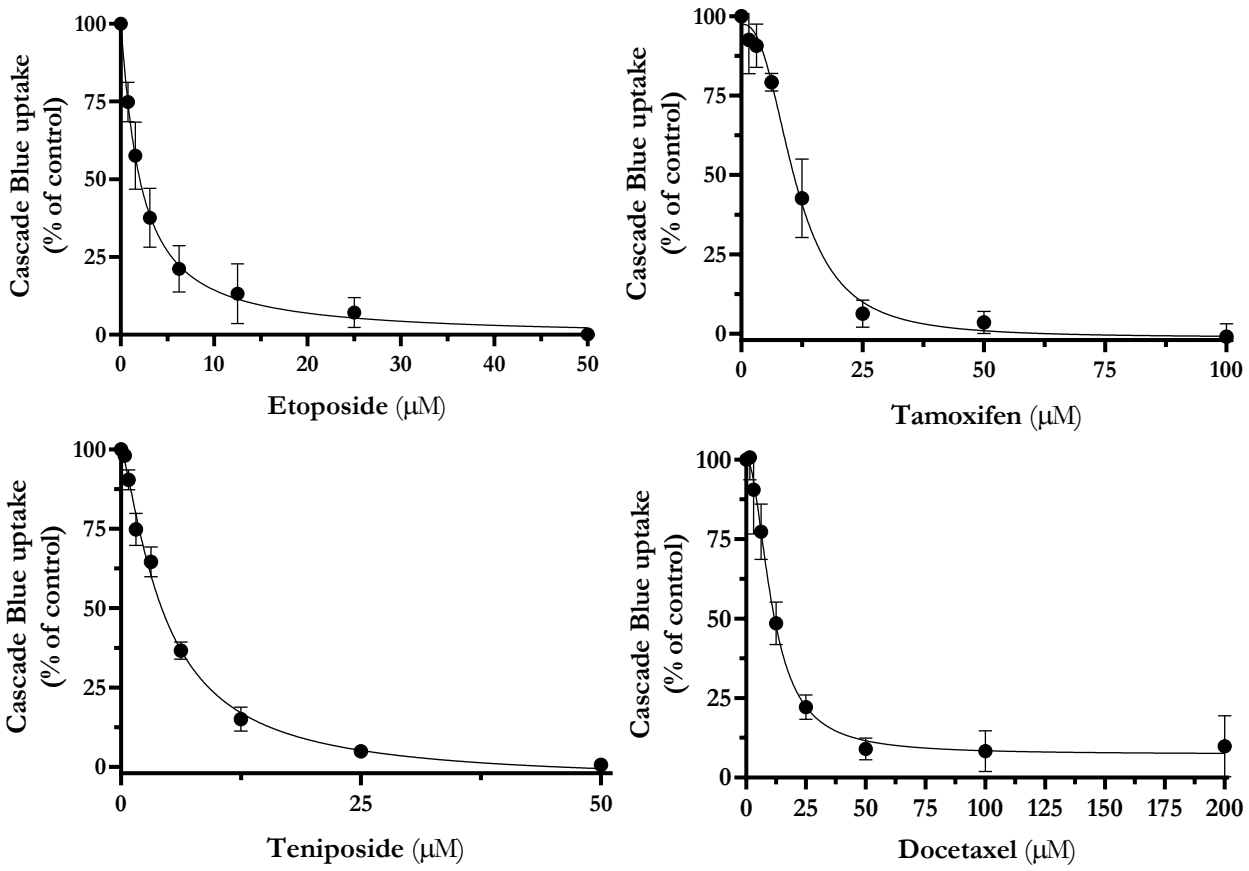

Figure 3.16 Inhibition of OATP2B1-mediated Cascade Blue (CB) uptake by the putative OATP2B1 substrates identified in the cytotoxicity screen. Transport of CB (10 μM) was measured for 30 min in increasing concentrations of the investigated compounds on 96-well plates. IC_{50} values were determined by measuring the intracellular accumulation of Cascade Blue in the presence of increasing concentrations of OATP2B1 interacting compounds. Experiments were performed in triplicates with three parallels in each biological replicate. Average ± SD values of IC_{50} values are shown.

3.4.2 The cancer specific isoform of OATP1B3-Where do we stand?

(The data presented here have not been published yet)

As it was mentioned in **Chapter I**, ectopic expression of OATP1B3 has been shown in multiple types of cancer [4,71]. Moreover, a number of studies have proved the existence of two cancer specific OATP1B3 variants, OATP1B3 CT and OATP1B3 V1 [72,73]. These isoforms seem to utilize alternative transcription initiation sites; therefore, the translated protein products lack the first 28 (OATP1B3 V1) or 47 (OATP1B3 CT) amino acids at the N-terminus of the canonical OATP1B3. Topology modeling predicts a transporter-like structure for both versions. While OATP1B3 V1 is predicted to have 12 transmembrane helices, which are the typical structure of OATPs, the CT isoform has only

10 TM helices indicating that this variant may not be functional (**Figure 3.17**). Studies have agreed that CT is localized intracellularly, and it might be functionally inactive.

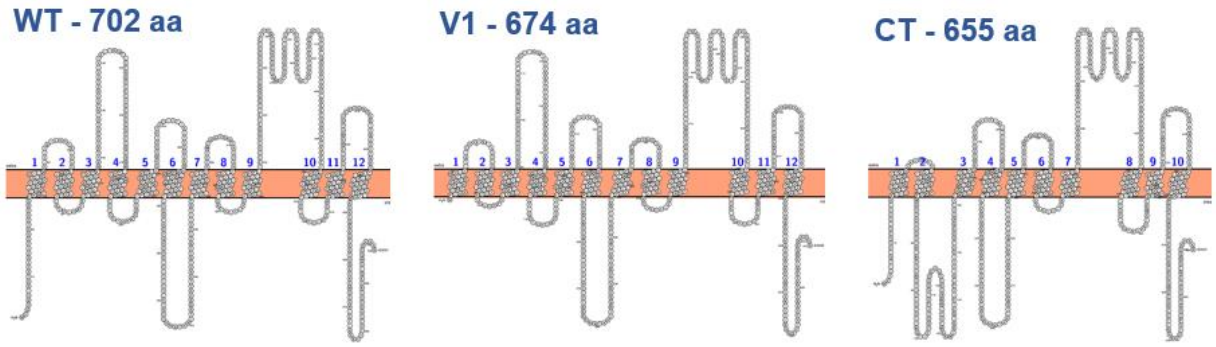

Figure 3.17 Predicted membrane topologies of the OATP1B3 isoforms. Topology was determined by CCTOP (Dobson et al. [207]), image was drawn by using the Protter program (http://wlab.ethz.ch/protter/start/).

However, there are discrepancies in the literature about the localization and function of OATP1B3 V1. Imai et al., showed that OATP1B3 V1 is localized to the plasma membrane with measurable transporter-mediated fluvastatin and rifampicin uptake [74], whereas Thakkar et al., and Chun et al. described no or very low level of transporter function and reduced plasma membrane localization [73,208]. Furthermore, Chun et al. was also showing that the first 50 amino acids are crucial for the plasma membrane localization of OATP1B3 [208].

Therefore, our goal here was to express these two isoforms of OATP1B3, CT and V1 in different cell lines and see whether they are localized to the plasma membrane and have any measurable transporter activity. A431 cell lines were previously shown as an ideal cell model for OATP expression related functional studies (Patik et al., and Windt et al. [142,206]), Therefore, we choose A431 cell as our reference point; and we also transduced colorectal carcinoma-derived cell lines where previous papers have been able to detect endogenous OATP1B3 expression by RT-PCR [71].

3.4.2.1 Cell lines expressing OATP1B3 isoforms

First, we transduced A431, HCT 8 (ileocecal colorectal adenocarcinoma) and HCT 116 (colorectal carcinoma) cell lines cells with the different OATP1B3 isoforms. Generating the cell lines with marked protein expression appeared to be challenging. Following our previous observations with OATP1B1 and OATP1B3 (wild type, **Chapter III, 3.3.2**), the cells did not tolerate forced OATP expression. Nevertheless, we tried to sort the cells using the truncated CD4 receptor encoded in our transfection vector (see Methods, Chapter III, 3.2.2), but we could only attain minor protein enrichment. Although

the available data are inconsistent with the function of the OATP1B3 V1 isoform, we tried to sort these CD4-presorted cells based on LDG positivity (described in Chapter III). This method proved to be useful again in the case of OATP1B3 WT and V1, as after four rounds of cell sorting, we got cells with detectable protein expression. However, in the case of OATP1B3 CT we did not detect any LDG positivity, therefore we applied repeated CD4-fragment based-sorting (data not shown). When we tested transporter function in these cell lines, we could detect increased OATP-mediated uptake of the well-documented substrate Fl-MTX in the LDG sorted OATP1B3 WT and OATP1B3 V1 cell lines, but only low transport in the CD4 sorted cells (**Figure 3.18** shows the results from HCT 8 cell lines). Furthermore, our results show that OATP1B3 V1 is a functional isoform. Although we did not detect OATP1B3 CT mediated Fl-MTX uptake, which could imply either a non-functional protein or lack of protein expression. Therefore, we had to examine whether this protein is present in these cell lines as CD4 expression does not necessarily correlate with OATP1B3 expression (See the results later in the text).

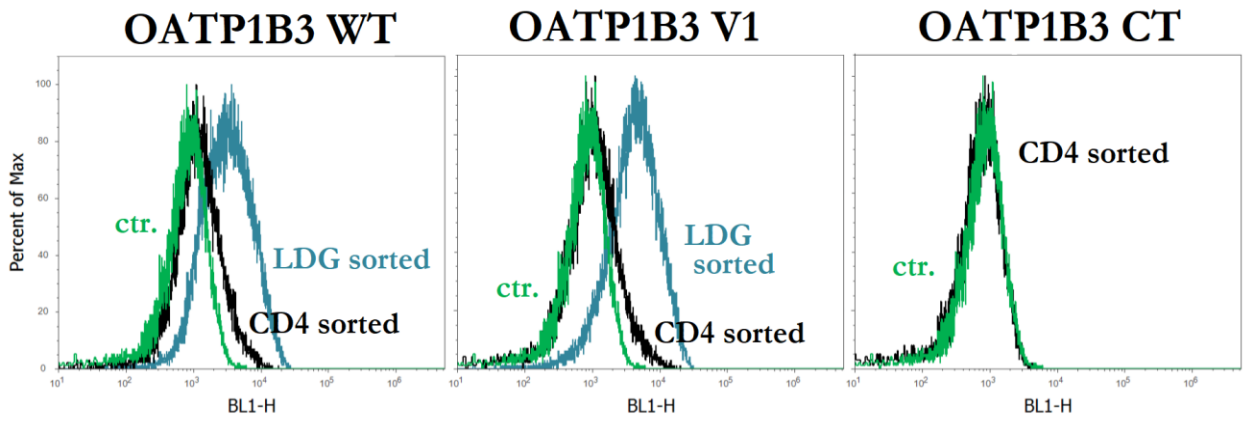

Figure 3.18 Fl-MTX uptake in HCT-8 cells expressing OATP1B3 WT, OATP1B3 V1 or OATP1B3 CT after sorting based on CD4 expression and/or LDG uptake. Cells were incubated with 1 μM Fl-MTX for 15 min at pH 5.5, 37°C. Fluorescence was detected by flow cytometry. Dead cells were excluded based on PI staining. **Ctr:** mock-transfected cells, **CD4**: cells were sorted based on labeling with the anti-CD4 antibody (Sigma) and anti-mouse Alexa-488 secondary antibody, **LDG:** cells sorted based on LDG positivity (see **Chapter III, 3.2.7**). Experiments were repeated three times, one representative experiment is shown.

3.4.2.2 Cellular localization of cancer-specific OATP1B3 isoforms

Visual examination of OATP1B3 expression by confocal microscopy revealed mainly plasma membrane localization for OATP1B3 WT and OATP1B3 V1. However, OATP1B3 CT showed mostly cytoplasmic localization in A431 (not shown) and HCT 8 cells (**Figure 3.19**) and very low

expression in HCT 116 cells (**Figure 3.20**). Low expression levels might be explained by improper folding and decreased protein stability of OATP1B3 CT.

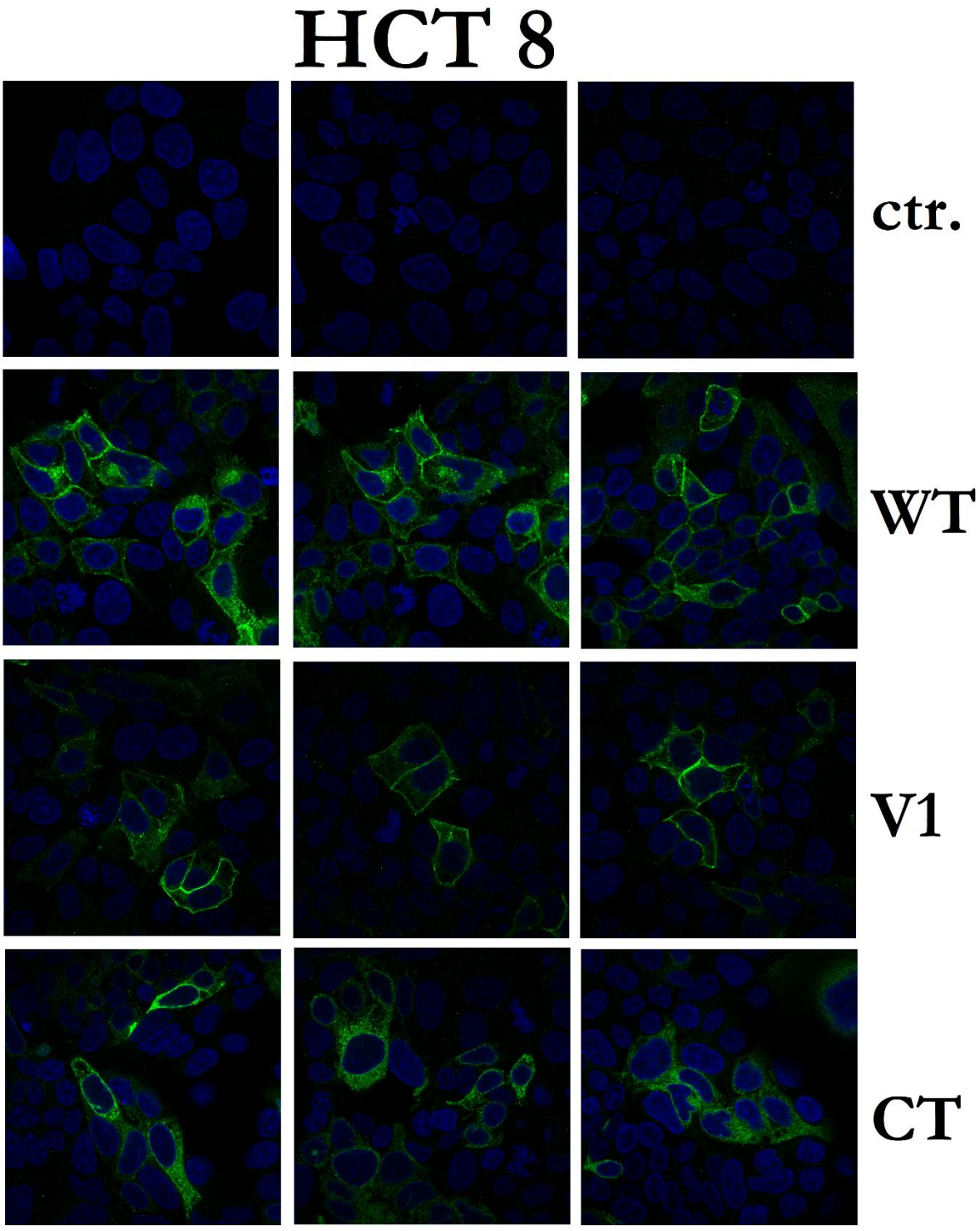

Figure 3.19 OATP1B3 expression in HCT 8 cells. Cells were labeled with an anti-OATP1B3 antibody (Atlas antibodies, 1:500 dilution) and Alexa-488-conjugate anti-rabbit secondary antibody (Sigma, 1: 250 dilution).

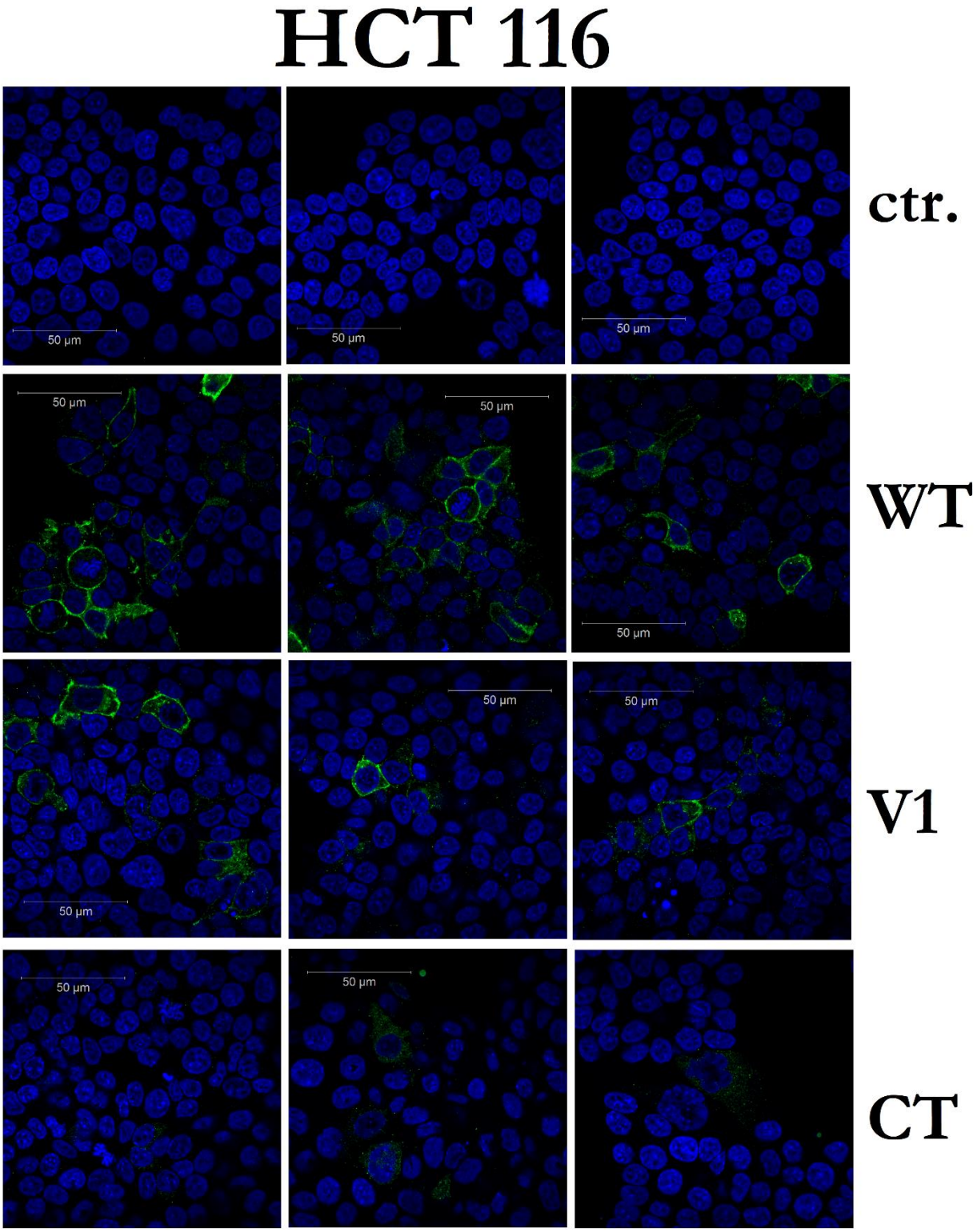

Figure 3.20 OATP1B3 expression in HCT 116 cells. The same antibodies were used as described above for HCT 8 cells.

Most cell-surface membrane proteins are glycosylated on their extracellular domains. Therefore, we assessed the glycosylation status of OATP1B3 WT and V1 after removing the N-linked oligosaccharides by PNGase F digestion. Western blot analysis of whole-cell lysates with and without PNGase treatment showed marked shifts in the molecular weight of OATP1B3 WT and OATPP1B3 V1 (**Figure 3.21**). As OATP1B3 CT only showed cytoplasmic localization, we excluded those samples here.

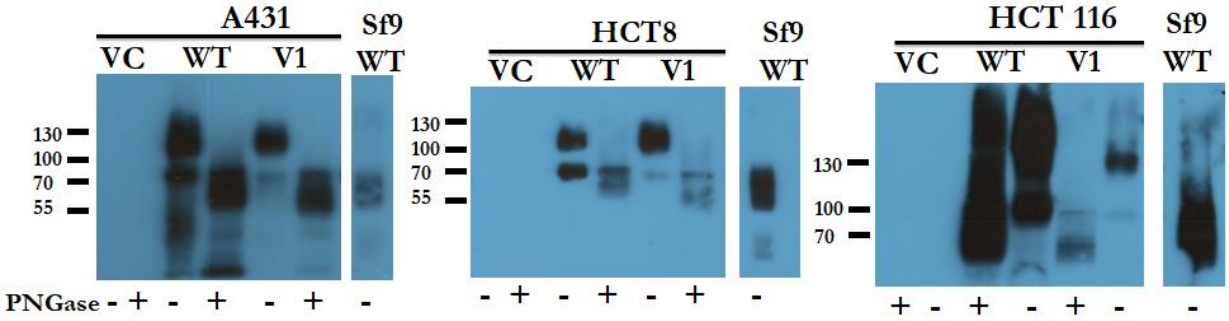

Figure 3.21 Western blot analysis of over-expressed OATP1B3 WT, OATP1B3 V1 in different cell lines. Whole-cell lysates with (+) or without (-) PNGase F treatment. 1:2000 anti-OATP1B3 antibody (Abcam), 1:20000 anti-mouse HRP. Total protein amounts: A431: 1 μg in VC (vector control), WT and V1, HCT 116: 10 μg in VC and WT, 20 μg in V1, HCT 8: 10 μg in VC and WT, 20 μg in V1. Sf9 OATP1B3 WT: 0.05 μg

Furthermore, using immunoblot analysis and confocal immunofluorescence microscopy, we demonstrated that OATP1B3 V1 expressed in A431, HCT 8 and HCT 116 cells show colocalization with E-cadherin in the plasma membrane. In **Figure 3.22**, expression of OATP1B3 V1 and E-cadherin were examined by confocal microscopy. Red staining (first row) shows E-cadherin, green (second row) shows OATP1B3 expression and the third row shows merged images.

Taken together, our preliminary results indicate that OATP1B3 V1 is localized to the plasma membrane and has a transporter function. In future studies, our laboratory would like to compare the function of OATP1B3 WT and V1 and test whether OATP1B3 V1 would result in increased sensitivity to chemotherapeutics.

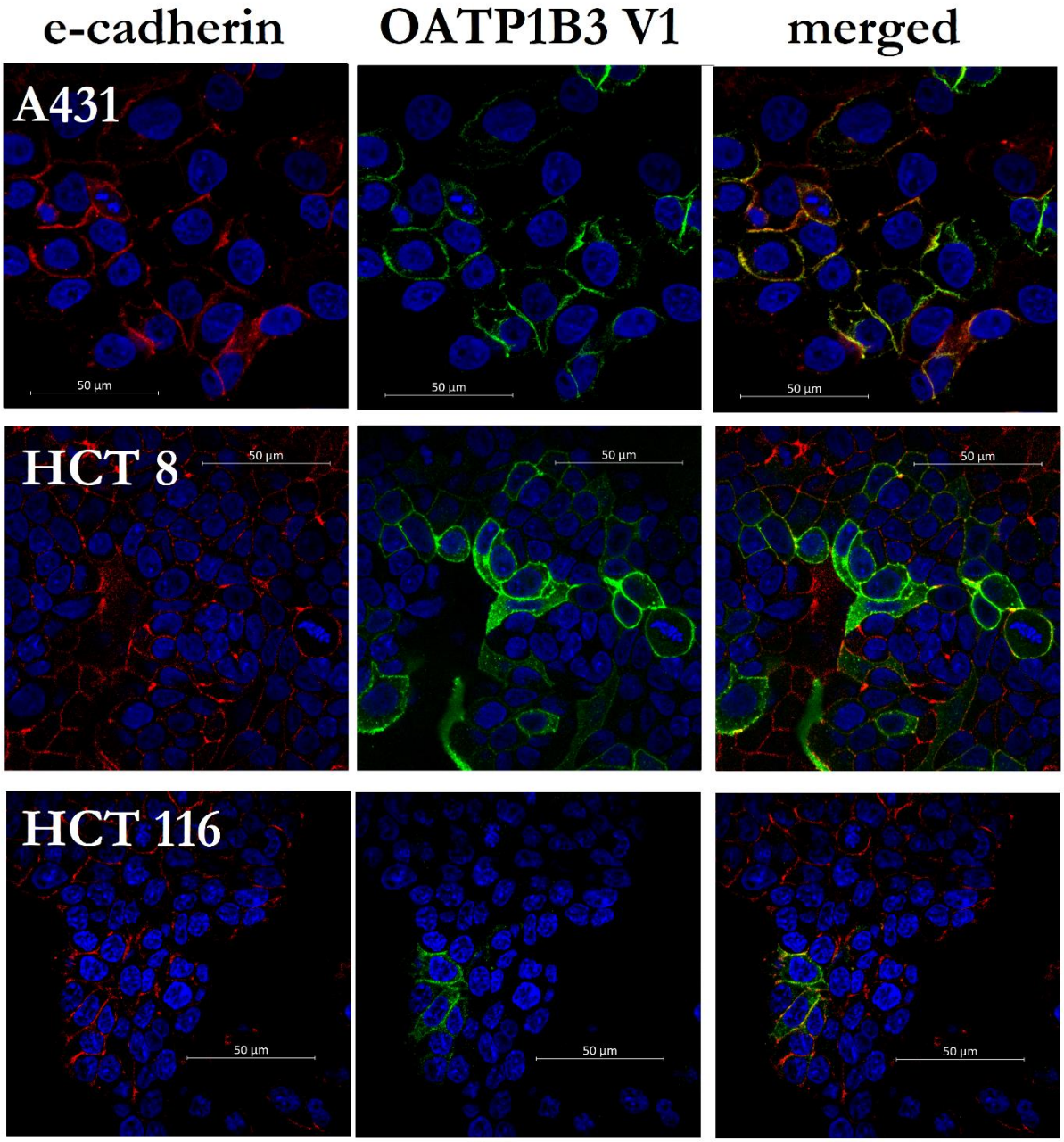

Figure 3.22 Colocalization of E-cadherin and OATP1B1 in three different cell lines. Using red for E-cadherin (**on the left**) and green fluorescent probes for OATP1B3 (**middle row**). When these images were merged, they showed a yellow signal, indicating that both proteins were colocalized (**on the right**). 1:1000 mouse anti-OATP1B3 (Abcam) and 1:100 anti-pan-cadherin (PA5-16766 rabbit-Thermo Fisher) were probed with 1:250 mouse Alexa-488 and 1:250 rabbit Alexa 647 (Sigma) as secondary antibodies.

3.5 Discussion

Hepatic OATPs are well-recognized players in transporter-mediated drug-drug interactions. The altered function of OATP1B1 and OATP1B3 due to mutations or drug-drug or food-drug interactions are directly implicated in the modification of drug pharmacokinetics and causing pharmacological toxicities [209] (e.g. bile acid congestion [100], statin-induced toxicity [50,210]). In addition, OATP2B1 is an emerging candidate for contributing to these effects due to its possible role in SN-38 mediated gastrointestinal toxicity [211] or statin-induced myopathy [22].

Moreover, OATPs are also recognized in cancer; not only as potential mediators of chemotherapy disposition but as potential future targets for cancer treatments or tumor markers [20].

Taken together, these are the key reasons why OATPs receive increasing attention. The ITS recognizes OATP1A2, OATP1B1, OATP1B3, and OATP2B1 as main determinants of drug PK and recommends the investigation of these transporters during early drug development [83]. The EMA also emphasizes the necessity to characterize specific transporter polymorphisms as they might alter drug absorption and efficacy [84]. The pharmaceutical industry follows the recommendations as the common goal is to ensure drug safety, develop new therapies and prevent potential complications. To meet regulatory requirements, *in vitro* systems are required to estimate drug-transporter interactions. Radioactively labeled drugs have been an excellent choice to track a compound through the body and determine pharmacokinetics.

Nevertheless, researchers are attempting to employ even better or newer techniques, such as mass spectroscopy (MS) to study ADME characteristics. Naturally, these techniques have limitations: they are costly and not applicable for larger compound screens. In order to increase the magnitude of these screens, new probes and more advanced assay technologies are required. Fluorescent tracers and compounds labeled with fluorescent tags are emerging as a cost-efficient substitution for radioligands. Also, fluorescent labeling promises higher flexibility in multicolor labeling. Several fluorescent OATP1B substrates have been identified in the past decade (e.g. Na-fluorescein and fluorescein-methotrexate [132,212]) and there were attempts to utilize these probes for semi-HTS or HTS formats [55,131,196]. However, due to sensitivity, stability and availability issues, these compounds are not ideal for larger compound screens [133]. An increasing evidence suggests that OATP2B1 needs to be considered as a new target for pharmacokinetic studies [22,92,213–215]. Interestingly, OATP2B1 has been reported to reach its highest transport activity under an acidic extracellular environment [1,136]. However, fluorescent functional assay to study OATP2B1's function on a larger scale has not been described.

Consequently, our goal was to develop experimental strategies to measure OATP-drug interactions with the help of fluorescent substrates. We bought commercially available fluorescent dyes with low cell-permeability, high quantum yield and pH independence. First, we choose to test amine-reactive viability dyes, and we identified Zombie Violet (ZV) and Live/Dead Green (LDG) as novel OATP1B1, OATP1B3 and OATP2B1 substrates (**Figure 3.6**). In the second set of experiments, we chose compounds (Cascade Blue Hydrazide and Alexa Fluor 405) from the same family but these are used to label proteins fluorescently.

We have used our previously developed Sf9 cell-based assay to test our candidate substrates by flow cytometry. ZV showed transporter-mediated uptake in cells expressing OATP1B1, OATP1B3 and OATP2B1, but not in any other OATP member (**Figure 3.3**). The transport was recapitulated in A431 cells overexpressing the same proteins (**Figure 3.8 and Figure 3.11**). The other viability dye that we discovered as a new substrate for hepatic OATPs was LDG. As both dyes label dead cells and cells with high OATP1B1, OATP1B3 and OATP2B1 expression, a secondary dye is required to exclude cells with compromised membranes (**Figure 3.1**). Also, there are cell types with endogenous OATP expression (e.g. hepatocytes), calling for caution when these dyes are used for live/dead cell discrimination as subpopulations of live cells are excluded because of LDG positivity. However, currently, we have no data about the influence/relevance of endogenous levels of OATPs on the uptake of these dyes.

For larger drug screens, we needed an adherent cell line with stable OATP expression. We generated A431 cells expressing OATP1B1, OATP1B3 and OATP2B1. Although this cell line has not been commonly used in pharmacological screens, it has been used before in microplate-based assay due to its strong adherence [216]. Though our vectors contained a CD4 fragment as a selection marker, our primary attempts yielded cell lines (A431, MDCKII, HEK293T, HCT8) with very low expression levels of OATP (**Figure 3.7 and Figure 3.18**). Without any other existing selection marker, we attempted to sort cells based on OATP-mediated LDG uptake. This method helped to increase OATP1B and OATP2B1 protein expression levels which were accompanied by elevated transporter function in multiple cell lines (**Figure 3.8-3.10** and **Figure 3.18).** According to our knowledge, using a fluorescent dye to enrich OATP-expression hasn't been done before. This could be used as a new tool to generate cell lines with high OATP1B and OATP2B1 expression. Furthermore, without this novel sorting method, we would not have been able to demonstrate that the cancer-specific OATP1B3 V1 has measurable transporter activity (**Figure 3.18**). With these cell lines, we could also demonstrate

plasma membrane localization for this protein in three different cell lines and made our contribution to the existing debate about these isoforms' cellular localization (**Figure 3.19-Figure 3.22**).

Our results measuring transporter activity in hepatic OATP expressing cell lines are consistent with previous studies showing enhanced OATP transporter activity under an acidic extracellular milieu [1,40,42,211,217]. In line with this, our newly identified OATP test substrates were almost exclusively transported at pH 6.5-5.5. Further studies are required to determine whether this enhancement is due to changes in the protonation levels in the transporter binding sites or in the substrates in an acidic environment. Nevertheless, the inhibition constants measured with this new assay are in full accordance with transport measurements carried out at neutral pH [133,204,205], indicating the usefulness of this system (**Table 3.3**).

Although ZV, LDG and LDV are excellent substrates for hepatic OATPs, the exact transport kinetics could not be determined as the molecular structure is proprietary. Therefore, we could only provide detailed transport kinetics for the well-established hepatic OATP substrate; fluorescein-methotrexate and the two novel OATP1B1, OATP1B3 and OATP2B1 substrates; Cascade Blue, Alexa Fluor 405 (**Figure 3.12**). OATPs had different affinities for different substrates. OATP1B1 and OATP2B1 exhibited higher affinity for Cascade Blue, and OATP1B3 showed a preference for Alexa Fluor 405 when compared to Cascade Blue and fluorescein-methotrexate (**Figure 3.11, Figure 3.12, Table 3.2**). OATP2B1 is an emerging candidate in drug-transporter interaction studies, however, there is no available large-scale fluorescence-based scaling method for OATP2B1. This assay might be the new approach to screen for OATP2B1-mediated DDIs.

Our new substrates are excellent candidates for the establishment of a new functional assay, given the high quantum yield, water-solubility, minimal membrane permeability and low pH-sensitivity. Moreover, they can be used to measure OATP function in a semi-high throughput format. Calculating the z-factor revealed that LDV and CB for OATP1B1 and OATP2B1, and ZV, LDG and AF405 for all three hepatic OATPs may be applied in larger-scale drug screening studies (**Table 3.2**). Additionally, using CB and AF405 as test substrates, we could detect OATP-drug interactions. First, we showed the inhibitory effect on OATP1B3, OATP1B3 and OATP2B1-mediated CB and AF405 transport with previously identified OATP interacting compounds (**Figure 3.14**). Furthermore, determining the IC50 values for the most used test substrate, estrone-3-sulphate was in good agreement with previous measurements (**Table 3.3** and kinetics can be seen in **Figure 3.15**). The value of the new fluorescent substrate-based assay was also further demonstrated when our group verified OATP2B1-drug interactions and determined IC_{50} values following a smaller scale (101 compounds)

toxicity screen between OATP2B1 and FDA approved drugs in A431 cells expressing OATP2B1 (**Chapter III-Results part II**, also Windt el al.[206]).

Unfortunately, indirect transport assays cannot reveal the true nature of the interaction (substrate or inhibitor) between the tested molecule and OATP, the transport should be confirmed by direct transport measurements, such as mass spectrometry or direct labeling. However, the use of *in vitro* cell-based test systems, like our new method is a cheaper way to screen more extensive compound libraries in the early stages of drug development.

Summary

In drug development, there is an increasing interest in transporter families, especially the ones with a multispecific substrate profile, such as OATPs. Methods to investigate and predict OATP-drug and OATP-food interactions are necessary for early drug development.

In this thesis, we developed new fluorescent methods to investigate the human OATP transport function. The investigation evaluated Sf9 cells and several mammalian cell lines as models for *in vitro* transport measurements and tested and identified several fluorescent compounds that can be transported by the human OATP family. In the first part of the dissertation, we identified sodium-fluorescein as a pan-OATP substrate and proved that Sf9 cells are suitable to express functional OATP proteins. These two components helped to develop a new fluorescent substrate-based functional assay to identify novel OATP-drug interactions. In the second part of the dissertation, we found additional fluorescent substrates for OATP1B1, OATP1B3 and OATP2B2: Zombie Violet, Live/Dead Violet, Live/Dead Green, Cascade Blue and Alexa Fluor 405. These test substrates are better suited for semi-high throughput assays compared to sodium-fluorescein and fluorescein-methotrexate.

We advanced our first system and established a new *in vitro* assay in mammalian cells that can be used in semi-high throughput compound library screens. Moreover, we demonstrated that Live/Dead Green can be used for OATP-function based enrichment of OATP1B1, OATP1B3 and OATP2B1 expression in different cell lines.

We further emphasized the fact that OATPs' transporter activity is highly influenced by the extracellular pH environment.

In summary, the use of in vitro cell-based test systems that overexpress OATPs may be helpful towards to predict human PK of pre- and clinical drugs and assess risk for possible DDIs. Such knowledge may clarify differences observed in tissue distribution regarding OATPs and their polymorphisms and transporter-drug interactions. Even more, it might help to utilize OATPs for targeted drug delivery.

Further application of the fluorescence-based methods developed during my Ph.D. work:

The newly developed fluorescence techniques opened new possibilities toward the establishment of model systems and methods for the investigation of human OATPs.

1. Based on the best performing viability dyes, we performed further screening among the available viability and other routinely applied fluorescent dyes. This search resulted in the identification of novel fluorescent substrates for OATP1A2 and OATP1C1 that allowed the

development of novel assays for determining their function and drug interactions (Bakos et al., 2019[140]).

2. The fluorescence-based sorting method allowed the generation of human (A431 and HEK 293) cell lines with high expression levels of OATPs that is often a challenge due to the unfavorable effect of forced expression of OATPs in cell lines[159]. The generation of these cell lines provided the basis for further screening of fluorescent substrates and the establishment of model cell lines appropriate for medium scale drug screenings (Windt et al., 2019[206]).
3. With the help of the established fluorescence methods, I contributed to the identification of a novel OATP2B1 drug substrate, erlotinib (Bauer et al., 2018[173]).

Összefoglalás

A gyógyszerfejlesztési ágazatban folyamatosan növekszik az érdeklődés olyan transzporter családok iránt, amelyek multispecifikus szubsztrát profillal rendelkeznek. Erre egy kiváló példa az OATP fehérjecsalád, hiszen a gyógyszerfejlesztési folyamat során szükség van OATP-gyógyszer és OATP-étel kölcsönhatások kimutatására alkalmas módszerek kidolgozására. Ez azért fontos, hogy már a fejlesztés korai stádiumában ki tudják szűrni, hogy egy esetleges jövőbeli gyógyszer, OATP-kel való kölcsönhatás révén okozhat e káros mellékhatásokat.

A dolgozatban új, általunk kifejlesztett fluoreszcens módszereket mutatunk be, melyek alkalmasak a humán OATP-k transzportfunkciójának vizsgálatára. A kifejlesztett *in vitro* módszerrel Sf9 és emlős sejtvonalakban expresszáltatott OATP fehérjéken teszteltünk transzporter funkciót és azonosítottunk új fluoreszcens OATP szubsztrátokat.

A disszertáció első részében bemutatjuk, hogy az Sf9 sejtek alkalmasak funkcionális OATP-k termeltetésére, ezen felül bemutatjuk, hogy a nátrium-fluoreszcein egy általános OATP-szubsztrát Ezen eredmények hozzájárultak egy új fluoreszcens szubsztrát-alapú funkcionális mérési módszer kidolgozásához; mellyel új OATP-gyógyszer kölcsönhatásokat vagyunk képesek azonosítani.

A disszertáció második részében további fluoreszcens OATP1B1, OATP1B3 és OATP2B1 szubsztrátokat fedeztünk fel, mint Zombie Violet, Live / Dead Violet, Live / Dead Green, Cascade Blue és Alexa Fluor 405. Ezek a teszt szubsztrátok az előzetes mérések során jobbnak bizonyultak közepes áteresztőképességű vizsgálatok lebonyolításához, mint a korábban leírt nátrium-fluoreszcein és fluoreszcein-metotrexát.

A korábbi módszerünket tovább fejlesztve, az újonnan felfedezett szubsztrátokat is felhasználva, egy *in vitro,* emlős sejt-alapú, közepes-áteresztőképességű esszét dolgoztunk ki gyógyszer könyvtárak tesztelésére. Továbbá bemutatjuk, hogy a Live/Dead Green festék használható OATP-funkció alapú sejt szortolásra, amivel növelhető az össz-OATP1B1, OATP1B3 és OATP2B1 fehérje mennyisége különböző sejtvonalakban.

Továbbá hangsúlyozzuk és példákkal szemléltetjük az OATP-k pH-függő transzporter aktivitását.

Az eredményeinket összefoglalva megállapíthatjuk, hogy egy *in vitro*, magas OATP-expressziót mutató sejt-alapú teszt rendszer alkalmas lehet preklinikai fázisban és már forgalomban lévő gyógyszerek farmakokinetikai paramétereinek és lehetséges gyógyszerkölcsönhatások becslésére. Az így megszerzett tudás segíthet jobban megérteni az OATP-k és izoformáik között megfigyelt funkcionális

és szöveti elolszlásbeli különbségeket és transzporter-gyógyszer kölcsönhatásokat. Továbbá, esetleges kaput nyit OATP-ken keresztüli célzott gyógyszer bejuttatásra.

További példák a doktori képzésem során kifejlesztett fluoreszcencia-alapú módszerek alkalmazhatóságára:

Az újonnan kifejlesztett fluoreszcens technikák lehetőséget teremtettek újabb modell rendszerek kidolgozására, melyekkel a humán OATP család vizsgálata válik lehetővé.

1. A jól teljesítő viabilitási festékekből kiindulva, további viabilitási és más általánosan elérhető fluoreszcens festékeket teszteltünk OATP-expresszáló sejtvonalakban. Ezzel új szubsztrátokat, továbbá új módszereket fejlesztett és írt le a csoportunk a kevésbé jellemzett OATP1A2 és OATP1C1 fehérjék és gyógyszerkölcsönhatásaik jellemzésére. (Bakos et al., 2019[140]).
2. A fluoreszcencia-alapú szortolási módszer lehetőséget teremtett magas OATP-expressziót mutató humán eredetű sejtvonalak (A431 és HEK293) létrehozásához, ami a legtöbb esetben már önmagában kihívás, hiszen a túl magas OATP-expressziót és a hozzá köthető funkciót rosszul tolerálják egyes sejtvonalak. (Cesar-Razquin et al., 2015[159]) Az OATP-ket nagy mennyiségben termelő sejtvonalak segítségével drog toxicitási vizsgálatokra alkalmas közepes áteresztő képességű teszt rendszer hoztunk létre. (Windt et al., 2019[206]).
3. Az általunk kifejlesztett fluoreszcens módszerek segítségével, hozzájárultunk egy új OATP2B1 szubsztrát (Erlotinib) felfedezéséhez és ezen kölcsönhatás jellemzéséhez (Bauer et al., 2018[173]).

Bibliography

1. Kobayashi, D. *et al.* Involvement of human organic anion transporting polypeptide OATP-B (SLC21A9) in pH-dependent transport across intestinal apical membrane. *J Pharmacol Exp Ther* **306**, 703–708 (2003).

2. Svoboda, M., Riha, J., Wlcek, K., Jaeger, W. & Thalhammer, T. Organic anion transporting polypeptides (OATPs): regulation of expression and function. *Curr. Drug Metab.* **12**, 139–53 (2011).

3. Lawrence Lin, Sook Wah Yee, Richard B. Kim, and K. M. G. SLC Transporters as Therapeutic Targets: Emerging Opportunities. *Nat Rev Drug Discov.* **14**, 543–560 (2015).

4. Kovacsics, D., Patik, I. & Özvegy-Laczka, C. The role of organic anion transporting polypeptides in drug absorption, distribution, excretion and drug-drug interactions. *Expert Opin. Drug Metab. Toxicol.* **Nov**, 1–16 (2016).

5. Lee, W. *et al.* Polymorphisms in human organic anion-transporting polypeptide 1A2 (OATP1A2): implications for altered drug disposition and central nervous system drug entry. *J Biol Chem* **280**, 9610–9617 (2005).

6. Bronger, H. *et al.* ABCC drug efflux pumps and organic anion uptake transporters in human gliomas and the blood-tumor barrier. *Cancer Res* **65**, 11419–11428 (2005).

7. Gao, B., Vavricka, S. R., Meier, P. J. & Stieger, B. Differential cellular expression of organic anion transporting peptides OATP1A2 and OATP2B1 in the human retina and brain: implications for carrier-mediated transport of neuropeptides and neurosteriods in the CNS. *Pflügers Arch. - Eur. J. Physiol.* **467**, 1481–1493 (2014).

8. Chan, T. *et al.* Human organic anion transporting polypeptide 1A2 (OATP1A2) mediates cellular uptake of all-trans-retinol in human retinal pigmented epithelial cells. *Br. J. Pharmacol.* **172**, 2343–2353 (2015).

9. Meier, Y., Eloranta, J. & Darimont, J. Regional distribution of solute carrier mRNA expression along the human intestinal tract. *Drug Metab. …* **35**, 590–594 (2007).

10. Wang, H. *et al.* Alteration in placental expression of bile acids transporters OATP1A2, OATP1B1, OATP1B3 in intrahepatic cholestasis of pregnancy. *Arch. Gynecol. Obstet.* **285**, 1535–1540 (2012).

11. Hubeny, A. *et al.* Expression of OATP1A2 in red blood cells and its potential impact on antimalarial therapy. *Drug Metab. Dispos.* **44**, 1562–1568 (2016).

12. Tamai, I. *et al.* Molecular identification and characterization of novel members of the human organic anion transporter (OATP) family. *Biochem. Biophys. Res. Commun.* **273**, 251–260 (2000).

13. König, J., Cui, Y., Nies, A. T. & Keppler, D. Localization and genomic organization of a new hepatocellular organic anion transporting polypeptide. *J. Biol. Chem.* **275**, 23161–23168 (2000).

14. Zu Schwabedissen, H. E. M. *et al.* OATP1B3 is expressed in pancreatic b-islet cells and enhances the insulinotropic effect of the sulfonylurea derivative glibenclamide. *Diabetes* **63**, 775–784 (2014).

15. Hagenbuch, B. & Stieger, B. The SLCO (former SLC21) superfamily of transporters. *Mol. Aspects Med.* **34**, 396–412 (2013).

16. Pizzagalli, F. *et al.* Identification of a novel human organic anion transporting polypeptide as a high affinity thyroxine transporter. *Mol. Endocrinol.* **16**, 2283–2296 (2002).

17. Kraft, M. E. *et al.* The prostaglandin transporter OATP2A1 is expressed in human ocular tissues and transports the antiglaucoma prostanoid latanoprost. *Invest. Ophthalmol. Vis. Sci.* **51**, 2504–11 (2010).

18. Kang, J. *et al.* Expression of human prostaglandin transporter in the human endometrium across the menstrual cycle. *J. Clin. Endocrinol. Metab.* **90**, 2308–2313 (2005).

19. Choi K, Zhuang H, Crain B, D. S. Expression and localization of prostaglandin transporter in Alzheimer disease brains and age-matched controls. *J Neuroimmunol.* **195**, 81–87 (2008).

20. Oswald, S. Organic Anion Transporting Polypeptide (OATP) transporter expression, localization and function in the human intestine. *Pharmacol. Ther.* **195**, 39–53 (2019).

21. Kullak-Ublick, G. A. & Meier, P. J. Mechanisms of cholestasis. *Clin. Liver Dis.* **4**, 357–385 (2000).

22. Knauer, M. J. *et al.* Human skeletal muscle drug transporters determine local exposure and toxicity of statins. *Circ. Res.* **106**, 297–306 (2010).

23. Huber, R. D. *et al.* Characterization of two splice variants of human organic anion transporting polypeptide 3A1 isolated from human brain. *Am. J. Physiol. Cell Physiol.* **292**, C795-806 (2007).

24. Gao, B. *et al.* Localization of organic anion transporting polypeptides in the rat and human ciliary body epithelium. *Exp. Eye Res.* **80**, 61–72 (2005).

25. Fujiwara, K. *et al.* Identification of thyroid hormone transporters in humans: Different molecules are involved in a tissue-specific manner. *Endocrinology* **142**, 2005–2012 (2001).

26. Sato, K. *et al.* Expression of organic anion transporting polypeptide E (OATP-E) in human placenta. *Placenta* **24**, 144–148 (2003).

27. Mikkaichi, T. *et al.* Isolation and characterization of a digoxin transporter and its rat homologue expressed in the kidney. *Proc. Natl. Acad. Sci. U. S. A.* **101**, 3569–3574 (2004).

28. Kindla, J. *et al.* Expression and localization of the uptake transporters OATP2B1, OATP3A1 and OATP5A1 in non-malignant and malignant breast tissue. *Cancer Biol Ther* **11**, 584–591 (2011).

29. Okabe, M. *et al.* Profiling SLCO and SLC22 genes in the NCI-60 cancer cell lines to identify drug uptake transporters. *Mol. Cancer Ther.* **7**, 3081–3091 (2008).

30. Obaidat, A., Roth, M. & Hagenbuch, B. The Expression and Function of Organic Anion Transporting Polypeptides in Normal Tissues and in Cancer. *Annu Rev Pharmacol Toxicol.* **52**, 135–151 (2012).

31. Lee, S.-Y. *et al.* Identification of the gonad-specific anion transporter SLCO6A1 as a cancer/testis (CT) antigen expressed in human lung cancer. *Cancer Immun.* **4**, 13 (2004).

32. Hagenbuch, B. & Meier, P. J. The superfamily of organic anion transporting polypeptides. *Biochim. Biophys. Acta* **1609**, 1–18 (2003).

33. Taylor-Wells, J. & Meredith, D. The Signature Sequence Region of the Human Drug Transporter Organic Anion Transporting Polypeptide 1B1 Is Important for Protein Surface Expression. *J. Drug Deliv.* **2014**, 1–10 (2014).

34. Emanuel Hanggi, Anne Freimoser Grundschober, Simone Leuthold, Peter J. Meier, and M. V. S.-P. *et al.* Functional Analysis of the Extracellular Cysteine Residues in the Human Organic Anion Transporting Polypeptide , OATP2B1. *Mol. Pharmacol.* **70**, 806–817 (2006).

35. Roth, M., Obaidat, A. & Hagenbuch, B. OATPs, OATs and OCTs: the organic anion and cation transporters of the SLCO and SLC22A gene superfamilies. *Br. J. Pharmacol.* **165**, 1260–87 (2012).

36. Tusnády, G. E. & Simon, I. The HMMTOP transmembrane topology prediction server. *Bioinformatics* **17**, 849–850 (2001).

37. Wang, P. *et al.* Interaction with PDZK1 is required for expression of organic anion transporting protein 1A1 on the hepatocyte surface. *J. Biol. Chem.* **280**, 30143–9 (2005).

38. Kato, Y., Yoshida, K., Watanabe, C., Sai, Y. & Tsuji, A. Screening of the Interaction Between Xenobiotic Transporters and PDZ Proteins. *Pharm. Res.* **21**, 1886–1894 (2004).

39. Yao, J. *et al.* N-Glycosylation dictates proper processing of organic anion transporting polypeptide 1B1. *PLoS One* **7**, e52563 (2012).

40. Leuthold, S. *et al.* Mechanisms of pH-gradient driven transport mediated by organic anion polypeptide transporters. *Am. J. Physiol. Cell Physiol.* **296**, C570–C582 (2009).

41. Meier-Abt, F., Mokrab, Y. & Mizuguchi, K. Organic anion transporting polypeptides of the OATP/SLCO superfamily: identification of new members in nonmammalian species, comparative modeling and a potential transport mode. *J. Membr. Biol.* **208**, 213–227 (2005).

42. Nozawa, T., Imai, K., Nezu, J.-I., Tsuji, A. & Tamai, I. Functional characterization of pH-sensitive organic anion transporting polypeptide OATP-B in human. *J. Pharmacol. Exp. Ther.* **308**, 438–45 (2004).

43. Varma, M. V *et al.* pH-Sensitive Interaction of HMG-CoA Reductase Inhibitors (Statins) with Organic Anion Transporting Polypeptide 2B1. *Mol. Pharm.* **8**, 1303–1313 (2011).

44. Gui, C. *et al.* Effect of pregnane X receptor ligands on transport mediated by human OATP1B1 and OATP1B3. *Eur. J. Pharmacol.* **584**, 57–65 (2008).

45. Stieger, Bruno; Hagenbuch, B. Organic Anion-Transporting Polypeptides. in *Current topics in Membranes* **73**, 205–232 (2014).

46. Funk, C. The role of hepatic transporters in drug elimination. *Expert Opin. Drug Metab. Toxicol.* **4**, 363–379 (2008).

47. Keogh, J. P. Membrane Transporters in Drug Development. *Adv. Pharmacol.* **63**, 1–42 (2012).

48. Generaux, G. T., Bonomo, F. M., Johnson, M. & Doan, K. M. M. Impact of SLCO1B1 (OATP1B1) and ABCG2 (BCRP) genetic polymorphisms and inhibition on LDL-C lowering and myopathy of statins. *Xenobiotica.* **41**, 639–51 (2011).

49. Chu, X., Bleasby, K. & Evers, R. Species differences in drug transporters and implications for translating preclinical findings to humans. *Expert Opin. Drug Metab. Toxicol.* **5255**, 1–16 (2012).

50. SEARCH Collaborative Group *et al.* SLCO1B1 Variants and Statin-Induced Myopathy — A Genomewide Study. *N. Engl. J. Med.* **359**, 789–799 (2008).

51. Kullak-Ublick, G. a *et al.* Molecular and functional characterization of an organic anion transporting polypeptide cloned from human liver. *Gastroenterology* **109**, 1274–82 (1995).

52. Ismair, M. G. *et al.* Hepatic uptake of cholecystokinin octapeptide by organic anion-transporting polypeptides OATP4 and OATP8 of rat and human liver. *Gastroenterology* **121**, 1185–90 (2001).

53. Lu, R., Kanai, N., Bao, Y. & Schuster, V. L. Cloning, in vitro expression, and tissue distribution of a human prostaglandin transporter cDNA(hPGT). *J. Clin. Invest.* **98**, 1142–9 (1996).

54. Hagenbuch, B. & Gui, C. Xenobiotic transporters of the human organic anion transporting polypeptides (OATP) family. *Xenobiotica.* **38**, 778–801 (2008).

55. Yamaguchi, H. *et al.* Transport of estrone 3-sulfate mediated by organic anion transporter OATP4C1: estrone 3-sulfate binds to the different recognition site for digoxin in OATP4C1. *Drug Metab. Pharmacokinet.* **25**, 314–317 (2010).

56. Van De Steeg, E. *et al.* Complete OATP1B1 and OATP1B3 deficiency causes human Rotor syndrome by interrupting conjugated bilirubin reuptake into the liver. *J. Clin. Invest.* **122**, 519–528 (2012).

57. Sanchez-Contreras, M. Y. *et al.* Replication of progressive supranuclear palsy genome-wide association study identifies SLCO1A2 and DUSP10 as new susceptibility loci. *Mol. Neurodegener.* **13**, 1–10 (2018).

58. Khan, R. A. W. *et al.* Analysis of association between common variants in the SLCO6A1 gene with schizophrenia, bipolar disorder and major depressive disorder in the Han Chinese population. *World J. Biol. Psychiatry* **17**, 140–146 (2016).

59. Ripke, S. *et al.* Genome-wide association analysis identifies 13 new risk loci for schizophrenia. *Nat. Genet.* **45**, 1150–1159 (2013).

60. Kenny, E. E. *et al.* A genome-wide scan of Ashkenazi Jewish Crohn's disease suggests novel susceptibility loci. *PLoS Genet.* **8**, e1002559 (2012).

61. Strømme, P. *et al.* Mutated thyroid hormone transporter OATP1C1 associates with severe brain hypometabolism and juvenile neurodegeneration. *Thyroid* **28**, 1406–1415 (2018).

62. Liu, T. & Li, Q. Organic anion-transporting polypeptides: a novel approach for cancer therapy. *J. Drug Target.* **22**, 14–22 (2014).

63. Tamai, I. Oral drug delivery utilizing intestinal OATP transporters. *Advanced Drug Delivery Reviews* **64**, 508–514 (2012).

64. Schulte, R. R. & Ho, R. H. Organic anion transporting polypeptides: Emerging roles in cancer pharmacology. *Mol. Pharmacol.* **95**, 490–506 (2019).

65. Thakkar, N., Lockhart, A. C. & Lee, W. Role of Organic Anion-Transporting Polypeptides (OATPs) in Cancer Therapy. *AAPS J.* **17**, 535–45 (2015).

66. Zu Schwabedissen, H. E. M., Tirona, R. G., Yip, C. S., Ho, R. H. & Kim, R. B. Interplay between the nuclear receptor pregnane X receptor and the uptake transporter organic anion transporter polypeptide 1A2 selectively enhances estrogen effects in breast cancer. *Cancer Res.* **68**, 9338–9347 (2008).

67. Muto, M. *et al.* Human liver-specific organic anion transporter-2 is a potent prognostic factor for human breast carcinoma. *Cancer Sci.* **98**, 1570–1576 (2007).

68. Nozawa, T. *et al.* Involvement of estrone-3-sulfate transporters in proliferation of hormone-dependent breast cancer cells. *J Pharmacol Exp Ther* **311**, 1032–1037 (2004).

69. Wright, J. L. *et al.* Expression of SLCO transport genes in castration-resistant prostate cancer and impact of genetic variation in SLCO1B3 and SLCO2B1 on prostate cancer outcomes. *Cancer Epidemiol Biomarkers PrevCancer Epidemiol. Biomarkers Prev.* **20**, 619–627 (2011).

70. Hamada, A. *et al.* Effect of SLCO1B3 haplotype on testosterone transport and clinical outcome in caucasian patients with androgen-independent prostatic cancer. *Clin Cancer Res* **14**, 3312–3318 (2008).

71. Furihata T, Sun Y, C. K. Cancer-type Organic Anion Transporting Polypeptide 1B3: Current Knowledge of the Gene Structure, Expression Profile, Functional Implications and Future Perspectives. *Curr. Drug Metab.* **16**, 474–85. (2015).

72. Nagai, M. *et al.* Identification of a new organic anion transporting polypeptide 1B3 mRNA isoform

primarily expressed in human cancerous tissues and cells. *Biochem. Biophys. Res. Commun.* **418**, 818–23 (2012).

73. Thakkar, N. *et al.* A cancer-specific variant of the SLCO1B3 gene encodes a novel human organic anion transporting polypeptide 1B3 (OATP1B3) localized mainly in the cytoplasm of colon and pancreatic cancer cells. *Mol. Pharm.* **10**, 406–16 (2013).

74. Imai, S. *et al.* Epigenetic regulation of organic anion transporting polypeptide 1b3 in cancer cell lines. *Pharm. Res.* **30**, 2880–2890 (2013).

75. Sun Y, Harada M, Shimozato O, Souda H, Takiguchi N, Nabeya Y, Kamijo T, Akita H, Anzai N, Chiba K, F. T. Cancer-type OATP1B3 mRNA has the potential to become a detection and prognostic biomarker for human colorectal cancer. *Biomark Med* **Jun 8**, (2017).

76. Morio, H. *et al.* Cancer-Type OATP1B3 mRNA in extracellular vesicles as a promising candidate for a serum-based colorectal cancer biomarker. *Biol. Pharm. Bull.* **41**, 445–449 (2018).

77. Sun, Y. *et al.* Cancer-type organic anion transporting polypeptide 1B3 is a target for cancer suicide gene therapy using RNA trans -splicing technology. *Cancer Lett.* **433**, 107–116 (2018).

78. Alam, K. *et al.* Regulation of organic anion transporting polypeptides (OATP) 1B1- and OATP1B3-mediated transport: An updated review in the context of OATP-mediated drug-drug interactions. *Int. J. Mol. Sci.* **19**, 1–20 (2018).

79. Shitara, Y. & Sugiyama, Y. Preincubation-dependent and long-lasting inhibition of organic anion transporting polypeptide (OATP) and its impact on drug-drug interactions. *Pharmacol. Ther.* **177**, 67–80 (2017).

80. Ivanyuk, A., Livio, F., Biollaz, J. & Buclin, T. Renal Drug Transporters and Drug Interactions. *Clin. Pharmacokinet.* **56**, 825–892 (2017).

81. Tamai, I. & Nakanishi, T. OATP transporter-mediated drug absorption and interaction. *Curr. Opin. Pharmacol.* **13**, 859–863 (2013).

82. Yu, J., Petrie, I. D., Levy, R. H. & Ragueneau-Majlessi, I. Mechanisms and clinical significance of pharmacokinetic-based drug-drug interactions with drugs approved by the U.S. Food and drug administration in 2017 s. *Drug Metab. Dispos.* **47**, 135–144 (2019).

83. Yee, S. W. *et al.* Influence of Transporter Polymorphisms on Drug Disposition and Response: A Perspective from the International Transporter Consortium. *Clin. Pharmacol. Ther.* **104**, 803–817 (2018).

84. European Medicines Agency. Guideline on key aspects for the use of pharmacogenomic methodologies in the pharmacovigilance evaluation of medicinal products (Draft). *Ema/281371/2013* **44**, 1–18 (2014).

85. Kato, K. *et al.* Intestinal absorption mechanism of tebipenem pivoxil, a novel oral carbapenem: Involvement of human OATP family in apical membrane transport. *Mol. Pharm.* **7**, 1747–1756 (2010).

86. Gao, B. *et al.* Organic anion-transporting polypeptides mediate transport of opioid peptides across blood-brain barrier. *J. Pharmacol. Exp. Ther.* **294**, 73–9 (2000).

87. van Montfoort JE1, Müller M, Groothuis GM, Meijer DK, Koepsell H, M. P. Comparison of " Type I " and " Type II " Organic Cation Transport by Organic Cation Transporters and Organic Anion-Transporting Polypeptides. *J Pharmacol Exp Ther.* **298**, 110–115 (2001).

88. Badagnani, I. *et al.* Interaction of Methotrexate with Organic-Anion Transporting Polypeptide 1A2

and Its Genetic Variants. *J. Pharmacol. Exp. Ther.* **318**, 521–529 (2006).

89. Yamakawa, Y. *et al.* Pharmacokinetic impact of SLCO1A2 polymorphisms on imatinib disposition in patients with chronic myeloid leukemia. *Clin. Pharmacol. Ther.* **90**, 157–163 (2011).

90. Misaka, S. *et al.* Green tea ingestion greatly reduces plasma concentrations of nadolol in healthy subjects. *Clin. Pharmacol. Ther.* **95**, 432–8 (2014).

91. Shirasaka, Y. *et al.* Species Difference in the Effect of Grapefruit Juice on Intestinal Absorption of Talinolol between Human and Rat. *J. Pharmacol. Exp. Ther.* **332**, 181–189 (2010).

92. Glaeser, H. *et al.* Intestinal drug transporter expression and the impact of grapefruit juice in humans. *Clin. Pharmacol. Ther.* **81**, 362–370 (2007).

93. Bailey, D. G., Dresser, G. K., Leake, B. F. & Kim, R. B. Naringin is a major and selective clinical inhibitor of organic anion-transporting polypeptide 1A2 (OATP1A2) in grapefruit juice. *Clin Pharmacol Ther* **81**, 495–502 (2007).

94. Su, Y., Zhang, X. & Sinko, P. J. Human organic anion-transporting polypeptide OATP-A (SLC21A3) acts in concert with P-glycoprotein and multidrug resistance protein 2 in the vectorial transport of Saquinavir in Hep G2 cells. *Mol. Pharm.* **1**, 49–56 (2004).

95. Shirasaka, Y., Suzuki, K., Nakanishi, T. & Tamai, I. Intestinal absorption of HMG-CoA reductase inhibitor pravastatin mediated by organic anion transporting polypeptide. *Pharm. Res.* **27**, 2141–2149 (2010).

96. Fischer, W. J. *et al.* Organic anion transporting polypeptides expressed in liver and brain mediate uptake of microcystin. *Toxicol. Appl. Pharmacol.* **203**, 257–263 (2005).

97. Bexten, M. *et al.* Expression of drug transporters and drug metabolizing enzymes in the bladder urothelium in man and affinity of the bladder spasmolytic trospium chloride to transporters likely involved in its pharmacokinetics. *Mol. Pharm.* **12**, 171–178 (2015).

98. Cheng, Z. *et al.* Hydrophilic anti-migraine triptans are substrates for OATP1A2, a transporter expressed at human blood-brain barrier. *Xenobiotica.* **42**, 880–90 (2012).

99. Gong, I. Y. & Kim, R. B. Impact of genetic variation in OATP transporters to drug disposition and response. *Drug Metab. Pharmacokinet.* **28**, 4–18 (2013).

100. König, J., Seithel, A., Gradhand, U. & Fromm, M. F. Pharmacogenomics of human OATP transporters. *Naunyn. Schmiedebergs. Arch. Pharmacol.* **372**, 432–443 (2006).

101. Dresser, G. K. *et al.* Fruit juices inhibit organic anion transporting polypeptide-mediated drug uptake to decrease the oral availability of fexofenadine. *Clin. Pharmacol. Ther.* **71**, 11–20 (2002).

102. Iusuf, D. *et al.* Human OATP1B1, OATP1B3 and OATP1A2 can mediate the in vivo uptake and clearance of docetaxel. *Int J Cancer* **136**, 225–233 (2015).

103. Parvez, M. M., Jung, J.-A., Shin, H.-J., Kim, D. H. & Shin, J.-G. Characterization of 22 anti-tuberculosis drugs for the inhibitory interaction potential on organic anionic transporter polypeptides (OATPs) mediated uptake. *Antimicrob. Agents Chemother.* **60**, 3096–3105 (2016).

104. Karlgren, M. *et al.* Classi fi cation of Inhibitors of Hepatic Organic Anion Transporting Polypeptides (OATPs): In fl uence of Protein Expression on Drug − Drug Interactions. *J. Med. Chem.* **55**, 4740–4763 (2012).

105. Lee, H. H. *et al.* Contribution of Hepatic Organic Anion-Transporting Polypeptides to Docetaxel Uptake and Clearance. *Mol. Cancer Ther.* **14**, 994–1003 (2015).

106. Brenner, S. *et al.* The effect of organic anion-transporting polypeptides 1B1, 1B3 and 2B1 on the antitumor activity of flavopiridol in breast cancer cells. *Int. J. Oncol.* **46**, 324–332 (2015).

107. Cynthia S. Lancaster, Jason A. Sprowl1, Aisha L. Walker, Shuiying Hu, A. A. G. & Sparreboom, and A. S. Modulation of OATP1B-type Transporter Function Alters Cellular Uptake and Disposition of Platinum Chemotherapeutics. *Mol. Cancer Ther.* **12**, 1537–1544 (2013).

108. Zimmerman, E. I. *et al.* Contribution of OATP1B1 and OATP1B3 to the disposition of sorafenib and sorafenib-glucuronide. *Clin. Cancer Res.* **19**, 1458–66 (2013).

109. Treiber, A., Schneiter, R., Häusler, S. & Stieger, B. Bosentan is a substrate of human OATP1B1 and OATP1B3: Inhibition of hepatic uptake as the common mechanism of its interactions with cyclosporin A, rifampicin, and sildenafil. *Drug Metab. Dispos.* **35**, 1400–1407 (2007).

110. Yamashiro W, Maeda K, Hirouchi M, Adachi Y, Hu Z, S. Y. Involvement of transporters in the hepatic uptake and biliary excretion of valsartan, a selective antagonist of the angiotensin II AT1-receptor, in humans. *Drug Metab. Dispos.* **34**, 1247–1254 (2006).

111. König, J. *et al.* Role of organic anion-transporting polypeptides for cellular mesalazine (5-aminosalicylic acid) uptake. *Drug Metab. Dispos.* **39**, 1097–1102 (2011).

112. Shitara, Y., Itoh, T., Sato, H., Li, A. P. & Sugiyama, Y. Inhibition of transporter-mediated hepatic uptake as a mechanism for drug-drug interaction between cerivastatin and cyclosporin A. *J. Pharmacol. Exp. Ther.* **304**, 610–616 (2003).

113. Shitara, Y., Hirano, M., Sato, H. & Sugiyama, Y. Gemfibrozil and Its Glucuronide Inhibit the Organic Anion Transporting Polypeptide 2 (OATP2/OATP1B1:SLC21A6)- Mediated Hepatic Uptake and CYP2C8-Mediated Metabolism of Cerivastatin: Analysis of the Mechanism of the Clinically Relevant Drug-Drug Interactio. *J. Pharmacol. Exp. Ther.* **311**, 228–236 (2004).

114. Monks, N. R. *et al.* Potent cytotoxicity of the phosphatase inhibitor microcystin LR and microcystin analogues in OATP1B1- and OATP1B3-expressing HeLa cells. *Mol. Cancer Ther.* **6**, 587–98 (2007).

115. Karlgren, M. *et al.* In Vitro and in silico strategies to identify OATP1B1 Inhibitors and Predict Clinical Drug-Drug Interactions. *Pharm. Res.* **29**, 411–426 (2012).

116. Prueksaritanont, T. *et al.* Pitavastatin is a more sensitive and selective organic anion-transporting polypeptide 1B clinical probe than rosuvastatin. *Br. J. Clin. Pharmacol.* **78**, 587–598 (2014).

117. Smith, N. F. *et al.* Variants in the SLCO1B3 gene: interethnic distribution and association with paclitaxel pharmacokinetics. *Clin. Pharmacol. Ther.* **81**, 76–82 (2007).

118. Nambu, T. *et al.* Association of SLCO1B3 polymorphism with intracellular accumulation of imatinib in leukocytes in patients with chronic myeloid leukemia. *Biol. Pharm. Bull.* **34**, 114–119 (2011).

119. Mandery, K. *et al.* Influence of cyclooxygenase inhibitors on the function of the prostaglandin transporter organic anion-transporting polypeptide 2A1 expressed in human gastroduodenal mucosa. *J. Pharmacol. Exp. Ther.* **332**, 345–351 (2010).

120. Glaeser, H., Bujok, K., Schmidt, I., Fromm, M. F. & Mandery, K. Organic anion transporting polypeptides and organic cation transporter 1 contribute to the cellular uptake of the flavonoid quercetin. *Naunyn. Schmiedebergs. Arch. Pharmacol.* **387**, 883–891 (2014).

121. Scialis, R. J. & Manautou, J. E. Elucidation of the Mechanisms through Which the Reactive Metabolite Diclofenac Acyl Glucuronide Can Mediate Toxicity. *J. Pharmacol. Exp. Ther.* **357**, 167–176 (2016).

122. Wei, S. C. *et al.* SLCO3A1, a novel Crohn's disease-associated gene, regulates NF-kB activity and associates with intestinal perforation. *PLoS One* **9**, e100515 (2014).

123. Chu, X. Y. *et al.* Transport of the dipeptidyl peptidase-4 inhibitor sitagliptin by human organic anion transporter 3, organic anion transporting polypeptide 4C1, and multidrug resistance P-glycoprotein. *J Pharmacol Exp Ther* **321**, 673–683 (2007).

124. He, J., Yu, Y., Prasad, B., Chen, X. & Unadkat, J. D. Mechanism of an unusual, but clinically significant, digoxin-bupropion drug interaction. *Biopharm. Drug Dispos.* **35**, 253–263 (2014).

125. Toyohara, T. *et al.* SLCO4C1 transporter eliminates uremic toxins and attenuates hypertension and renal inflammation. *Ther. Res.* **31**, 1221–1223 (2010).

126. Hamilton *et al.* Organic Anion Transporting Polypeptide 5A1 (OATP5A1) in Small Cell Lung Cancer (SCLC) Cells: Possible Involvement in Chemoresistance to Satraplatin. *Biomark. Cancer* **Jun**, 31–40 (2011).

127. Solon, E. G. Use of radioactive compounds and autoradiography to determine drug tissue distribution. *Chem. Res. Toxicol.* **25**, 543–555 (2012).

128. Hong Lu, Supratim Choudhuri, K. O. et al. *et al.* Characterization of Organic Anion Transporting Polypeptide 1b2-null Mice: Essential Role in Hepatic Uptake/Toxicity of Phalloidin. *Toxicol Sci* **May**, 35–45 (2008).

129. Kanai, N., Lu, R., Bao, Y., Wolkoff, a W. & Schuster, V. L. Transient expression of oatp organic anion transporter in mammalian cells: identification of candidate substrates. *Am. J. Physiol.* **270**, F319-25 (1996).

130. Hirano, M., Maeda, K., Shitara, Y. & Sugiyama, Y. Drug-drug interaction between pitavastatin and various drugs via OATP1B1. *Drug Metab. Dispos.* **34**, 1229–1236 (2006).

131. De Bruyn, T. *et al.* Sodium Fluorescein is a Probe Substrate for Hepatic Drug Transport Mediated by OATP1B1 and OATP1B3. *J. Pharm. Sci.* **100**, 5018–5030 (2011).

132. Gui, C., Obaidat, A., Chaguturu, R. & Hagenbuch, B. Development of a cell-based high-throughput assay to screen for inhibitors of organic anion transporting polypeptides 1B1 and 1B3. *Curr. Chem. Genomics* **4**, 1–8 (2010).

133. Izumi, S. *et al.* Investigation of Fluorescein Derivatives as Substrates of Organic Anion Transporting Polypeptide (OATP) 1B1 To Develop Sensitive Fluorescence-Based OATP1B1 Inhibition Assays. *Mol Pharm* **13**, 438–448 (2016).

134. Yamaguchi, H. *et al.* Transport of fluorescent chenodeoxycholic acid via the human organic anion transporters OATP1B1 and OATP1B3. *J. Lipid Res.* **47**, 1196–1202 (2006).

135. de Waart, D. R. *et al.* Hepatic transport mechanisms of cholyl-L-lysyl-fluorescein. *J. Pharmacol. Exp. Ther.* **334**, 78–86 (2010).

136. Patik, I. *et al.* Functional expression of the 11 human Organic Anion Transporting Polypeptides in insect cells reveals that sodium fluorescein is a general OATP substrate. *Biochem. Pharmacol.* **98**, 649–658 (2015).

137. Martin, M. M. & Lindqvist, L. The pH dependence of fluorescein fluorescence. *J. Lumin.* **10**, 381–390 (1975).

138. Doughty, M. J. PH dependent spectral properties of sodium fluorescein ophthalmic solutions revisited. *Ophthalmic Physiol. Opt.* **30**, 167–174 (2010).

139. Kullak-Ublick, G. a. *et al.* Organic anion-transporting polypeptide B (OATP-B) and its functional comparison with three other OATPs of human liver. *Gastroenterology* **120**, 525–533 (2001).

140. Bakos, É. *et al.* A novel fluorescence-based functional assay for human OATP1A2 and OATP1C1 identifies interaction between third-generation P-gp inhibitors and OATP1A2. *FEBS J.* (2019). doi:10.1111/febs.15156

141. Forster, S., Thumser, A. E., Hood, S. R. & Plant, N. Characterization of rhodamine-123 as a tracer dye for use in in vitro drug transport assays. *PLoS One* **7**, (2012).

142. Patik, I. *et al.* Identification of novel cell-impermeant fluorescent substrates for testing the function and drug interaction of Organic Anion-Transporting Polypeptides, OATP1B1/1B3 and 2B1. *Sci. Rep.* **8**, 2630 (2018).

143. Izumi, S. *et al.* Substrate-dependent inhibition of organic anion transporting polypeptide 1B1: comparative analysis with prototypical probe substrates estradiol-17β-glucuronide, estrone-3-sulfate, and sulfobromophthalein. *Drug Metab. Dispos.* **41**, 1859–1866 (2013).

144. Oshida, K., Shimamura, M., Seya, K., Ando, A. & Miyamoto, Y. Identification of Transporters Involved in Beraprost Sodium Transport In Vitro. *Eur. J. Drug Metab. Pharmacokinet.* **42**, 117–128 (2017).

145. Abe, T. *et al.* Identification of a novel gene family encoding human liver-specific organic anion transporter LST-1. *J. Biol. Chem.* **274**, 17159–17163 (1999).

146. Schnell, C. *et al.* The multispecific thyroid hormone transporter OATP1C1 mediates cell-specific sulforhodamine 101-labeling of hippocampal astrocytes. *Brain Struct. Funct.* **220**, 193–203 (2013).

147. van Montfoort, J. E. *et al.* Polyspecific organic anion transporting polypeptides mediate hepatic uptake of amphipathic type II organic cations. *J. Pharmacol. Exp. Ther.* **291**, 147–52 (1999).

148. Hu, S. *et al.* Interaction of imatinib with human organic ion carriers. *Clin. Cancer Res.* **14**, 3141–3148 (2008).

149. De Graaf, W. *et al.* Transporters involved in the hepatic uptake of 99mTc-mebrofenin and indocyanine green. *J. Hepatol.* **54**, 738–745 (2011).

150. Kanai, N. *et al.* Identification and characterization of a prostaglandin transporter. *Science (80-.).* **268**, 866–869 (1995).

151. Tschantz, W. R. *et al.* Expression, purification and characterization of the human membrane transporter protein OATP2B1 from Sf9 insect cells. *Protein Expr. Purif.* **57**, 163–71 (2008).

152. Sai, Y. *et al.* Predominant contribution of organic anion transporting polypeptide OATP-B (OATP2B1) to apical uptake of estrone-3-sulfate by human intestinal Caco-2 cells. *Drug Metab. Dispos.* **34**, 1423–1431 (2006).

153. Lee, W. *et al.* Overexpression of OATP1B3 confers apoptotic resistance in colon cancer. *Cancer Res.* **68**, 10315–23 (2008).

154. Wen Zhao, Jeremiah D. Zitzow, Y. W. et al. Organic Anion Transporting Polypeptides Contribute to the Disposition of Perfluoroalkyl Acids in Humans and Rats. *Toxicol Sci* **156**, 84–95 (2017).

155. Satlin, Lisa M.;Amin, Vipul; Wolkoff, A. W. *et al.* Organic Anion Transporting Polypeptide Mediates Organic Anion/HCO3- Exchange*. *J. Biol. Chem.* **272**, 26340–26345 (1997).

156. Lu, J. *et al.* Effects of beta-blockers and tricyclic antidepressants on the activity of human organic anion transporting polypeptide 1A2 (OATP1A2). *J Pharmacol Exp Ther* **352**, 552–558 (2015).

157. Durmus, S. *et al.* In vivo disposition of doxorubicin is affected by mouse Oatp1a/1b and human OATP1A/1B transporters. *Int. J. Cancer* **135**, 1700–1710 (2014).

158. Jung, D. *et al.* Characterization of the human OATP-C (SLC21A6) gene promoter and regulation of liver-specific OATP genes by hepatocyte nuclear factor 1 alpha. *J. Biol. Chem.* **276**, 37206–37214 (2001).

159. César-Razquin, A. *et al.* A Call for Systematic Research on Solute Carriers. *Cell* **162**, 478–487 (2015).

160. Kopplow, K., Letschert, K., König, J., Walter, B. & Keppler, D. Human Hepatobiliary Transport of Organic Anions Analyzed by Quadruple-Transfected Cells. *Mol. Pharmacol.* **68**, 1031–1038 (2005).

161. Sato, T. *et al.* Single Lgr5 stem cells build crypt-villus structures in vitro without a mesenchymal niche. *Nature* **459**, 262–5 (2009).

162. Sawant-basak, A. & Obach, R. S. Emerging Models of Drug Metabolism , Transporters , and Toxicity. *Drug Metab Dispos* **46**, 1556–1561 (2018).

163. Godoy, P. *et al. Recent advances in 2D and 3D in vitro systems using primary hepatocytes, alternative hepatocyte sources and non-parenchymal liver cells and their use in investigating mechanisms of hepatotoxicity, cell signaling and ADME. Archives of Toxicology* **87**, (2013).

164. Li, M., de Graaf, I. A. M. & Groothuis, G. M. M. Precision-cut intestinal slices: alternative model for drug transport, metabolism, and toxicology research. *Expert Opin. Drug Metab. Toxicol.* **12**, 175–190 (2016).

165. Contreras-Gómez, A., Sánchez-Mirón, A., García-Camacho, F., Molina-Grima, E. & Chisti, Y. Protein production using the baculovirus-insect cell expression system. *Biotechnol. Prog.* **30**, 1–18 (2014).

166. Vaidyanathan, J., Yoshida, K., Arya, V. & Zhang, L. Comparing Various In Vitro Prediction Criteria to Assess the Potential of a New Molecular Entity to Inhibit Organic Anion Transporting Polypeptide 1B1. *J. Clin. Pharmacol.* **56**, S59–S72 (2016).

167. Evers, R. & Chu, X. Y. Role of the murine organic anion-transporting polypeptide 1b2 (Oatp1b2) in drug disposition and hepatotoxicity. *Mol Pharmacol* **74**, 309–311 (2008).

168. Zaher, H. *et al.* Targeted disruption of murine organic anion-transporting polypeptide 1b2 (oatp1 b2/slco1b2) significantly alters disposition of prototypical drug substrates pravastatin and rifampin. *Mol. Pharmacol.* **74**, 320–329 (2008).

169. Durmus, S. *et al.* Preclinical Mouse Models To Study Human OATP1B1- and OATP1B3-Mediated Drug-Drug Interactions in Vivo. *Mol Pharm* **12**, 4259–4269 (2015).

170. Durmus, S., van Hoppe, S. & Schinkel, A. H. The impact of Organic Anion-Transporting Polypeptides (OATPs) on disposition and toxicity of antitumor drugs: Insights from knockout and humanized mice. *Drug Resist. Updat.* **27**, 72–88 (2016).

171. Kaneko, K. ichi *et al.* A clinical quantitative evaluation of hepatobiliary transport of [11 C] Dehydropravastatin in humans using positron emission tomography. *Drug Metab. Dispos.* **46**, 719–728 (2018).

172. Shingaki, T. *et al.* Evaluation of oatp and Mrp2 activities in hepatobiliary excretion using newly developed positron emission tomography tracer [11C] dehydropravastatin in rats. *J. Pharmacol. Exp. Ther.* **347**, 193–202 (2013).

173. Bauer, M. *et al.* Influence of OATPs on Hepatic Disposition of Erlotinib Measured With Positron

Emission Tomography. *Clin. Pharmacol. Ther.* **104**, 139–147 (2018).

174. A. Ufuk, R. E. Kosa, H. Gao, YA. Bi, S. Modi, D. Gates, A. D. Rodrigues, L. M. Tremaine , M. V. S. Varma, J. B. H. and A. G. In vitro – in vivo extrapolation of OATP1B-mediated drug-drug interactions in cynomolgus monkey. *J. Pharmacol. Exp. Ther.* **365**, 1–43 (2018).

175. Shen, H. *et al.* Evaluation of rosuvastatin as an organic anion transporting polypeptide (OATP) probe substrate: in vitro transport and in vivo disposition in cynomolgus monkeys. *J. Pharmacol. Exp. Ther.* **353**, 380–91 (2015).

176. Shen, H. *et al.* Coproporphyrins I and III as Functional Markers of OATP1B Activity: In Vitro and In Vivo Evaluation in Preclinical Species. *J Pharmacol Exp Ther* **357**, 382–393 (2016).

177. Shitara, Y. *et al.* Clinical significance of organic anion transporting polypeptides (OATPs) in drug disposition: Their roles in hepatic clearance and intestinal absorption. *Biopharm. Drug Dispos.* **34**, 45–78 (2013).

178. Maeda, K. & K., M. Organic anion transporting polypeptide (OATP)1B1 and OATP1B3 as important regulators of the pharmacokinetics of substrate drugs. *Biol. Pharm. Bull.* **38**, 155–168 (2015).

179. Huang, S.-M., Zhang, L. & Giacomini, K. M. The International Transporter Consortium: a collaborative group of scientists from academia, industry, and the FDA. *Clin. Pharmacol. Ther.* **87**, 32–36 (2010).

180. Morrissey, K. M. *et al.* The UCSF-FDA TransPortal: a public drug transporter database. *Clin. Pharmacol. Ther.* **92**, 545–6 (2012).

181. Kienana, M. *et al.* Endogenous metabolites that are substrates of Organic Anion Transporter's (OATs) predict methotrexate clearance. *Pharmacol. Res.* 121–132 (2016). doi:10.1016/j.phrs.2016.05.021

182. Baldes, C. *et al.* Development of a fluorescence-based assay for screening of modulators of human Organic Anion Transporter 1B3 (OATP1B3). *Eur. J. Pharm. Biopharm.* **62**, 39–43 (2006).

183. Özvegy, C. *et al.* Characterization of drug transport, ATP hydrolysis, and nucleotide trapping by the human ABCG2 multidrug transporter. Modulation of substrate specificity by a point mutation. *J. Biol. Chem.* **277**, 47980–47990 (2002).

184. Vaughn, J. L., Goodwin, R. H., Tompkins, G. J. & McCawley, P. The establishment of two cell lines from the insect spodoptera frugiperda (lepidoptera; noctuidae). *In Vitro* **13**, 213–217 (1977).

185. Schneider, E. H. & Seifert, R. Sf9 cells: A versatile model system to investigate the pharmacological properties of G protein-coupled receptors. *Pharmacol. Ther.* **128**, 387–418 (2010).

186. Stieger, B., Fattinger, K., Madon, J., Kullak-Ublick, G. a & Meier, P. J. Drug- and Estrogen-Induced Cholestasis through Inhibition of the Hepatocellular Bile Salt Export Pump (Bsep) of Rat Liver. *Gastroenterology* **118**, 422–430 (2000).

187. Ozvegy, C. *et al.* Functional characterization of the human multidrug transporter, ABCG2, expressed in insect cells. *Biochem. Biophys. Res. Commun.* **285**, 111–117 (2001).

188. Vidigal, J. *et al.* A cell sorting protocol for selecting high-producing sub-populations of Sf9 and High Five™ cells. *J. Biotechnol.* **168**, 436–439 (2013).

189. Shi, X. & Jarvis, D. Protein N-Glycosylation in the Baculovirus-Insect Cell System. *Curr. Drug Targets* **8**, 1116–1125 (2007).

190. Sarkadi, B., Price, E. M., Boucher, R. C., Germann, U. A. & Scarborough, G. A. Expression of the human multidrug resistance cDNA in insect cells generates a high activity drug-stimulated membrane

ATPase. *J. Biol. Chem.* **267**, 4854–4858 (1992).

191. Szakács, G., Ozvegy, C., Bakos, E., Sarkadi, B. & Váradi, A. Role of glycine-534 and glycine-1179 of human multidrug resistance protein (MDR1) in drug-mediated control of ATP hydrolysis. *Biochem. J.* **356**, 71–75 (2001).

192. Holló, Z., Homolya, L., Davis, C. W. & Sarkadi, B. Calcein accumulation as a fluorometric functional assay of the multidrug transporter. *BBA - Biomembr.* **1191**, 384–388 (1994).

193. Meier-Abt, F., Faulstich, H. & Hagenbuch, B. Identification of phalloidin uptake systems of rat and human liver. *Biochim. Biophys. Acta - Biomembr.* **1664**, 64–69 (2004).

194. Grube, M. *et al.* Modification of OATP2B1-mediated transport by steroid hormones. *Mol. Pharmacol.* **70**, 1735–1741 (2006).

195. Kindla, J., Müller, F., Mieth, M., Fromm, M. F. & König, J. Influence of non-steroidal anti-inflammatory drugs on Organic Anion Transporting Polypeptide (OATP) 1B1- and OATP1B3-mediated drug transport. *Drug Metab. Dispos.* **39**, 1047–1053 (2011).

196. Yamaguchi, H. *et al.* Rapid screening of antineoplastic candidates for the human organic anion transporter OATP1B3 substrates using fluorescent probes. *Cancer Lett.* **260**, 163–169 (2008).

197. Gál, Z. *et al.* Mutations of the central tyrosines of putative cholesterol recognition amino acid consensus (CRAC) sequences modify folding, activity, and sterol-sensing of the human ABCG2 multidrug transporter. *Biochim. Biophys. Acta - Biomembr.* **1848**, 477–487 (2015).

198. Liu, X. *et al.* Generation of mammalian cells stably expressing multiple genes at predetermined levels. *Anal. Biochem.* **280**, 20–28 (2000).

199. Kolacsek, O. *et al.* Reliable transgene-independent method for determining Sleeping Beauty transposon copy numbers. *Mob. DNA* **2**, (2011).

200. Tátrai, P. *et al.* Combined introduction of Bmi-1 and hTERT immortalizes human adipose tissue-derived stromal cells with low risk of transformation. *Biochem. Biophys. Res. Commun.* **422**, 28–35 (2012).

201. Zhang, J. H., Chung, T. D. Y. & Oldenburg, K. R. A simple statistical parameter for use in evaluation and validation of high throughput screening assays. *J. Biomol. Screen.* **4**, 67–73 (1999).

202. Whitaker, J. E. *et al.* Cascade Blue derivatives: Water soluble, reactive, Blue emission dyes evaluated as fluorescent labels and tracers. *Anal. Biochem.* **198**, 119–130 (1991).

203. Izumi, S. *et al.* Investigation of the impact of substrate selection on in vitro organic anion transporting polypeptide 1B1 inhibition profiles for the prediction of drug-drug interactions. *Drug Metab. Dispos.* **43**, 235–247 (2015).

204. Bednarczyk, D. Fluorescence-Based Assays for the Assessment of Drug Interaction with the Human Transporters OATP1B1 and OATP1B3. *Anal. Biochem.* **405**, 50–58 (2010).

205. Karlgren, M. *et al.* Classification of inhibitors of hepatic organic anion transporting polypeptides (OATPs): Influence of protein expression on drug-drug interactions. *J. Med. Chem.* **55**, 4740–4763 (2012).

206. Windt, T. *et al.* Identification of anticancer OATP2B1 substrates by an in vitro triple-fluorescence-based cytotoxicity screen. *Arch. Toxicol.* **93**, 953–964 (2019).

207. Dobson, L., Reményi, I. & Tusnády, G. E. CCTOP: A Consensus Constrained TOPology prediction web server. *Nucleic Acids Res.* **43**, W408–W412 (2015).

208. Chun, S.-E. *et al.* The N-terminal region of organic anion transporting polypeptide 1B3 (OATP1B3) plays an essential role in regulating its plasma membrane trafficking. *Biochem. Pharmacol.* **131**, 98–105 (2017).

209. Kalliokoski, A. & Niemi, M. Impact of OATP transporters on pharmacokinetics. *Br. J. Pharmacol.* **158**, 693–705 (2009).

210. Deepak V, Svati HS, Spasojevic I, Shazia A, E. A. The SLCO1B1* 5 genetic variant is associated with statin-induced side effects. *J. Am. Coll. Cardiol.* **54**, 1609–1616 (2009).

211. Fujita, D., Saito, Y., Nakanishi, T. & Tamai, I. Organic anion transporting polypeptide (OATP)2b1 contributes to gastrointestinal toxicity of anticancer drug sn-38, active metabolite of irinotecan hydrochloride. *Drug Metab. Dispos.* **44**, 1–7 (2016).

212. Tang, H. *et al.* Development of novel, 384-well high-throughput assay panels for human drug transporters: drug interaction and safety assessment in support of discovery research. *J. Biomol. Screen.* **18**, 1072–83 (2013).

213. Shirasaka, Y., Mori, T., Murata, Y., Nakanishi, T. & Tamai, I. Substrate- and dose-dependent drug interactions with grapefruit juice caused by multiple binding sites on OATP2B1. *Pharm. Res.* **31**, 2035–2043 (2014).

214. Hussner, J. *et al.* Expression of OATP2B1 as determinant of drug effects in the microcompartment of the coronary artery. *Vascul. Pharmacol.* **72**, 25–34 (2015).

215. McFeely, S. J., Wu, L., Ritchie, T. K. & Unadkat, J. Organic anion transporting polypeptide 2B1 – More than a glass-full of drug interactions. *Pharmacol. Ther.* #pagerange# (2018). doi:10.1016/j.pharmthera.2018.12.009

216. Usuda, J. *et al.* Breast cancer resistant protein (BCRP) is a molecular determinant of the outcome of photodynamic therapy (PDT) for centrally located early lung cancer. *Lung Cancer* **67**, 198–204 (2010).

217. Visentin, M., Chang, M.-H., Romero, M. F., Zhao, R. & Goldman, I. D. Substrate- and pH-specific antifolate transport mediated by organic anion-transporting polypeptide 2B1 (OATP2B1-SLCO2B1). *Mol. Pharmacol.* **81**, 134–42 (2012).

List of publications

Publications presented in this dissertation:

- **Patik I**, Kovacsics D, Nemet O, Gera M, Varady G, Stieger B, Hagenbuch B, Szakacs G, Ozvegy-Laczka Cs., Functional Expression of the 11 Human Organic Anion Transporting Polypeptides in Insect Cells Reveals that Sodium Fluorescein is a General OATP Substrate. **Biochemical Pharmacology** 98:649-58 (2015) , doi: 10.1016/j.bcp.2015.09.015
- Kovacsics D, **Patik I**, Ozvegy-Laczka Cs., The role of organic anion transporting polypeptides in drug absorption, distribution, excretion and drug-drug interaction. **Expert Opin. Drug Metab. Toxicol.** Nov (2016) 1–16., doi:10.1080/17425255.2017.1253679.
- **Patik I**, Szekely V, Nemet O, Szepesi A, Kucsma N, Varady G, Szakacs G, Bakos E, Ozvegy-Laczka Cs., Identification of novel cell-impermeant fluorescent substrates for testing the function and drug interaction of Organic Anion-Transporting Polypeptides, OATP1B1/1B3 and 2B1. **Sci Rep.** 2018 Feb 8;8(1):2630., doi: 10.1038/s41598-018-20815-1.

Other publications:

- Bauer M, Matsuda A, Wulkersdorfer B, Philippe C, Traxl A, Ozvegy-Laczka C, Stanek J, Nics L, Klebermass EM, Poschner S, Jager W, Patik I, Bakos E, Szakacs G, Wadsak W, Hacker M, Zeitlinger M, Langer O., Influence of OATPs on Hepatic Disposition of Erlotinib Measured With Positron Emission Tomography. Clin Pharmacol Ther. 2017 Sep 22., doi: 10.1002/cpt.888.
- Windt T., Toth Sz, Patik I, Sessler J, Kucsma N,Szepesi A, Zdrazil B, Ozvegy-Laczka Cs, Szakacs G., Identification of anticancer OATP2B1 substrates by an in vitro triple-fluorescence-based cytotoxicity screen. Arch. Toxicol. 93, 953–964 2019 doi:10.1007/s00204-019-02417-6.
- Bakos E, Nemet O, Patik I, Kucsma N, Varady Gy, Szakacs G and Ozvegy-Laczka Cs., A novel fluorescence-based functional assay for human OATP1A2 and OATP1C1 identifies interaction between third-generation P-gp inhibitors and OATP1A2. FEBS J. (2019). doi: 10.1111/febs.15156
- O'Hara J M, Redhu N S,Cheung E, Robertson N G, Patik I, El Sayed S, Thompson C M, Herd M, Lucas K B, Conaway E, Morton C C, Farber D L, Malley R and Horwitz B H., The Generation of protective pneumococcal-specific nasal resident memory CD4+ T cells via

parenteral immunization. Mucosal Immunology 13, 172-182 (2020) doi: 10.1038/s41385-019-0218-5.

ADATLAP

a doktori értekezés nyilvánosságra hozatalához

I. A doktori értekezés adatai

A szerző neve: Izabel Patik
MTMT-azonosító: 10052823
A doktori értekezés címe és alcíme: Development of novel fluorescence-based assays for the investigation of human Organic anion transporting polypeptides, uptake transporters with emerging pharmacological relevance
DOI-azonosító: 10.15476/ELTE.2020.04
A doktori iskola neve: Biológia Doktori Iskola
A doktori iskolán belüli doktori program neve: Immunológia program
A témavezető neve és tudományos fokozata: Laczka-Özvegy Csilla, PhD
A témavezető munkahelye: MTA-TTK, Enzimológiai Intézet

II. Nyilatkozatok

1. A doktori értekezés szerzőjeként
a) hozzájárulok, hogy a doktori fokozat megszerzését követően a doktori értekezésem és a tézisek nyilvánosságra kerüljenek az ELTE Digitális Intézményi Tudástárban. Felhatalmazom a Természettudományi kar Dékáni Hivatal Doktori, Habilitációs és Nemzetközi Ügyek Csoportjának ügyintézőjét, hogy az értekezést és a téziseket feltöltse az ELTE Digitális Intézményi Tudástárba, és ennek során kitöltse a feltöltéshez szükséges nyilatkozatokat.
b) kérem, hogy a mellékelt kérelemben részletezett szabadalmi, illetőleg oltalmi bejelentés közzétételéig a doktori értekezést ne bocsássák nyilvánosságra az Egyetemi Könyvtárban és az ELTE Digitális Intézményi Tudástárban;
c) kérem, hogy a nemzetbiztonsági okból minősített adatot tartalmazó doktori értekezést a minősítés (*dátum*)-ig tartó időtartama alatt ne bocsássák nyilvánosságra az Egyetemi Könyvtárban és az ELTE Digitális Intézményi Tudástárban;
d) kérem, hogy a mű kiadására vonatkozó mellékelt kiadó szerződésre tekintettel a doktori értekezést a könyv megjelenéséig ne bocsássák nyilvánosságra az Egyetemi Könyvtárban, és az ELTE Digitális Intézményi Tudástárban csak a könyv bibliográfiai adatait tegyék közzé. Ha a könyv a fokozatszerzést követőn egy évig nem jelenik meg, hozzájárulok, hogy a doktori értekezésem és a tézisek nyilvánosságra kerüljenek az Egyetemi Könyvtárban és az ELTE Digitális Intézményi Tudástárban.
2. A doktori értekezés szerzőjeként kijelentem, hogy
a) az ELTE Digitális Intézményi Tudástárba feltöltendő doktori értekezés és a tézisek saját eredeti, önálló szellemi munkám és legjobb tudomásom szerint nem sértem vele senki szerzői jogait;
b) a doktori értekezés és a tézisek nyomtatott változatai és az elektronikus adathordozón benyújtott tartalmak (szöveg és ábrák) mindenben megegyeznek.
3. A doktori értekezés szerzőjeként hozzájárulok a doktori értekezés és a tézisek szövegének plágiumkereső adatbázisba helyezéséhez és plágiumellenőrző vizsgálatok lefuttatásához.

Kelt: Boston, 2020. március 9.

……
a doktori értekezés szerzőjének aláírása